Forecasting Research

Met O 11 Technical Note No. 25

Development of a new physics package for the global forecast model

by

C.A. Wilson and J. Slingo

January 1989

Me O 11)
London Road G12 2SZ, England

MET O 11 TECHNICAL NOTE NO 25

DEVELOPMENT OF A NEW PHYSICS PACKAGE FOR THE GLOBAL FORECAST MODEL

by

C A WILSON AND J M SLINGO

LONDON, METEOROLOGICAL OFFICE.
Met.O.11 Technical Note (New Series) No.25

Development of a new physics package for the global forecast model.

08730289 551.509.313 FH2A
551.588

Met O 11
(Forecasting
Research)
London Road
Bracknell
Berkshire
RG12 2SZ.

January 1989

DEVELOPMENT OF A NEW PHYSICS PACKAGE FOR THE GLOBAL FORECAST MODEL

C. Wilson & J. Slingo, Met O 11
January 1989

1. INTRODUCTION.

At present there are many differences in the physical parametrization schemes between the fine-mesh and coarse-mesh (global) models. A new package of physics routines including many of the changes introduced into the fine-mesh over the past two years underwent a trial in the global model producing forecasts for several test cases (Bell ,1986).The major change is the replacement of the climatological radiation scheme by an interactive scheme with radiation fluxes and heating rates dependent upon the model's temperature, humidity and model generated cloud, as well as carbon dioxide and ozone. (In the first trial the effects of ozone on the solar beam only were treated.) Other changes were :- the inclusion of a 4-layer soil temperature model and a surface resistance to evaporation; modifications to the convection scheme to include the effects of mixing by detrainment, impose a critical cloud depth threshold for the formation of precipitation and restrict evaporation of precipitation to that falling below cloud base; an implicit method of solution of the vertical diffusion equations of the boundary layer so allowing the removal of the overdeepening correction.

The results of the first trial were rather disappointing. Scores of objective verification against observations were often worse than the control (operational) version of the model, especially for the heights and temperatures in the northern hemisphere extra-tropics in summer. The model's rather poor humidity structure, particularly at stratospheric levels, and a tendency to diagnose excessive cloudiness with low cloud amount increasing during the forecast, were major defects resulting in unrealistic cooling rates from the interactive radiation scheme.

A revised version of the package was made in an attempt to remedy these faults. Stratospheric humidity fields were reinitialised to remove the excessive moisture and negative humidities, produced by the finite difference equations of motion, were reset in a more conservative way. The threshold relative humidity for the prediction of cloud amounts was increased to 90% (95% at level 2) from 85% and the final detrainment of convective parcels was split between the last level of buoyancy and that above to take account of shallow convection. In addition the long-wave effects of ozone were also included and the roughness length over the sea was made wind-speed dependent.

A new trial (hereafter referred to as trial2) was carried out with the revised package. Cloud prediction was improved substantially with global average amounts at 5 days being 30% for high, 27% for medium and 28% for low cloud with a much more realistic geographical distribution. However the cold bias of the previous trial still remained. As a consequence the height field errors, particularly in the tropics and summer hemisphere were still significantly greater than the operational model (Bell, 1987). Despite the improved verification of surface temperatures, it was clear that measures to improve the cold bias

were required before the interactive radiation scheme could be implemented operationally.

This note describes how the package has been subsequently changed and corrected to improve its performance. A single case, DT 12Z 13/6/85, was selected for investigation . This was chosen since the worst height and temperature errors, compared to the control (operational model), were found for the tropics and extra-tropics of the northern hemisphere summer. Objective verification against observations (Tables 1,2) for this case, and zonal mean differences of T+120 forecast heights and temperatures from the verifying analyses (Figures 1,2), for the control and trial2, also show the trial to be worse in these regions . The case is therefore representative. The errors in the southern hemisphere extra-tropics are large in both and little attention will be given to this region in the following. It should also be noted that the *pattern* of height errors is very similar in both the control and trial with largest negative biases in the tropics and around 60° N and 60° S and the smallest biases in the sub-tropics.

Unlike the control, the trial shows negative temperature errors of at least 1 K near the surface in the tropics. Once the near surface air is too cold the rest of the troposphere will be cold also. The reason for this cooling becomes apparent when the globally meaned temperature increments from the diabatic and adiabatic processes are compared (Figure 3). In the lower atmosphere the two versions of the model show quite different behaviours. The boundary fluxes are enhanced in the trial due to more heating over land with the diurnal cycle and interactive cloud (versus zonally averaged cloud). Correspondingly the convection shows more cooling near the surface and heating above presumably again as a result of a shallow dry adjustment process associated with the additional heating over land. However these two effects are almost compensatory and the lower tropospheric net cooling in the trial can be attributed to the greater radiative cooling. It would be wrong though to cite this as an error of the interactive package. Indeed it is the unrealistic lack of cooling in the climatological radiation scheme which allows the control to perform better. This insufficient cooling in the bottom 4 layers is due to the term for radiation exchange with the surface which is only applied in these layers. This term was extended to operate in these layers (rather than just the first layer) in an attempt to alleviate the model tendency to cool, particularly in the tropics (Foreman, 1982) which was noticed soon after the model became operational.

In the middle and upper troposphere the trial again shows more net cooling than the control. This can be attributed to a weakening of the convection associated with increased low level stability as a result of the greater near surface cooling.

The conclusion to be drawn from these results is that the net cooling in the trial is due primarily to inadequate heating from other processes. It is a common assumption, incorrectly made, that cooling in a model must be due to radiative processes but it may equally be associated with lack of heating by convection as was amply demonstrated in the ECMWF model when changes in the convective parameterization changed the bias from cold to warm (Tiedtke et al,

1988). Whilst the radiation code has been checked for errors, considerable emphasis has therefore been placed on improving the performance of the convection scheme. Some constraints on the scheme which were included for numerical stability, have been found to be unnecessarily pessimistic and may be removed. The prediction of cloudiness and the placement of clouds in the vertical have also been revised. Some minor adjustments to the boundary layer code were also found to be required to eliminate unrealistic small amounts of precipitation which resulted from the vertical shift of clouds in the lowest atmospheric layers.

Whilst the modifications to the package have improved its performance considerably it is still not possible to outperform the operational model in terms of the height and temperature errors. It should be stressed again that the operational model has unrealistic radiational cooling in the lowest 4 layers which gives it a distinct advantage. As noted by Burridge et al.(1986), in most models there is a systematic trend to cool the troposphere and the forecast model is no exception (even without interactive radiation). Zonal mean temperature errors at 5 days from the NCAR community climate model, the spectral model of the Bureau of Meteorology Research Centre, and the GFDL model (Puri and Gauntlett, 1987) all show a systematic cold bias of up to 4° C throughout most of the troposphere. The NMC global spectral model also shows a similar cooling trend with largest errors around 700 mb which are established over the first 5 days (White, 1988). The reasons for these common errors may not be the same for all models; however it does appear that where a simple radiation scheme is used such as in the operational model, or in the 'Emeraude' model (Coiffier et al, 1987), the temperature bias is less or absent. The inclusion of a more realistic scheme tends to expose deficiences in the model and produce a worse bias. This has been found in the NMC nested grid model where inclusion of an interactive scheme in place of a simple scheme resulted in more cooling and worse height errors (Hoke, personal communication). This has been overcome in the hemispheric version by the imposing hemispheric conservation of potential temperature in each layer (NOAA-NWS,1987; also see Section 8). Yang et al,(1988) also report the deterioration of the equatorial thermal structure in the AFGL global model upon the introduction of an interactive radiation scheme. Climate models used in the Meteorological Office also show a cold bias. Mitchell et al,(1987) note that the zonal mean temperatures in the troposphere are generally too cold by 2 to 3 K in both the 11 layer and 5 layer models; both models used similar radiation codes with zonally meaned climatological clouds. More recent versions of the 11 layer model including gravity wave drag or envelope orography parameterisations (Slingo and Pearson,1987), or at lower horizontal resolution but including an interactive ocean surface and model generated clouds (Wilson and Mitchell,1987) also have a cold bias. Extended range forecasts using the 11 layer model in Met O 13 also show a similar cold trend (Milton, personal communication). In the ECMWF model there is now a warm bias throughout much of the troposphere (as noted above). An examination of the global energy budget (Tiedtke et al,1988) shows that much of the warming is explained by the initial 'spin-up' of the convection scheme with convective rainfall much larger than evaporation over the first few days. However it is a little difficult to assess whether there is a cooling trend since at present the radiation scheme operates without including the effects of the water vapour continuum (Miller, personal communication) which

are largely responsible for the increased radiational cooling in the lower atmosphere (see Section 8). Omitting the effects of the continuum can lead to significant differences in model behaviour (see Harshvardhan and Randall,1986).

The long digression above on the behaviour of other models is to emphasise that the cooling shown by the 15 level model is present to a greater or lesser degree in many other models and seems to be related to the use of more realistic radiation codes. However the cause of the cooling may well be a lack of heating or some other deficiency in the dynamical formulation. For example Black and Janjic,(1988) using the same radition code as the NMC nested grid model but a modified σ coordinate (η) and the Betts-Miller convective adjustment scheme reduced the cooling significantly.

Whilst we have not been able to improve the heating of the model sufficiently we have removed some of the undesireable aspects of the convection scheme and checked the radiation code for errors. Two short term remedies are available to control the growth of the cold bias (omit the continuum effects or impose global conservation of temperature) whilst the problem is investigated further and other improvements sought for the physical parametrizations.

The model's poor humidity structure with excessive humidity at upper levels was found to be quickly re-established (see Appendix) within a few days of being initialised to climatological values. The cause of this systematic error requires further investigation but as a temporary measure humidity fields can be re-initialised daily.

2.CHANGES MADE AS A RESULT OF SENSITIVITY TESTS.

This section descibes a series of minor changes designed to bring the model into line with the fine mesh model and Met O 20 model. The changes will be described briefly and their impact on the performance of the model summarised. A fuller discussion of the convection and radiation changes will be given in later sections.

2.1 Solar constant and high/medium cloud height

The value of the solar constant used in the trial was 1395 Wm^{-2} which is ~ 1.5% larger than recent estimates. This was reduced to 1373 Wm^{-2} (Slingo, 1985). In the trial, medium cloud was predicted from the largest relative humidity of layers 5 to 9 and high cloud from that of layers 10 to 12. Since the optical properties specified for high cloud (albedo=0.2, emissivity=0.75) and for medium cloud (albedo=0.6, emissivity=1.0) are quite different it is probably unrealistic to allow medium cloud up to ~350 mb in polar and mid-latitudes. In a sensitivity test medium cloud was restricted everywhere to layer 7 or below so that the tops are not above ~550 mb. This produced a decrease in medium cloud amount of 7% of total global cover and a corresponding increase in high cloud amount. Much of the middle and lower atmosphere was warmer as a result of increased solar heating because less incoming solar flux is reflected by high clouds.

Changing the layers used to predict medium cloud had a beneficial effect in the northern hemisphere where heights and temperatures were improved. Therefore a latitude dependence was introduced so that the relative humidities up to layer 9 are used in the tropics whereas only the realtive humidities up to layer 7 are used polewards of 30° . Subsequently the cloud scheme was rewritten (see Section 6) and a more extensive latitude dependence of cloud toop height was incorporated.

2.2 Global conservation of mass.

In the trial the globally averaged surface pressure decreased by about 0.15 mb d^{-1} and so the model did not conserve total mass. This was because mean sea-level pressure was filtered during the forecast . Global conservation is imposed at each timestep by rescaling surface pressure everywhere by the same factor after the filtering and updating. Although the temperature errors remained almost the same this change had a substantial effect on the height biases below 100 mb in the northern hemisphere. Improvements of ~0.4 dm at day 3 and of ~0.6 dm at day 5, were obtained with surface pressure (PMSL) negative biases reduced by ~0.5 mb and ~0.8 mb respectively.

2.3 Evaporation of precipitation .

In trial2 the evaporation of precipitation, formed dynamically or in the convection scheme, was independent of the rate of precipitation. Essentially this meant that convective rainfall was evaporated more rapidly than dynamic precipitation. This inconsistency was removed from the operational fine-mesh model by a new formulation whereby the rate of evaporation depended upon the rate of precipitation (Hammon and Wilson, 1987). At the same time the liquid water retained by the cloud, after the commencement of precipitation, was reduced from 1 g Kg^{-1} to 0.1 g kg^{-1} (or it is replaced by the saturated humidity if that is smaller, which is generally the case above ~500 mb.). This decreased the moistening and cooling when the cloud finally detrained. Since the new scheme reduced the evaporation of all but the heaviest convective rainfall it would probably lead to a warming and drying of the lower atmosphere.In a sensitivity test the troposphere below 400mb was ~0.5 to 1 degree K warmer in northern mid-latitudes with a corresponding improvement in heights .

2.4 Soil moisture

Operationally there are only two non-frozen land surface types :-temperate and arid land with soil moisture specified as 5cm or 0cm. In the trial these were also used and, over temperate land evaporation is only restricted by a surface resistance whilst over arid land there is no evaporation. Over much land in summer the assumption of easily available soil moisture is wrong. Therefore soil moisture over temperate land was allowed any value between 0 and 15 cm as specified from a new geographically varying data-set depending on the time of

year (obtained via Met O 8 from the data of Willmott and Rowe, University of Delaware, see Willmott et al.,1985).

Using a realistic geographical distibution produced a warming near the surface over much of the northern hemisphere land and a slight improvement in northern hemisphere heights .

2.5 Performance with all changes included

There was a significant improvement in the performance of the model with all the changes described above included (Figure 4, Table 3). The near surface air and much of the troposphere were warmer (by ~0.5 K at day 5) and heights in the tropics and northern hemisphere improved (by 1 to 2 dm at day 5). The surface pressure verify better than the control as do the 850 mb heights but in general the height and temperature biases and rms errors are still worse than for the operational model. Further improvements to increase the diabatic heating of the lower atmosphere are therefore required.

3. CONVECTION CHANGES.

The global mean temperature increments due to convection (Figure 3) show that there is less heating in the trial than in the control for the layers above layer 4. Over a large depth of the atmosphere the heating is ~0.25 K d^{-1} less. Although there is more dry convective adjustment within the boundary layer in the trial, deep convection is suppressed. To encourage greater heating a modification was made to the initiation of convection. The convection scheme derives a mass flux from the degree of instability between model levels. For numerical stability the mass flux is restricted to be smaller than the thinnest model layer. In order that convection should not be artificially suppressed the very thin bottom layer of the model is excluded from consideration. Instead the first test for instability assumes parcels to have temperature and humidity characteristic of a mean of layers 1 and 2 (with the final temperature and humidity changes applied equally to both levels). In reality deep convection is more likely to be initiated by the lifting of air from the surface. It would seem more reasonable therefore to restrict the convection scheme to layer 2 and above but to calculate the initial buoyancy of the parcels using the temperature and humidity of the first layer. In general this will mean a larger buoyancy and so stimulate more vigorous convection and larger heating. Enhanced heating does result ,particularly during the first 24 hours. However, applying the same convective increments to levels 1 and 2 tends to dry out and warm level 2 which results in unphysical profiles since level 2 is effectively uncoupled from level 1 and the surface fluxes. The convective precipitation increases rapidly over the first few hours before declining to almost the previous level after 2 days. Such a change is therefore not physically reasonable.

Further investigation showed that the scheme need not be restricted to operate from level 2 and above since, if all levels were treated in the same way and convection allowed to initiate from level 1, only a few points (about 12 in 6000 convectively active) have their mass flux restricted because of numerical stability. However the heating rates are little different above the boundary

layers (Figure 5) from the previous trial.(Heat and moisture are now permitted to mix in unstable situations by the boundary layer routine which accounts for the discrepancy here). Altering various parameters of the scheme such as the constants used to specify the intial mass flux or the excess temperature and humidity of the parcel only changes the heating rates very slightly. This low sensitivity shows the scheme is robust but there appears to be little scope for extra diabatic heating to compensate the radiative cooling..

4. CHANGE OF MODEL LEVELS.

Although no physically reasonable change to the convection scheme was found to significantly improve the heating rates ,the global temperature increments (Figure 5) are rather unevenly distibuted in the vertical. This is also evident for the previous trial and control (Figure 3) and so is likely to be a numerical artifact. The oscillating behaviour of the increments corresponds to the uneven distibution of the model layer thicknesses; thinner layers have larger increments and thicker layers smaller increments (Figure 3). Such obviously unphysical behaviour is undesireable and leads to vertical profiles of temperature and humidities with a similar structure. It is unfortunate also that the minima in heating tend to coincide with the standard levels used for verification.

The problem is caused by the uneven distribution of layer thicknesses. In the convection scheme the mass flux is modified by entrainment and detrainment. The entrainment is parameterized in terms of layer thickness and so leads to a marked variation of mass flux and hence heating between thick and thin layers. A simplified analysis of the convection scheme shows how this happens. If we ignore the effects of both mixing and forced detrainment the main heating of the enviromental air surrounding the cloud ensemble is by subsidence (Bell and Dickinson, 1987); the change in potential temperature is given by :-

$$\Delta\theta_k = M_k(1+\varepsilon_{k+\frac{1}{4}})(\theta_{k+1}-\theta_k)/\Delta\sigma \qquad (1)$$

(see Figure 6) where M_k is the mass flux at level k and is predicted by

$$M_{k+1} = (1+\varepsilon_{k+\frac{1}{4}})(1+\varepsilon_{k+\frac{3}{4}})M_k \qquad (2)$$

and $\varepsilon_{k+\frac{1}{4}}$, $\varepsilon_{k+\frac{3}{4}}$ are the fractional entrainment rates at levls k+¼,k+¾ and are given by :-

$$\varepsilon_{k+\frac{1}{4}} = 4.5\sigma_k(\sigma_k-\sigma_{k+\frac{1}{2}}) \simeq 4.5\sigma_k\tfrac{1}{2}\Delta\sigma_k$$

$$\varepsilon_{k+\frac{3}{4}} = 4.5\sigma_{k+\frac{1}{2}}(\sigma_{k+\frac{1}{2}}-\sigma_{k+1}) \simeq 4.5\sigma_{k+\frac{1}{2}}\tfrac{1}{2}\Delta\sigma_{k+1} \qquad (3)$$

If $\Delta\sigma_{k+1}$ is thin and $\Delta\sigma_k$ is thick, as illustrated in figure 6, then M_{k+1} will be large ; this and the $\Delta\sigma_{k+1}$ in the denominator of (1) will tend to make $\Delta\theta_{k+1}$ large. Similarly if $\Delta\sigma_{k+1}$ is thick and $\Delta\sigma_k$ is thin then $\Delta\theta_{k+1}$ will tend to be small.

A new set of levels (or rather layer boundaries) was therefore chosen so that the layer thickness varied more smoothly (Figure 7) and the initial data interpolated to these. The convective increments forecast using these new levels (Figure 7) are certainly smoother. The net overall warming of the atmosphere is also larger possibly as a result of a slightly thicker layer 2 which allows a larger mass flux. Several different sets of levels have been tried with similar results. The final choice of levels is not critical for the convection scheme to perform reasonably as long as the thickness variation is relatively smooth.

5. AMENDMENTS TO THE RADIATION CODE.

Using a single column version of the radiation scheme, several errors were identified in the code. The fluxes and heating rates for an idealised tropical atmosphere (McClatchey et al.,1973) were compared with those computed using a single column version of the Met O 20 code adapted to run on the same vertical grid as the forecast model. Initial results showed considerable differences in the clear sky heating infrared rates between the Met O 11 and Met O 20 codes (Figure 8: solid and dotted lines). The Met O 11 code does not show the expected increase in cooling in the lower troposphere associated with the continuum absorption in the atmospheric window. There were also some considerable differences in the middle and upper troposphere. Although the Met O 11 code is derived from that used in Met O 20 there are subtle differences in the formulation. As described in Slingo (1985), the downward and upward longwave fluxes at pressure p are given by :-

$$F\downarrow(p) = B(0)\varepsilon(0,p) - \int_{p}^{0} dp' a(p',p) dB(p')/dp'$$

$$F\uparrow(p) = B(p_s) + \int_{p_s}^{p} dp' a(p',p) dB(p')/dp' \qquad (4)$$

where $B(p)$ is the Planck flux for the air temperature at pressure p, $\varepsilon(0,p)$ is the slab emissivity of the atmosphere from the top down to pressure p and $a(p,p')$ is the slab absorptivity from the dummy pressure p' to p. These equations are solved numerically by a trapezoidal rule to calculate the fluxes at the layer boundaries. The terms which contribute to the upward and downward clear sky fluxes at any level are illustrated in Figure 9 . Apart from the half layers marked with an asterisk, adjacent to the level in question, the contribution from the integral in equation (4) to the flux at level n from each layer k is quite simply :-

$$a(u^{k}_{n})\ (B_{k} - B_{k-1}) \qquad (5)$$

where u^{k}_{n} is the pathlength from the level k to level n. For the half layers however, the Met O 11 and Met O 20 codes differ in their computation. In the Met O 20 code the contribution from the half layer adjacent to the level n is:-

$$\tfrac{1}{2}a(\tfrac{1}{2}u^{n-1}_{n})\ \tfrac{1}{2}(B_{n} - B_{n-1}) \qquad (6)$$

whilst for the Met O 11 code it is more correctly given as:-

$$a(\tfrac{1}{4}u^{n-1}_{n})\ (B_{n} - B_{n-\frac{1}{2}}) \qquad (7)$$

where $B_{n-½}$ is computed from $T_{n-½}$, linearly derived from T_n and T_{n-1} and u^{n-1}_n is the pathlength of the payer adjacent to level n. Since neither a nor B are linear functions of u and T then the two formulations can give substantial differences, particularly in regions of strong absorption, such as near the surface. When the Met O 20 code was modified to compute the half layer terms as in equation (7) a marked decrease in the near surface cooling was found for the McClatchey tropical profile (dashed line, figure 8). There were also quite large differences in the middle and upper troposphere. Thus a substantial part of the difference between the Met O 11 and Met O 20 codes could be attributed to the half layers. This result raises important questions about the accuracy of the emissivity approximation as currently used.

It is clear from figure 8 that the Met O 11 code is still underestimating the cooling near the surface. This was traced to an error in the definition of the continuum term for all half layers, An error in the computation of the Planck flux difference for the bottom model layer was also found. Once these were corrected the Met O 11 code gave clear sky cooling rates in very good agreement (to within 0.01 K d^{-1}) with the revised Met O 20 code (dashed line on figure 8). The agreement will not be exact because of other slight differences in the code such as the treatment of ozone.

As far as the cloudy fluxes and heating rates are concerned the operational Met O 11 code cannot be directly compared with the Met O 20 code because the clouds are positioned differently with respect to the model levels (see section 6). However a study of the results from the McClatchey tropical profile with various cloud geometries revealed two errors in the treatment of convective cloud. One gave a spurious longwave heating just below cloud top. The other, potentially more serious, involved the treatment of reflected shortwave radiation from a layer cloud adjacent to a convective cloud. The nature of the error was an underestimate of the reflected flux thus giving excessive convergence of solar radiation in the cloud layer. Heating rate errors of several K/day could be generated particularly when the sun is at its zenith. These corrections had only a small impact on the model. The global mean temperature increments (Figure 10) show only minor changes in the radiative cooling near the surface. Figure 11 shows the latitude height cross sections of the height and temperature errors for a five day forecast with the convection changes, new vertical levels (see section 4) and corrections to the radiation code. Compared with the previous version of Section 2 (Figure 4) the modifications to the convection scheme and these radiative corrections make a small improvement to the biases.

6 CHANGES TO THE TREATMENT OF CLOUDS.

When the interactive radiation scheme was recoded for the Met O 11 forecast models it was considered computationally more efficient to place the clouds between model levels rather than between layer boundaries as is done in the Met O 20 code and indeed in all interative radiation codes. This difference in the placement of clouds has important physical implications which require consideration. Figure 12 shows schematically the relationship between boundary layer cloud, the implied radiative heating and the temperature and humidity

structure for the two placements of the cloud. In the existing Met O 11 radiation code, although the cloud is diagnosed from the T and q at the base of the inversion the cloud extends , unrealistically right through the inversion. By effectively splitting the cloud between two model layers the radiative heating profile shows a large cooling in the upper layer and warming below. Thus the radiation will attempt to erode the inversion in an unrealistic fashion. Although it could be argued that in reality a boundary layer cloud does cool at its top and warm below (Slingo at al, 1982) not only does this occur on a vertical scale not resolved by the model, but the cooling is still concentrated below the inversion. The other undesirable aspect of the scheme is that the T and q used to diagnose the cloud are not representative of the whole cloud layer. As is evident from figure 12 this very nicely avoids the recurrent problem in models of cloud radiative cooling inducing an increase in cloudiness, particularly for the boundary layer cloud.

The lower part of figure 12 demonstrates what happens when the cloud is placed between model layers, consistent with the T and q profiles. Now the radiation scheme gives a simple cooling of the cloud layer with a tendency, in the absence of any other processes, to strengthen the inversion. It is clear from this example that the placement of clouds between model levels is physically unrealistic. However problems with the cooling of the inversion when the clouds are positioned between layers are anticipated and will be discussed later.

Considerable recoding of the radiation code was required to move the clouds between model layers. Again the code was checked by comparing with the results of a single column test with those from the modified version of the Met O 20 code described in section 5.

The opportunity was taken to modify the cloud prediction scheme to incorporate a more extensive dependence of cloud top height on latitude (see section 2.1). Table 4 shows the heights used for each layer cloud. The scheme was also generalised to make it more independent of vertical resolution. After a number of sensitivity experiments the dependence of low cloud amount (C_L) on the strength of the inversion ($\Delta\theta/\Delta p$) and the relative humidity at the base of the inversion (RH_{base}) (Slingo, 1987) was reintroduced as follows :-

$$C'_L = -16.67\ \Delta\theta/\Delta p - 1.167 \quad \text{for } \Delta\theta/\Delta p < 0.07$$

$$C_L = C'_L \quad \text{if } RH_{base} > 0.80$$

$$C_L = C'_L\ (0.8 - RH_{base})/0.2 \quad \text{for } 0.6 \leq RH_{base} \leq 0.8$$

$$C_L = 0.0 \quad \text{otherwise.}$$

These changes have improved the predicted low cloud field as can be seen in figure 13. With the original scheme (Fig. 13(a)) the tropics have very little low cloud and there is no evidence of the extensive stratocumulus sheets over the eastern subtropical oceans. The new scheme (Fig. 13(b)) performs much better in this respect.

Despite a better simulation of the clouds, which could be a useful additional forecast product, the impact of the new cloud representation on the model errors is slight. However, as anticipated the model now shows an undesireable response to the radiative cooling of the cloud topped boundary layer in those regions where convection is not active such as over the cold oceans of the eastern subtropics. The radiative coooling of the layer is compensated by the production of dynamic rain as shown in figure 14. This rainfall is unrealistic and clearly the model lacks the correct compensatory mechanism.

7 TREATMENT OF THE BOUNDARY LAYER.

The boundary layer diffusion equations are treated implicitly (Kitchen,1985), as in the fine mesh. There is a constant resistance to evaporation over land and over the sea the roughness length depends upon wind speed according to the Charnock formula. Here we describe the modifications to the scheme with low cloud placed in model layers.

Typically, the bulk radiative cooling of a boundary layer cloud is of the order of 10 K d^{-1} which is equivalent to a flux divergence of about 60 Wm^{-2} for a cloud of average thickness. When the underlying surface is relatively cool, such as in the eastern subtropical oceans, the upward flux of energy from the surface, which might compensate the radiative cooling of the cloud layer, is likely to be small. However it is generally considered (e.g. Lilly 1968; Randall 1980) that the entrainment of warm, dry air through the cloud top is an important warming mechanism for the cloud. This entrainment is driven by convective instability within the cloud, arising from the strong radiative cooling of the cloud top and weak warming below, assisted by condensational warming near the cloud base and evaporative cooling of the cloud drops into the entrained enviromental air at the cloud top. Whilst the overall energy balance of a stratocumulus cloud is a subtle mixture of radiative, turbulent and condensational processes there is no doubt that cloud top entrainment is a key component. Because the detailed structure of the in-cloud processes is not resolved by the model the cloud top entrainment process is not represented. The result is a cooling of the cloud layer until saturation is reached and dynamic rain forms. The cooling is then compensated by latent heat release and the cloud 'drizzles'. If the cloud is situated under a boundary layer inversion the model's vertical diffusion process will, in its present form, give very little exchange between the cloud and the warm, dry enviroment above because stable diffusion coefficients will be implied. To overcome the problem of dynamic rain from stratocumulus it was decided to represent, albeit crudely, the cloud top entrainment by enhancing the diffusion through the cloud top. Consistent with studies of cloud topped boundary layers this is only applied in convectively stable situations; in other words we are not trying to represent the additional mixing by shallow (trade-wind) cumulus which is a different process, convectively driven from the surface. Thus when the predicted convective cloud amount is less than 10% (i.e. very weak convection) and low cloud (C_L) exists, the diffusion coefficient at the cloud top is enhanced by an amount k_c given by :-

$k_e = A\ C_L$ where A is a constant.

The value of A has to be determined from sensitivity experiments. A value of 0.01 was found sufficient to eliminate the dynamic rain by entraining enough warm enviromental air to compensate the radiative cooling. On the other hand it was small enough to avoid dissipation of the cloud which can occur if too much mixing of dry air occurs.

When this extra diffusion was applied in the model the dynamic rain was greatly improved over the eastern subtropical oceans (Figure 15) whilst the low cloud field still showed a reasonable simulation (Figure 16). The impact of this change on the model errors was negligible.

8. ASSESSMENT AND RECOMMENDATIONS.

The final package including the new cloud scheme and changes to the boundary layer (Figure 17 and Table 5) still preforms worse overall than the operational model (cf Figure 1a and Table 1) despite the general reduction in cooling compared to the previous trial (Figure 2a). A winter case (not shown) was also generally slightly colder than the operational model, although many of the verification scores were comparable or better. The package cannot therefore be introduced without increasing the systematic errors of the model. Since it is desireable to introduce the new physics for the improved prediction of surface temperatures, precipitaion (especially convective) and the prediction of cloud, there are two possible methods available to control the cold bias.

The first method is to recognise that the water vapour continuum term is responsible for much of the radiative cooling in the lower atmosphere (Figure 18; see also Harshvardhan et al,1987 (Fig.2,Table 2), Stephens,1984 (Fig.2))and so simply remove it completely. This is rather unphysical since ,although the molecular nature of its cause and its magnitude is subject to some debate (Roach et al,1988) it is generally recognised as being important (Cox,1973, Luther et al,1988). The parameterisation of the absorption coefficient for the continuum (Slingo, 1985) might be rather too strong since the downward flux at the surface is larger than that obtained with more detailed line-by-line radiation codes. For example, for the tropical profile the flux of 412 Wm^{-2} is about 20 Wm^{-2} larger (Luther et al,1988). A possible modification suggested by K. Shine (personal communication), which removes the pressure-dependent foreign broadening and reduces the self-broadening coefficient for the absorption in the band 800 to 1200 cm^{-1}, reduces the cooling rates (Figure 18). However the cooling rates still increase as the surface is approached and the impact on the cold bias, especially in the Tropics, is likely to be slight. More field observations of the water vapour continuum absorption are required before its dependence on temperature and pressure can be better represented in radiation codes. If the continuum effects are omitted altogether (despite its known importance) the mean height and temperature errors (Figure 19) are reduced and generally the forecast verifies as well or better than the operational model.

The second method is by the imposition of global conservation of mass-weighted temperature on each model layer (Figure 20) which reduces the errors by more. This method also verifies better (Table 6) and is less prejudiced as to the cause of the temperature bias. It should therefore be used until further improvements to the physical parameterisations can be found.

Another systematic model error that requires further investigation is the tendency to produce excessive humidities at upper levels. These are re-established within a few days of being initialised to realistic climatological values (see Appendix). As a temporary measure the upper level humidities may be re-initialised daily. The effect of this on the tropospheric errors is slight (Figure 21).

The revised package including these measures to control the systematic errors has been shown to compete in forecast performance with the operational model for this one case. An extended trial of the package should now be done including the package in the assimilation model as well so that a full assessment of its impact on the analyses and forecasts can be made.

APPENDIX

Upper level humidities

In early tests of the interactive radiation scheme with the global model there was excessive cooling in the stratosphere. Partly this was due to excessive water vapour in the initial anlysis. Values of specific humidity at stratospheric heights were 10 to 100 times observed values which are generally ~2 to 3 X 10^{-6} kg kg^{-1}. To correct this the humidities were initialised as follows :- the tropopause was determined by where the lapse rate fell to 0.002 K m^{-1} (above 500mb). Above this level the specific humidity was set to 3 X 10^{-6} kg kg^{-1} or reduced until the relative humidity did not exceed 10%. At the model level immediately below the tropopause an interpolation between the stratospheric and tropospheric values was used. The effect of this on the intial analysis is shown in figure A1. (N.B. The region above 70mb should be disregarded since level 15,σ=0.025 does not carry any water vapour.) The relative humidity is reduced by 30 to 40% at 300mb in the extratropics and at 250mb in the tropics.

Several factors may be responsible for the build up of moisture at upper levels. Since very few routine observations are made at stratospheric heights the analysis is largely determined by the model's climatology. The model's advection equations poorly handle large gradients of specific humidity in both the vertical and horizontal directions. The finite difference procedure may produce negative values which have to be reset to zero in a globally conservative way. The model convection scheme may also detrain relatively large quantities of water vapour at upper levels where convection is curtailled. The net effect of these processes can be seen in figure A3 of the differences in relative humidity between a 3-day forecast and the initial analysis (after setting the stratospheric humidities). The increases at upper levels are very similar to the excess humidity removed by initialising (Figure A2). The evolution of the global mean relative humidity (Figure A4) shows the most rapid increase occurs over the first day. In view of this it is recommended that the upper level humidities be re-initialised daily.

References.

Bell, R S 1986 The global impact of the recent developments of the physical parametrisation schemes. Met O 11 Technical Note No 243

Bell, R S 1987 Report to WGDOS on results of second trial of the new coarse- mesh physics package.

Bell R S and A Dickinson 1987
The Meteorological Office operational weather prediction system. Meteorological Office Scientific Paper No.41, London:H.M.S.O.

Black, T L and Z I Janjic 1988
Preliminary forecast results for a step mountain eta coordinate regional model. In preprints from Eighth Conference on Numerical Weather Prediction. February 22-26,1988, Baltimore, Maryland. p442-447.

Burridge, D M, K Miyakoda and R Sadourny 1986 Review of the influence of model formulation (parameterisations and numerical treatment) on model errors. Appendix B to Report of second session of CAS/JSC Working Group on Numerical Experimentation, Japan,Meteorological Agency, Tokyo, Japan. 11-15 August,1986.

Coiffier J, Y Ernie, J-F Geleyn,J Clochard, J Hoffman and F Dupont 1987 The operational model at the French Meteorological Service.In Short and Medium Range Numerical Weather Prediction (ed. T Matsuno)- papers presented at WMO/IUGG NWP Symposium, Tokyo, Japan,4-8 August,1986. p337-345.

Foreman, S J 1982 Modifications of the new operational model to reduce cooling in the tropics. Met O 11 Working Paper No 44.

Hammon, O and C A Wilson 1987
Results from a fine-mesh model trial using a modified and evaporation scheme. Met O 11 Technical Note No 263

Harshvardhan and D Randall 1986
Cloud and radiation experiments with a general circulation model. 6th Conference on Atmospheric Radiation,AMS,44-47.

Harshvardhan, R Davies, D Randall, and T G Corsetti 1987
A fast radiation parameterization for Atmospheric Circulation Models. J. Geophys. Res. 92,1009-1016.

Kitchen, J E 1985 An implicit version of the operational boundary layer routine. Met O 11 Technical note No 222.

Lilly 1968 Models of cloud-topped mixed layers under a strong inversion. Q.J.R.Met.Soc. **94**,292-309.

Luther, F M, R G Ellingson, Y Fouquart, S Fels, N A Scott and W J Wiscombe 1988 Intercomparison of radiation codes in climate models (ICRCCM) results - a workshop summary. Bull. Amer. Met. Soc.,**69**, 40-48.

McClatchey, R A et al 1973 'AFCRL atmospheric absorption line parameters compilation',Bedford, Mass., Air Force Cambridge Research Labs. Enviromental Research Papers, No 434, AFCRL-TR-0096.

Mitchell, J F B, C A Wilson and W M Cunnington 1987 On CO_2 climate sensitivity and model dependence of results. Q.J.R. Met. Soc. **113**, p223-323.

NOAA - National Weather Service 1987 Temperature calculations in the nested grid model. Technical Procedures Bulletin No 373.

Puri, K and D J Gauntlett 1987 Numerival weather prediction in the Tropics.In Short and Medium Range Numerical Weather Prediction (ed. T Matsuno) - papers presented at WMO/IUGG NWP Symposium, Tokyo, Japan,4-8 August,1986. p605-631.

Roach, W T, J S Foot, F Rawlins and C G Kilsby 1988 Radiative transfer studies at the Meteorological Research Flight. MRF Internal Note No. 46.

Randall, D A 1980 Entrainment into a stratocumulus layer with distributed radiative heating. J. Atmos. Sci. **37**,148-149.

Slingo, A 1985 Handbook of the Meteorological Office 11-layer atmospheric general circulation model. DCTN 29.

Slingo, J M 1987 The development and verification of a cloud prediction scheme for the ECMWF model. Q.J.R.Met.Soc. **113**,899-927.

Slingo, A and D W Pearson 1987 A comparison of the impact of envelope orography and of a parametrization of gravity-wave drag on model simulations.Q.J.R. Met. Soc. **113**, p847-871.

Slingo, A, R Brown and C L Wrench 1982 A field study of nocturnal stratocumulus: III. High

resolution radiative and microphysical observations. Q.J.R.Met.Soc. **108**,145-165.

Stephens, G L 1984 The parameterization of radiation for numerical weather prediction and climate models. Mon. Wea. Rev. **112**, 826-867.

Tiedtke, M, W A Heckley and J Slingo 1988 Tropical forecasting at ECMWF: On the influence of physical parameterisation on the mean structure of the forecasts and analyses. Q.J.R.Met.Soc.,**114**,638-664.

White, G H 1988 Systematic performance of the NMC dynamical extended range forecasts. In preprints from Eighth Conference on Numerical Weather Prediction. February 22-26,1988, Baltimore, Maryland. p855-860.

Willmott, C J, C M Rowe and Y Mintz 1985 Climatology of the terrestial seasonal water cycle. J. Climatol. **5**,589-606.

Wilson C A and J F B Mitchell 1987 A doubled CO_2 climate sensitivity experiment with a global climate model including a simple ocean. J. Geophys. Res. **92**, 13,315-13,343.

TABLE 1.

Verification against observations at T+72 :case DT 12Z 13/6/85. (c=control, t2=trial2)

	Mean errors						R.m.s. errors					
	N.hem		Tropics		S.hem		N.hem		Tropics		S.hem	
T+72	c	t2	c	t2	c	t2	c	t2	c	t2	c	t2
pmsl												
land	-3.1	-2.7	-1.0	-0.8	0.8	-0.9	6.1	5.7	3.9	3.5	4.0	4.0
sea	-1.7	-2.3	0.0	-0.2	2.2	0.9	4.7	4.7	3.3	3.5	6.7	6.5
hts												
850mb	-2.5	-2.8	-1.6	-1.7	0.7	-0.5	4.3	4.5	3.1	2.9	3.1	3.2
700mb	-2.9	-3.7	-1.9	-2.3	-0.4	-1.6	4.5	5.1	2.9	3.3	3.5	4.2
500mb	-3.2	-5.0	-1.9	-3.3	-2.2	-3.3	5.5	6.6	3.1	4.3	5.0	5.9
250mb	-2.4	-5.6	-1.7	-4.9	-2.2	-3.6	6.6	8.5	4.7	6.8	6.7	7.4
100mb	-4.2	-8.2	-2.3	-5.0	-7.6	-8.6	6.5	9.8	7.2	8.5	8.6	9.7
temps												
850mb	-0.8	-1.6	-0.4	-1.3	-0.8	-1.1	3.3	3.2	2.4	2.7	3.5	3.4
700mb	-0.7	-1.8	-0.6	-1.4	-2.8	-2.8	2.7	3.0	2.2	2.3	3.3	3.4
500mb	-0.1	-1.0	0.1	-0.6	-1.9	-1.7	2.3	2.3	1.7	1.8	3.0	3.0
250mb	1.2	0.5	0.1	-0.7	1.2	1.0	3.5	3.1	2.1	2.1	2.9	3.6
100mb	-0.3	0.0	2.0	2.8	-0.9	-0.5	2.3	2.4	4.0	4.5	3.7	3.5
wind												
850mb							14.6	13.8	14.2	12.9	14.7	14.6
700mb							13.7	13.4	13.2	12.2	19.0	20.1
500mb							16.1	15.8	14.4	14.8	22.3	23.5
250mb							25.0	24.6	19.3	20.9	27.1	30.5

N.B. N.hem = north of 30° N
Tropics = 30° N - 30° S
S.hem = south of 30° S

TABLE 2.

Verification against observations at T+120 :case DT 12Z 13/6/85. (c=control, t2=trial2)

	Mean errors						R.m.s. errors					
	N.hem		Tropics		S.hem.		N.hem.		Tropics		S.hem.	
T+72	c	t2	c	t2	c	t2	c	t2	c	t2	c	t2
pmsl												
land	-1.2	-1.2	-1.3	-0.9	3.5	1.5	6.3	5.9	3.8	3.6	8.3	7.5
sea	-3.0	-3.6	-0.5	-0.9	4.9	3.2	7.1	6.9	3.3	3.5	10.7	10.3
hts												
850mb	-1.5	-2.6	-1.8	-2.2	1.1	0.0	4.7	5.2	3.1	3.4	8.7	7.4
700mb	-1.9	-3.5	-1.8	-2.8	-0.8	-2.0	5.0	6.0	2.9	3.9	8.9	8.4
500mb	-2.2	-4.9	-1.8	-4.1	-3.2	-4.4	6.1	7.7	3.3	5.3	10.9	11.2
250mb	-2.0	-6.3	-1.5	-6.0	-4.0	-4.8	8.0	10.7	4.9	7.7	14.1	15.5
100mb	-2.7	-8.5	-2.7	-6.3	-9.4	-9.5	6.9	11.0	6.3	8.7	12.0	12.2
temps												
850mb	-0.9	-1.8	-0.2	-1.3	-1.5	-1.5	3.7	3.8	2.7	3.1	3.0	3.3
700mb	-0.4	-1.6	-0.5	-1.7	-3.3	-2.9	2.7	3.2	2.5	2.8	5.3	5.5
500mb	-0.5	-1.4	0.0	-0.9	-0.7	-0.9	2.6	3.1	1.8	1.9	3.3	3.6
250mb	1.3	0.2	0.3	-0.5	-0.6	-0.3	4.0	3.9	1.9	2.1	3.5	3.1
100mb	-0.1	0.7	1.8	3.2	-1.1	-0.4	2.4	2.7	3.5	4.3	3.5	3.7
wind												
850mb							17.1	17.7	15.4	14.9	27.4	27.1
700mb							16.9	17.8	16.2	16.9	24.5	23.7
500mb							20.7	21.6	17.1	18.5		
250mb							28.1	31.5	23.3	24.3	36.5	34.5

N.B. N.hem = north of 30° N
Tropics = 30° N - 30° S
S.hem = south of 30° S

TABLE 3.

Verification against observations at T+72, T+120 :case DT 12Z 13/6/85. As trial2 but with **geographical distribution of soil moisture, evaporation of rain dependent upon rainfall rate, reduced solar constant, medium cloud height dependent upon latitude and global mass conservation.**

	Mean errors			R.m.s. errors			Mean errors			R.m.s. errors		
	N.H	T.	S.H	N.H	T.	S.H	N.H	T.	S.H	N.H	T.	S.H
	T+72						T+120					
pmsl												
land	-1.8	-0.2	-0.3	5.3	3.5	3.8	0.2	0.0	2.6	5.7	3.3	7.6
sea	-1.5	0.5	1.3	4.2	3.1	6.5	-2.3	0.0	4.3	6.2	3.2	10.2
hts												
850mb	-1.9	-1.1	0.0	4.0	2.6	3.0	-1.2	-1.2	0.9	4.5	2.7	7.0
700mb	-2.7	-1.8	-0.9	4.3	2.9	3.8	-2.0	-1.8	-0.8	5.1	3.2	7.8
500mb	-3.8	-2.8	-2.3	5.6	3.8	3.2	-3.0	-3.2	-2.8	6.4	4.7	10.2
250mb	-3.8	-4.0	-1.9	7.2	6.1	7.2	-3.8	-4.6	-1.9	9.1	6.7	14.1
100mb	-7.3	-3.1	-9.1	9.0	7.4	10.0	-7.3	-3.9	-9.6	10.4	7.3	12.1
temps												
850mb	-1.5	-1.2	-0.9	3.3	2.7	3.5	-1.5	-1.2	-1.1	3.6	3.0	2.9
700mb	-1.6	-1.3	-2.4	2.9	2.4	3.0	-1.3	-1.7	-2.6	3.0	2.7	4.9
500mb	-0.6	-0.7	-1.6	2.2	1.8	2.9	-0.8	-1.1	-0.6	2.7	2.1	3.3
250mb	1.0	0.1	1.9	3.4	2.2	3.6	0.6	0.5	1.5	4.0	2.4	3.4
100mb	-0.4	1.7	-0.8	2.6	4.0	3.7	-0.1	1.9	-1.2	2.9	3.5	4.2
wind												
850mb				14.2	13.5	14.6				17.3	14.7	26.7
700mb				13.5	12.7	20.3				17.2	16.3	24.6
500mb				16.1	15.3	23.6				20.3	18.5	
250mb				24.8	21.4	29.4				29.7	25.2	37.4

N.B. N.H = north of 30° N
T. = 30° N - 30° S
S.H = south of 30° S

TABLE 4
Maximum cloud top heights (σ_{H+M}) in revised cloud scheme.

Latitude	C_L	C_M	C_H
$\leq 30°$	.736	.366	.116
30° - 60°	.816	.456	.166
60° - 90°	.816	.546	.276

TABLE 5.

Verification against observations at T+72 : case DT 12Z 13/6/85. As Table2 but with **new levels, convection allowed from level 1 ,new cloud scheme with cloud placed in layers and diffusion at low cloud top..**

	Mean errors			R.m.s. errors		
	N.H	T.	S.H	N.H	T.	S.H
T+72						
pmsl						
land	-1.7	-0.7	-0.2	5.2	3.5	3.7
sea	-1.3	-0.2	1.3	4.1	3.0	6.3
hts						
850mb	-1.8	-1.5	0.5	3.9	2.7	3.0
700mb	-2.6	-2.0	-0.3	4.3	3.0	3.7
500mb	-3.5	-2.5	-1.8	5.4	3.7	5.0
250mb	-3.8	-3.6	-2.2	7.0	5.8	6.7
100mb	-4.7	1.0	-5.6	7.5	6.6	6.7
temps						
850mb	-1.5	-1.1	-0.6	3.5	3.2	3.4
700mb	-1.2	-0.8	-2.0	2.8	2.2	3.0
500mb	-0.3	0.0	-1.2	1.6	1.8	1.7
250mb	1.0	0.7	1.4	3.3	2.0	2.6
100mb	1.3	5.5	1.1	2.7	6.4	3.5
wind						
850mb				14.2	13.5	15.0
700mb				13.7	12.9	20.6
500mb				16.5	14.9	24.3
250mb				24.5	20.5	29.4

N.B. N.H = north of 30° N
T. = 30° N - 30° S
S.H = south of 30° S

TABLE 6.

Verification against observations at T+72 : case DT 12Z 13/6/85. As Table5 but with **global conservation of mass-weighted temperature in each model layer.**

	Mean errors			R.m.s. errors		
	N.H	T.	S.H	N.H	T.	S.H
T+72						
pmsl						
land	-2.1	-0.7	-0.3	5.5	3.5	3.9
sea	-1.5	0.1	1.4	4.3	3.1	6.4
hts						
850mb	-1.5	-1.0	-0.8	3.9	2.6	3.0
700mb	-2.0	-1.3	0.4	4.0	2.6	3.7
500mb	-2.4	-1.6	-0.9	4.8	3.1	4.7
250mb	-1.0	-1.5	0.3	6.0	4.8	6.3
100mb	-1.7	3.5	-3.6	6.1	7.4	4.6
temps						
850mb	-0.3	-0.1	-0.7	3.2	2.7	3.7
700mb	-0.7	-0.6	-1.8	2.6	2.1	2.7
500mb	0.0	-0.1	-1.0	2.2	1.6	2.6
250mb	1.9	0.0	2.4	3.6	2.6	3.1
100mb	1.1	5.4	1.0	2.6	6.3	3.5
wind						
850mb				14.6	13.8	15.2
700mb				14.0	13.4	20.4
500mb				16.6	15.4	24.0
250mb				24.6	20.1	28.6

N.B. N.H = north of 30° N
T. = 30° N - 30° S
S.H = south of 30° S

FIGURES

Figure 1 Zonal mean differences of height (upper) and temperature (lower) for a)T+72, b)T+120 control forecast and verifying analysis for case DT 12Z 13/06/87. Contours every 1 X 10m and every 0.5K, negative differences shaded. N.B. Extrapolation above 100mb.

Figure 2 As Figure 1 but for Trial2 forecast.

Figure 3 Global mean temperature increments for day 1 from each process : a) operational model ,b) previous trial.

Figure 4 As Figure 2 but with revised package as described in section 2 : T+120

Figure 5 Global mean temperature increments for day 1 from convection showing effect of allowing convection to be initiated from level 1.

Figure 6 Fluxes and entrainment in the convection scheme.

Figure 7 Global mean temperature increments for day 1 from convection showing effect of changing levels.

Figure 8 Clear sky heating rates for a tropical atmosphere.

Figure 9 Contributions of layers and half-layers to the infra-red flux calculation. (Shown here for 11 layers as in the Met O 20 climate model.)

Figure 10 Global mean temperature increments for day 1 from radiation showing effect of amendments to code and new cloud scheme.

Figure 11 As Figure 2 but with revised package as described in section 2, new levels, convection allowed from level1 and corrections to radiation code : T+120

Figure 12 Vertical placement of clouds and schematic heating rates.

Figure 13 Low cloud forecast at T+72 for a) old cloud scheme, b) new cloud scheme. Contours every 20%, shaded >40% ; c) Meteosat infrared picture at verification time.

Figure 14 Accumulated precipitation for day 3 produced dynamically in forecast with new cloud scheme. Contours every 2 mm d^{-1}, horizontal shading 4 to 10 mm d^{-1}, dotted shading >10 mm d^{-1}.

Figure 15 Accumulated precipitation for day 3 produced dynamically in forecast with new cloud scheme with extra diffusion at low cloud top. Contours and shading as in figure 14.

Figure 16 Low cloud forecast at T+72 for new cloud scheme with extra diffusion at low cloud top. Contours every 20%, shaded >40% .

Figure 17 As Figure 2 but with final revised package including new cloud scheme with extra diffusion at low cloud top : T+72.

Figure 18 As Figure 8 but showing the effects of different treatments of the water vapour continuum.

Figure 19 As Figure 17 but omitting the water vapour continuum term.

Figure 20 As Figure 17 but with global conservation of mass-weighted temperature in each layer.

Figure 21 As Figure 17 but with global conservation of mass-weighted temperature in each layer and resetting upper level humidities every 24 hours.

Figure A1 Zonal mean relative humidities for initial analysis: a) uninitialised at upper levels, b) initialised .

Figure A2 Zonal mean differences of relative humidity : initialised-uninitialised analyses.

Figure A3 Zonal mean differences of relative humidity : 3-day forecast-initialised analysis.

Figure A4 Evolution of global mean relative humidities at upper levels during a 3-day forecast following initialisation.

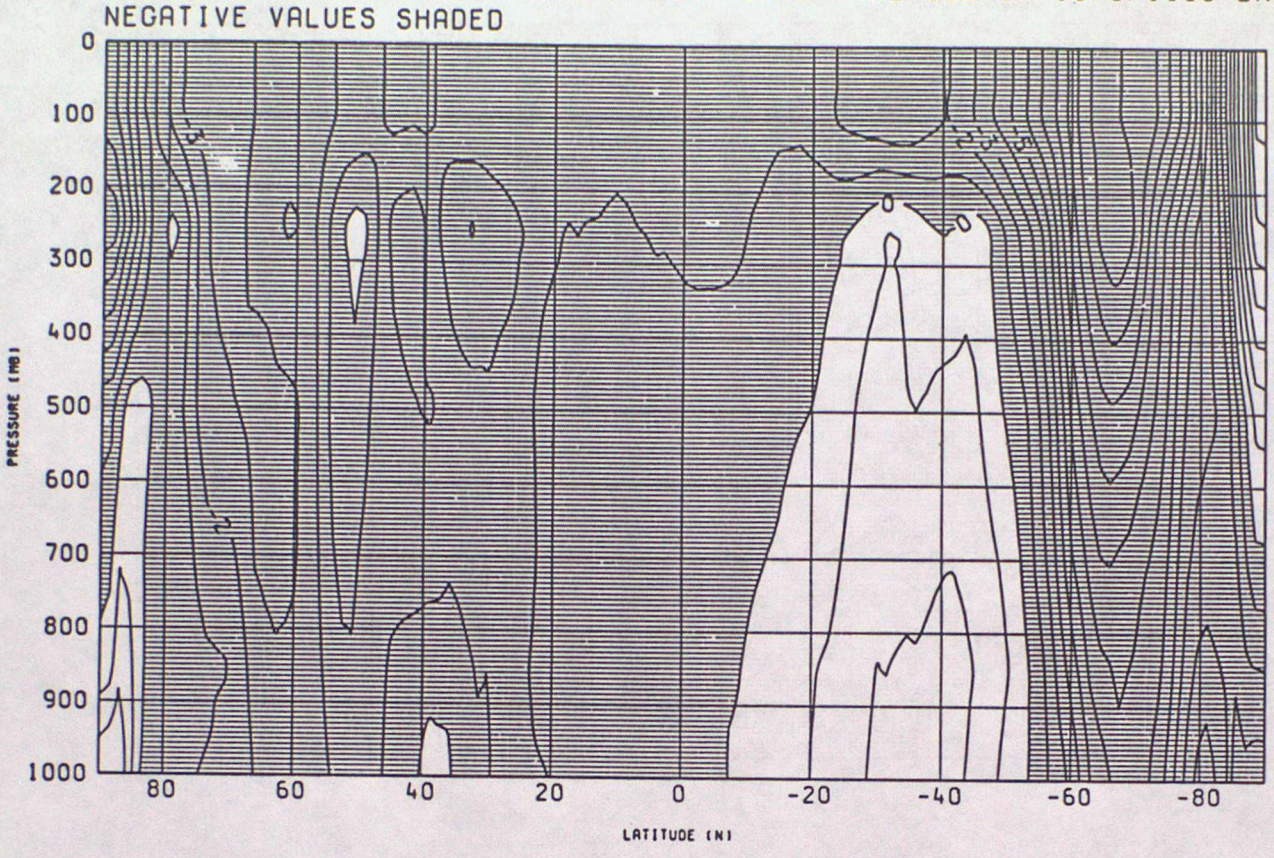
1SUM CASE.CONTROL-VER
HEIGHT
ZONAL MEAN DIFFERENCE
VALID AT 12Z ON 16/6/1985 DAY 167 DATA TIME 12Z ON 13/6/1985 DAY 164
NEGATIVE VALUES SHADED
PRESSURE (MB)
0
100
200
300
400
500
600
700
800
900
1000
80
60
40
20
0
-20
-40
-60
-80
LATITUDE (N)

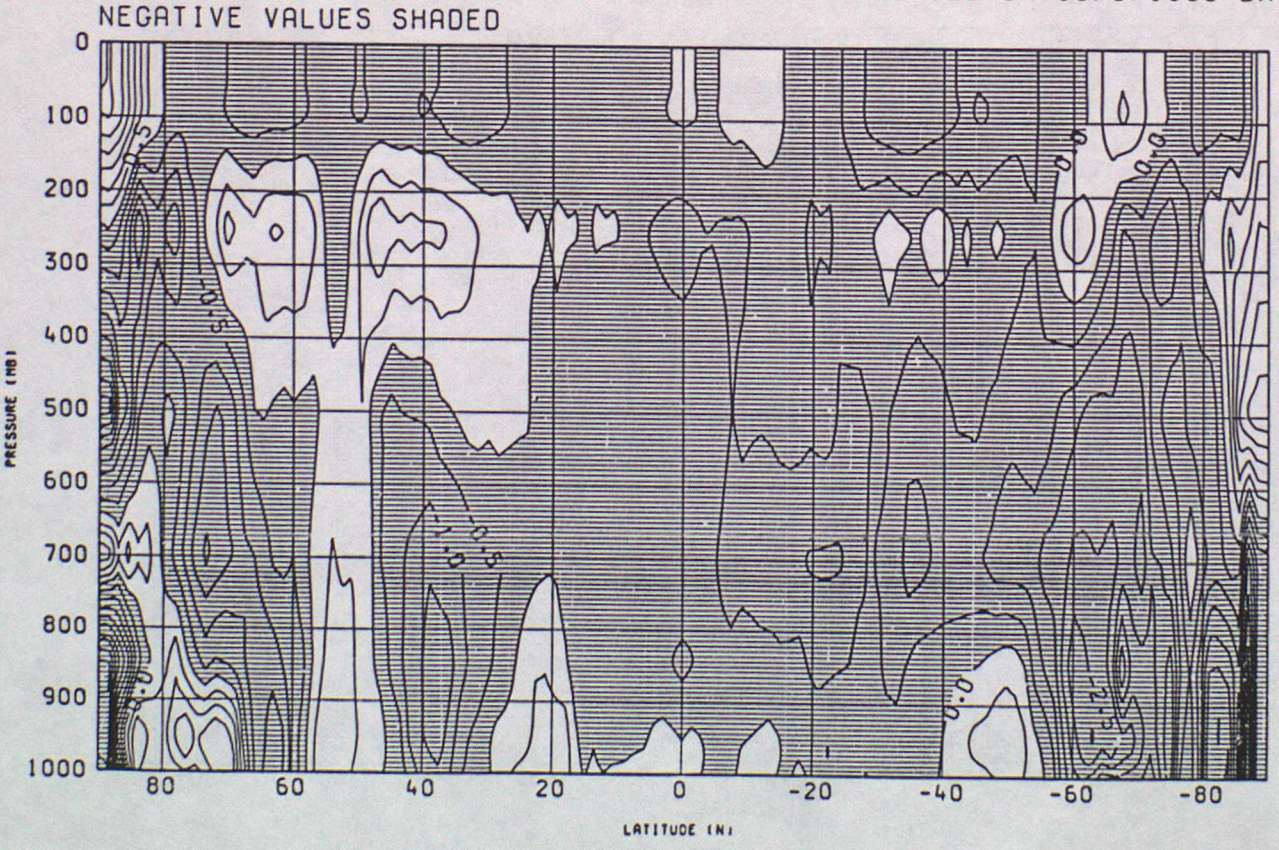
1SUM CASE.CONTROL-VER
TEMPERATURE
ZONAL MEAN DIFFERENCE
VALID AT 12Z ON 16/6/1985 DAY 167 DATA TIME 12Z ON 13/6/1985 DAY 164
NEGATIVE VALUES SHADED
PRESSURE (MB)
0
100
200
300
400
500
600
700
800
900
1000
80
60
40
20
0
-20
-40
-60
-80
LATITUDE (N)

Figure 1a

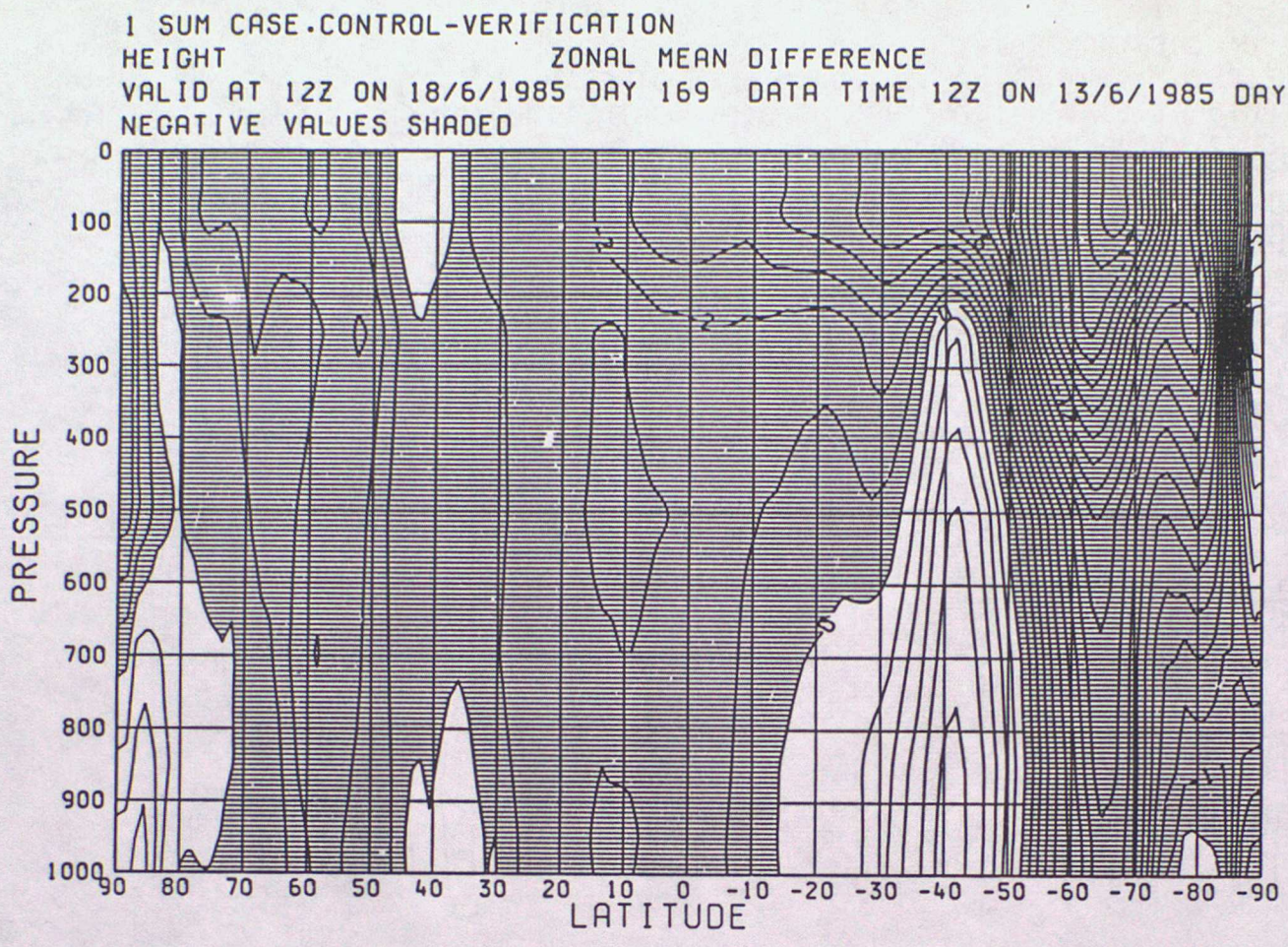
1 SUM CASE.CONTROL-VERIFICATION
HEIGHT ZONAL MEAN DIFFERENCE
VALID AT 12Z ON 18/6/1985 DAY 169 DATA TIME 12Z ON 13/6/1985 DAY 164
NEGATIVE VALUES SHADED
PRESSURE
0
100
200
300
400
500
600
700
800
900
1000
90 80 70 60 50 40 30 20 10 0 -10 -20 -30 -40 -50 -60 -70 -80 -90
LATITUDE

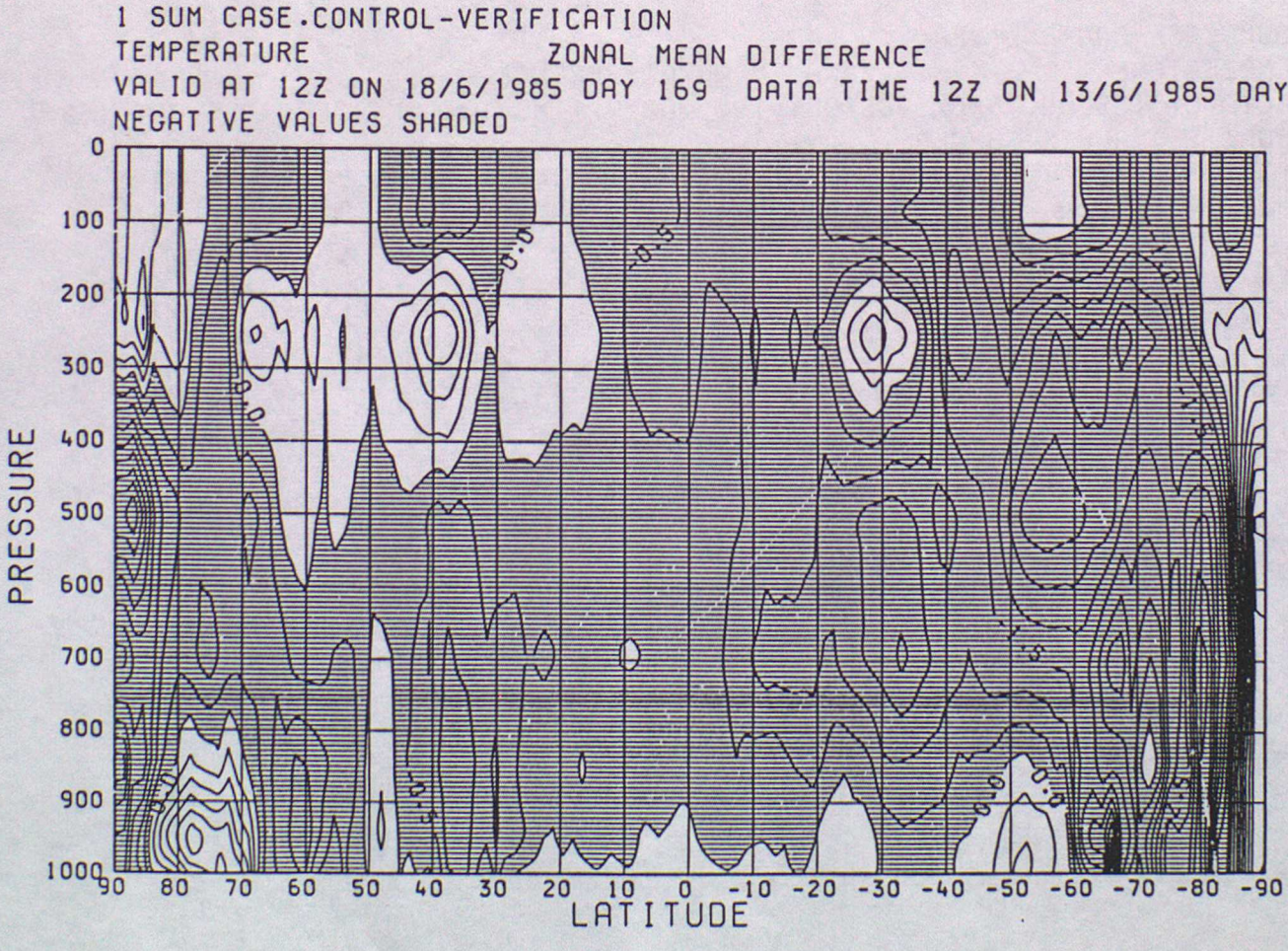
1 SUM CASE.CONTROL-VERIFICATION
TEMPERATURE ZONAL MEAN DIFFERENCE
VALID AT 12Z ON 18/6/1985 DAY 169 DATA TIME 12Z ON 13/6/1985 DAY 164
NEGATIVE VALUES SHADED
PRESSURE
0
100
200
300
400
500
600
700
800
900
1000
90 80 70 60 50 40 30 20 10 0 -10 -20 -30 -40 -50 -60 -70 -80 -90
LATITUDE

Figure 1b

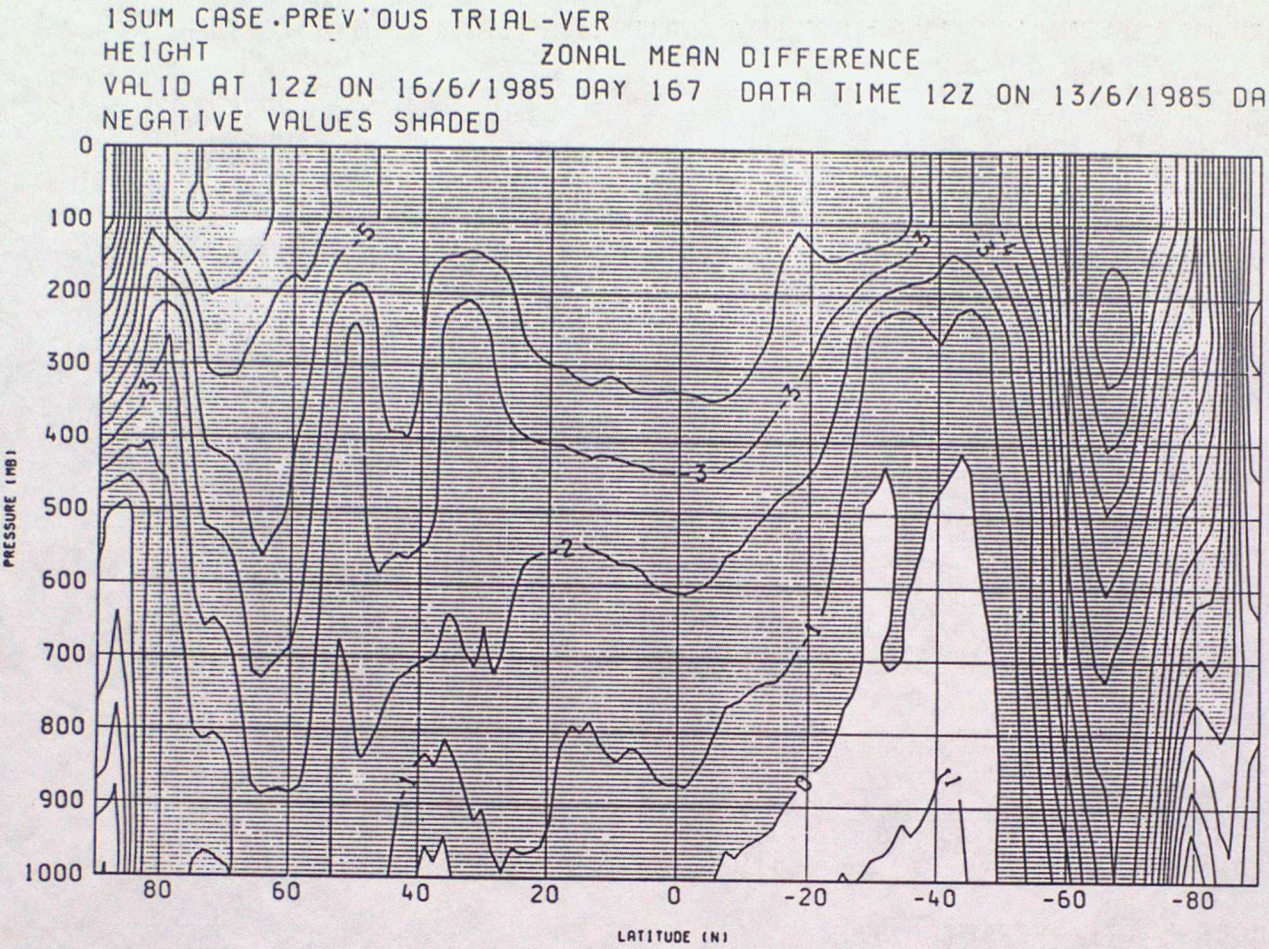
1SUM CASE.PREV'OUS TRIAL-VER
HEIGHT ZONAL MEAN DIFFERENCE
VALID AT 12Z ON 16/6/1985 DAY 167 DATA TIME 12Z ON 13/6/1985 DAY 164
NEGATIVE VALUES SHADED
PRESSURE (MB)
LATITUDE (N)

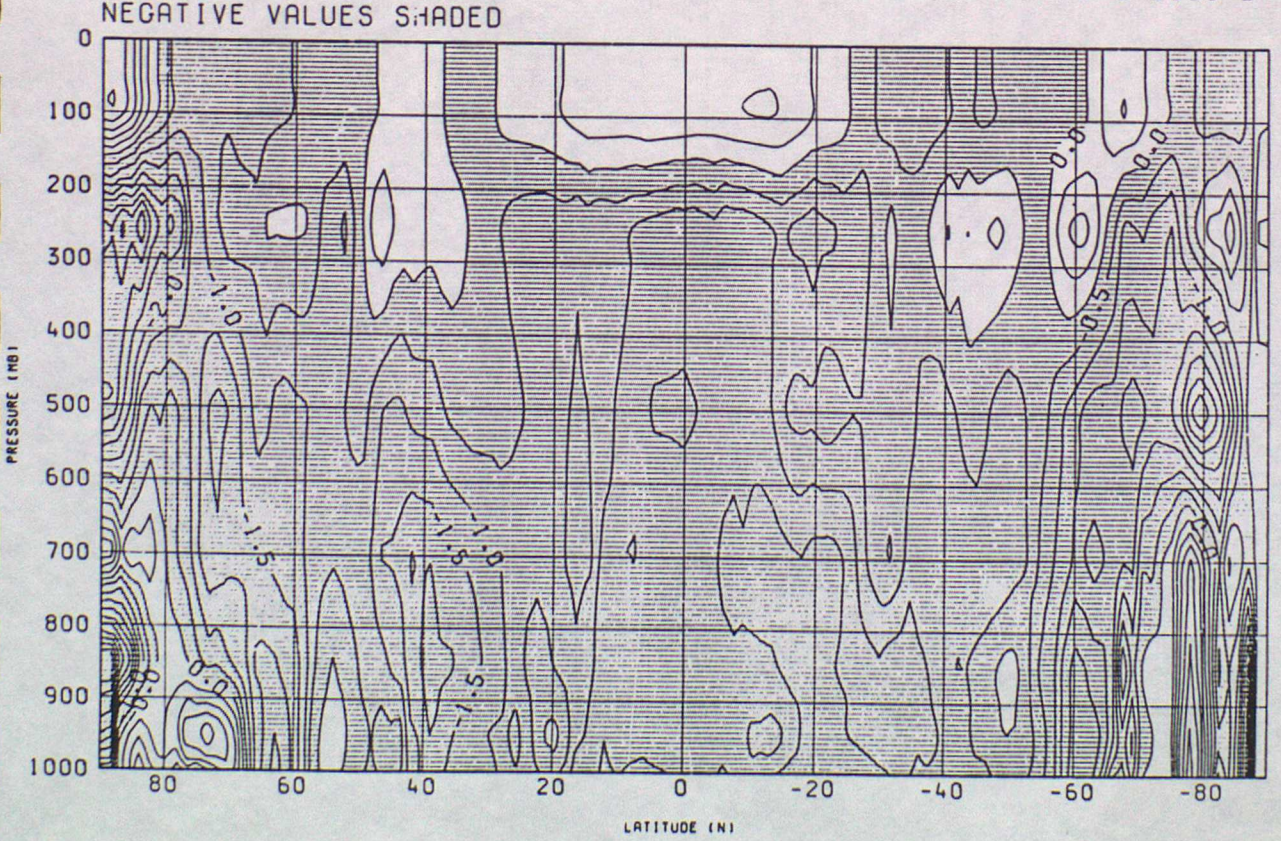
1SUM CASE.PREVIOUS TRIAL-VER
TEMPERATURE ZONAL MEAN DIFFERENCE
VALID AT 12Z ON 16/6/1985 DAY 167 DATA TIME 12Z ON 13/6/1985 DAY 164
NEGATIVE VALUES SHADED
PRESSURE (MB)
LATITUDE (N)

Figure 2a

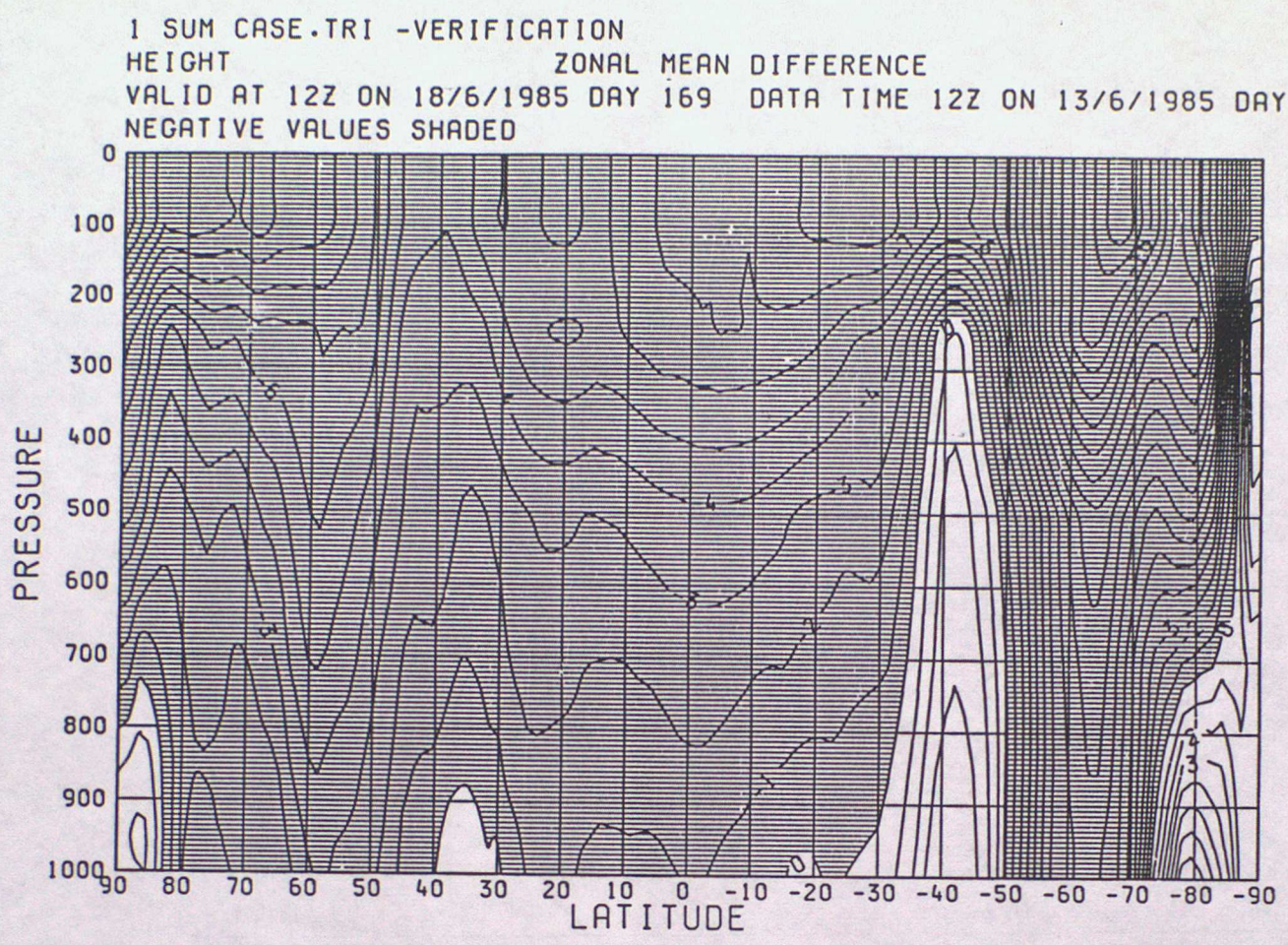
1 SUM CASE.TRI -VERIFICATION
HEIGHT ZONAL MEAN DIFFERENCE
VALID AT 12Z ON 18/6/1985 DAY 169 DATA TIME 12Z ON 13/6/1985 DAY 164
NEGATIVE VALUES SHADED
PRESSURE
0
100
200
300
400
500
600
700
800
900
1000
90 80 70 60 50 40 30 20 10 0 -10 -20 -30 -40 -50 -60 -70 -80 -90
LATITUDE

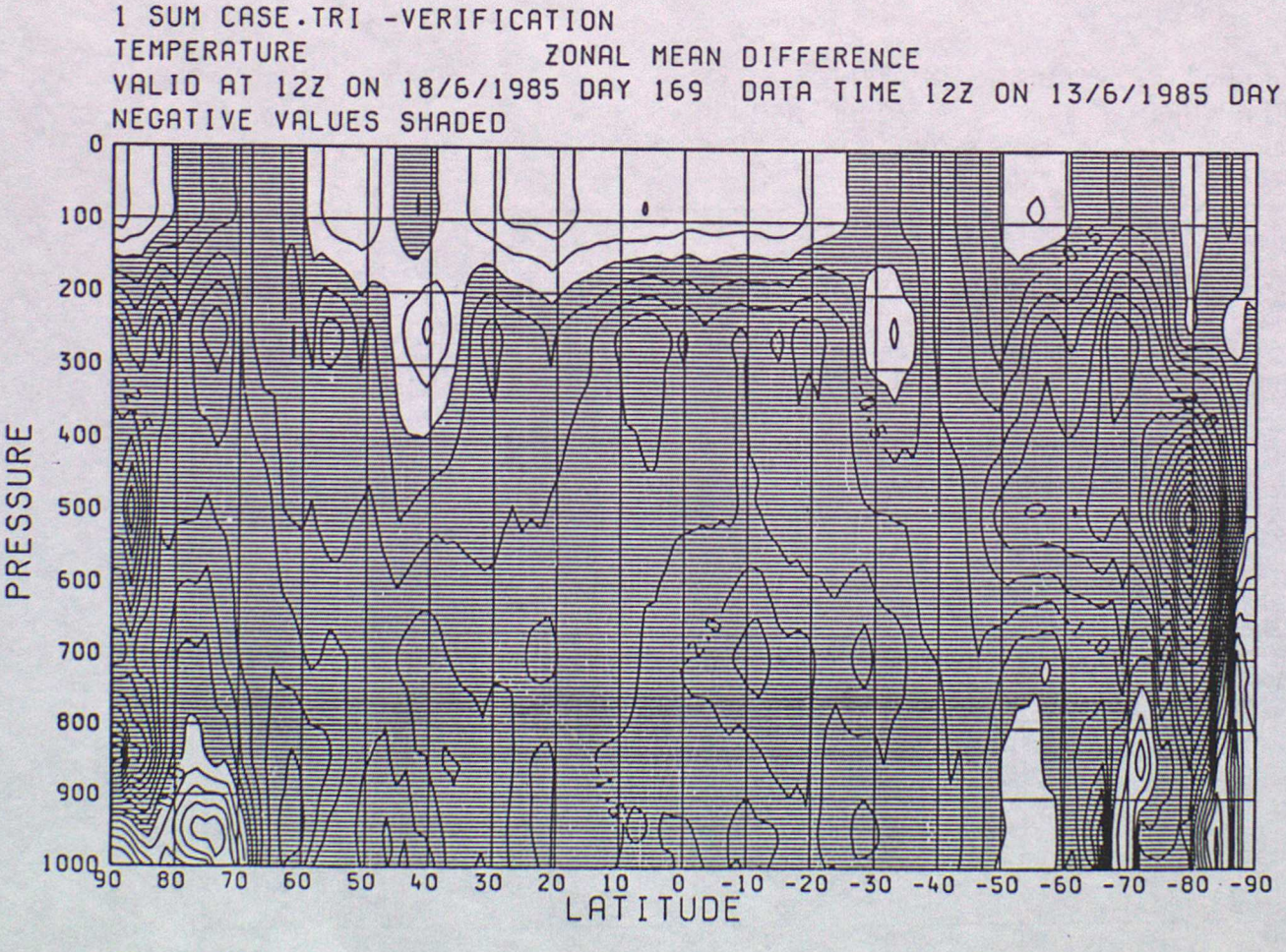
1 SUM CASE.TRI -VERIFICATION
TEMPERATURE ZONAL MEAN DIFFERENCE
VALID AT 12Z ON 18/6/1985 DAY 169 DATA TIME 12Z ON 13/6/1985 DAY 164
NEGATIVE VALUES SHADED
PRESSURE
0
100
200
300
400
500
600
700
800
900
1000
90 80 70 60 50 40 30 20 10 0 -10 -20 -30 -40 -50 -60 -70 -80 -90
LATITUDE

Figure 2b

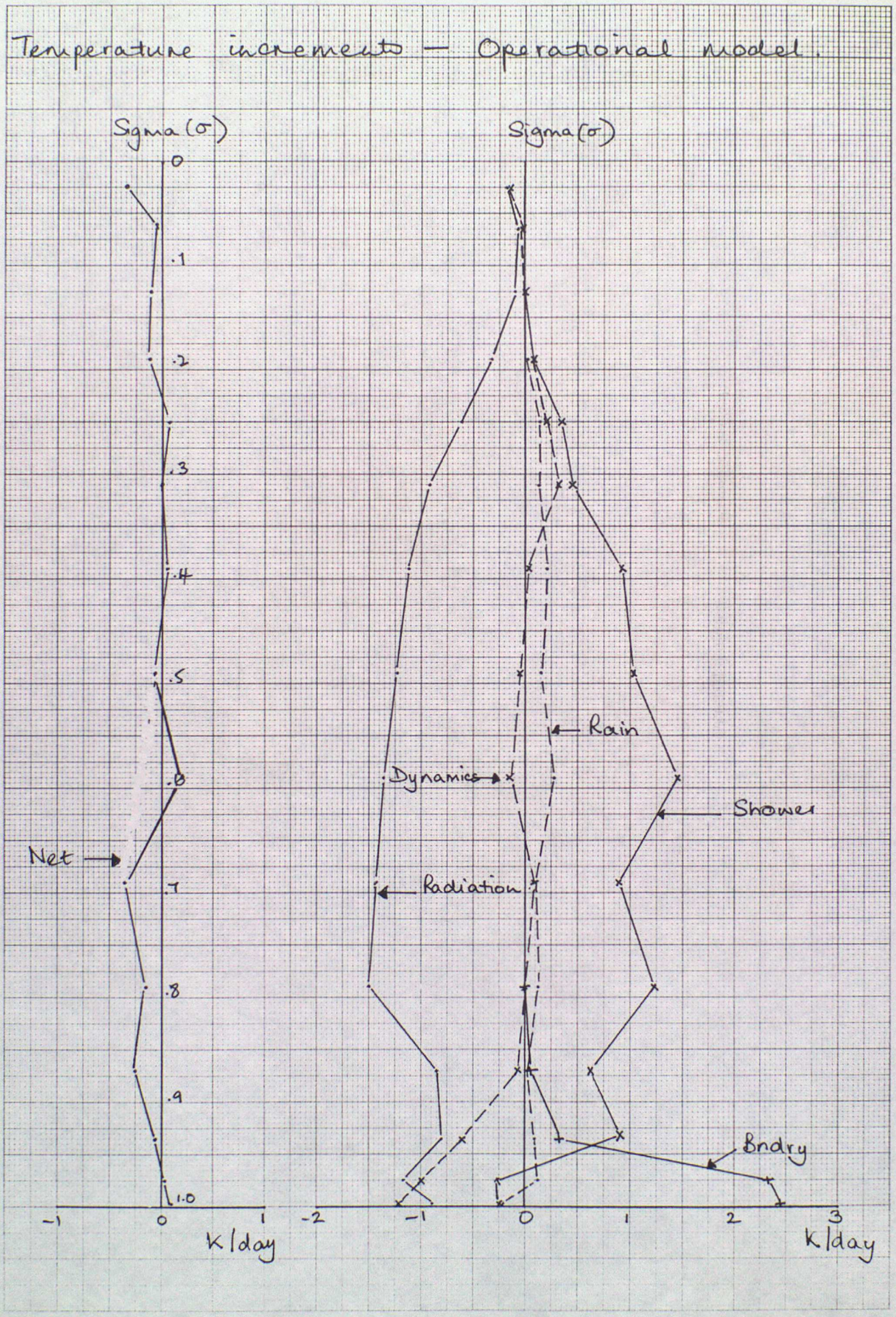

Figure 3a

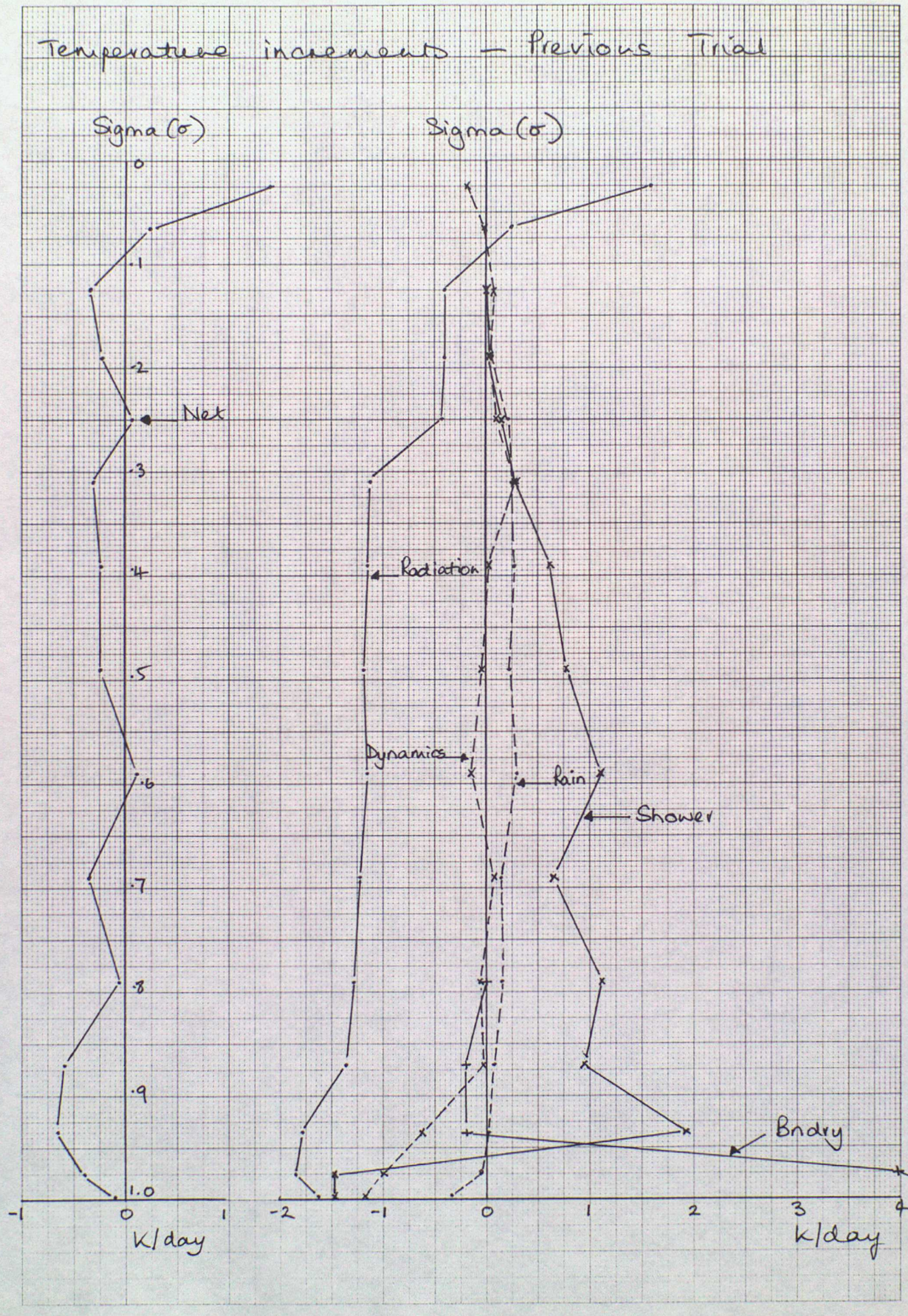

Figure 3b

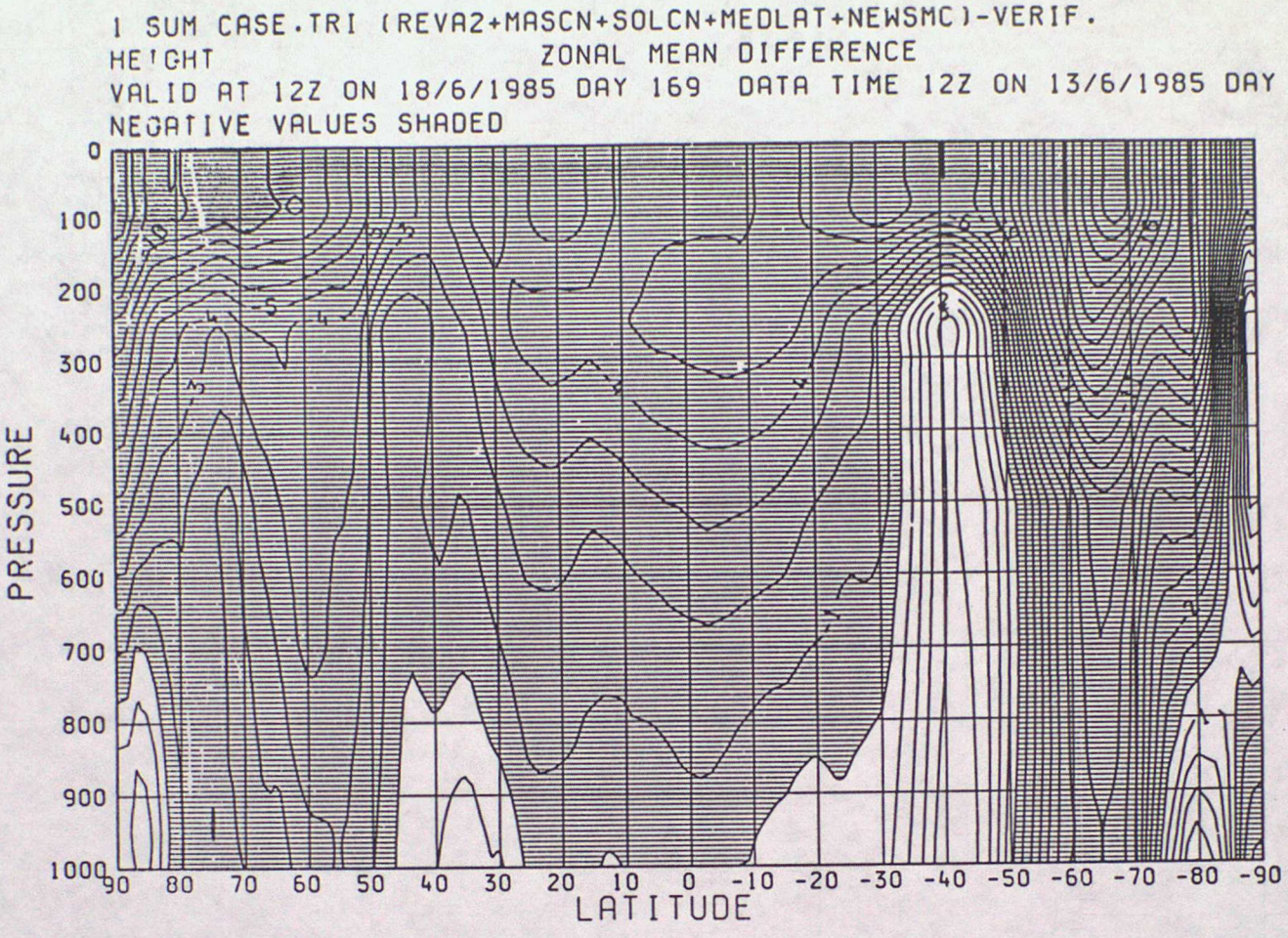
1 SUM CASE.TRI (REVA2+MASCN+SOLCN+MEDLAT+NEWSMC)-VERIF.
HEIGHT ZONAL MEAN DIFFERENCE
VALID AT 12Z ON 18/6/1985 DAY 169 DATA TIME 12Z ON 13/6/1985 DAY 164
NEGATIVE VALUES SHADED
PRESSURE
0
100
200
300
400
500
600
700
800
900
1000
90 80 70 60 50 40 30 20 10 0 -10 -20 -30 -40 -50 -60 -70 -80 -90
LATITUDE

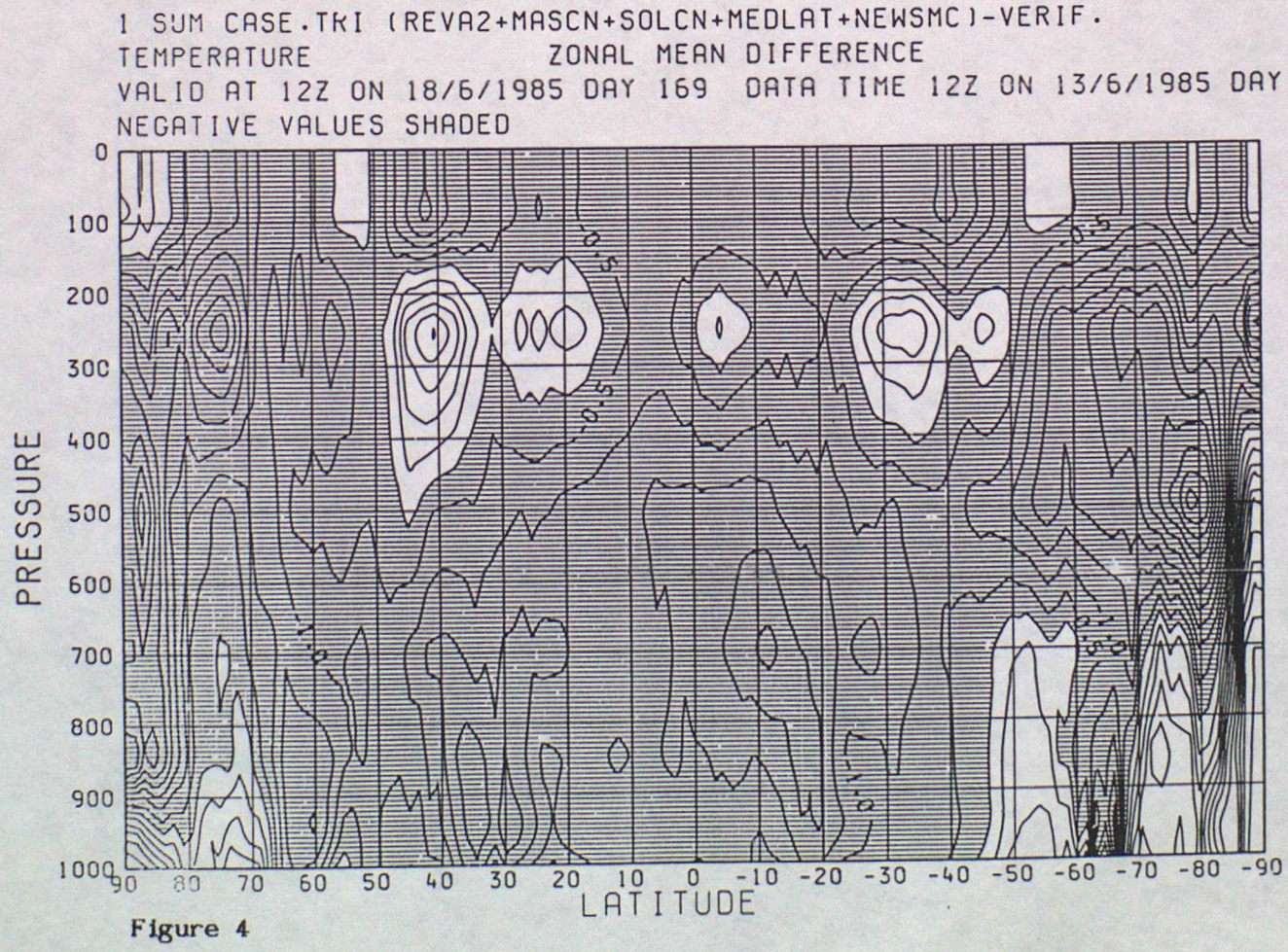
1 SUM CASE.TRI (REVA2+MASCN+SOLCN+MEDLAT+NEWSMC)-VERIF.
TEMPERATURE ZONAL MEAN DIFFERENCE
VALID AT 12Z ON 18/6/1985 DAY 169 DATA TIME 12Z ON 13/6/1985 DAY 164
NEGATIVE VALUES SHADED
PRESSURE
0
100
200
300
400
500
600
700
800
900
1000
90 80 70 60 50 40 30 20 10 0 -10 -20 -30 -40 -50 -60 -70 -80 -90
LATITUDE

Figure 4

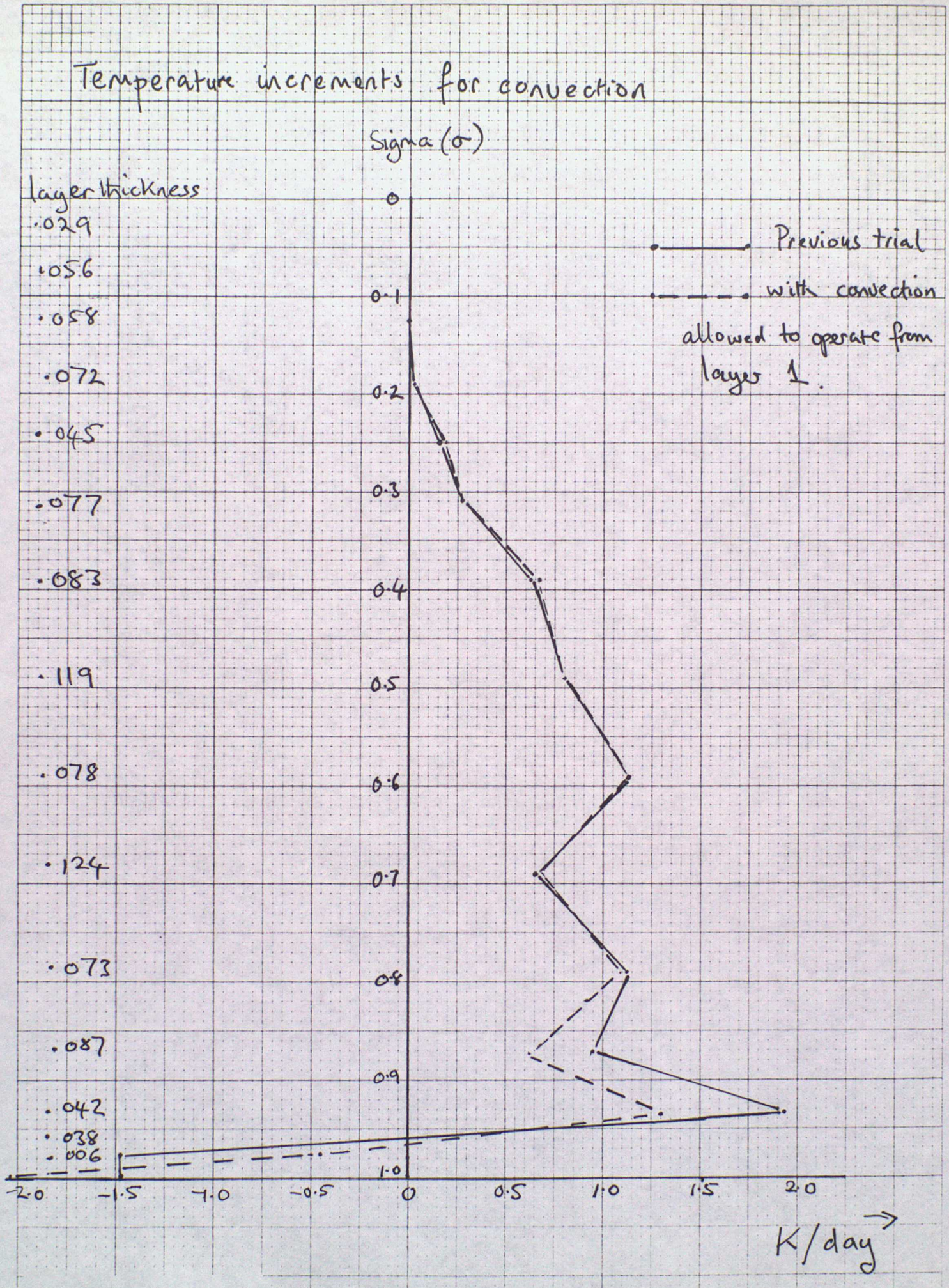
Temperature increments for convection
Sigma (σ)
layer thickness
.029
.056
.058
.072
.045
.077
.083
.119
.078
.124
.073
.087
.042
.038
.006
0
0.1
0.2
0.3
0.4
0.5
0.6
0.7
0.8
0.9
1.0
Previous trial
with convection allowed to operate from layer 1.
-2.0
-1.5
-1.0
-0.5
0
0.5
1.0
1.5
2.0
K/day

Figure 5

Vertical fluxes and entrainment in the convection scheme (forced and mixing detrainment omitted)

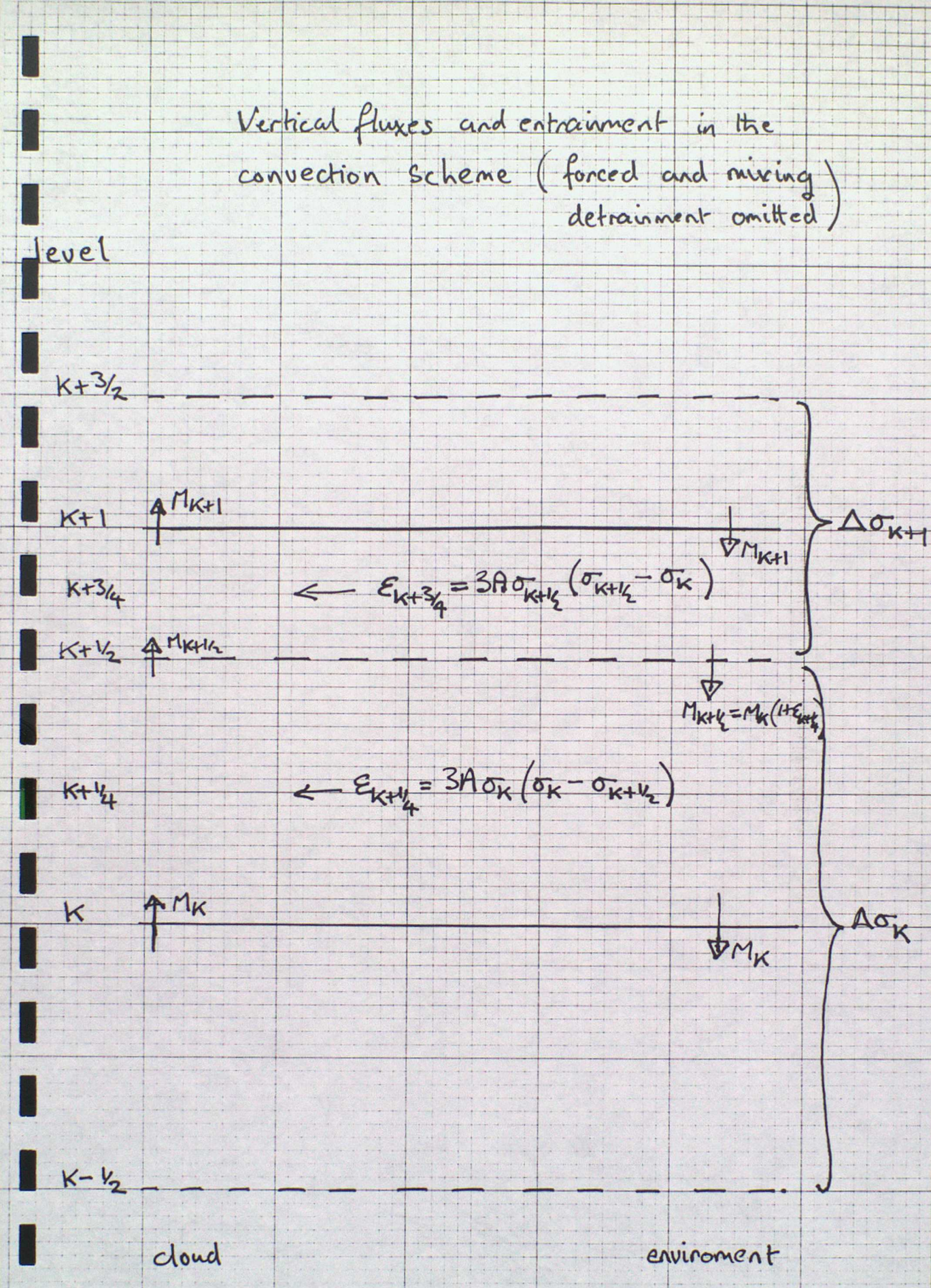

Figure 6

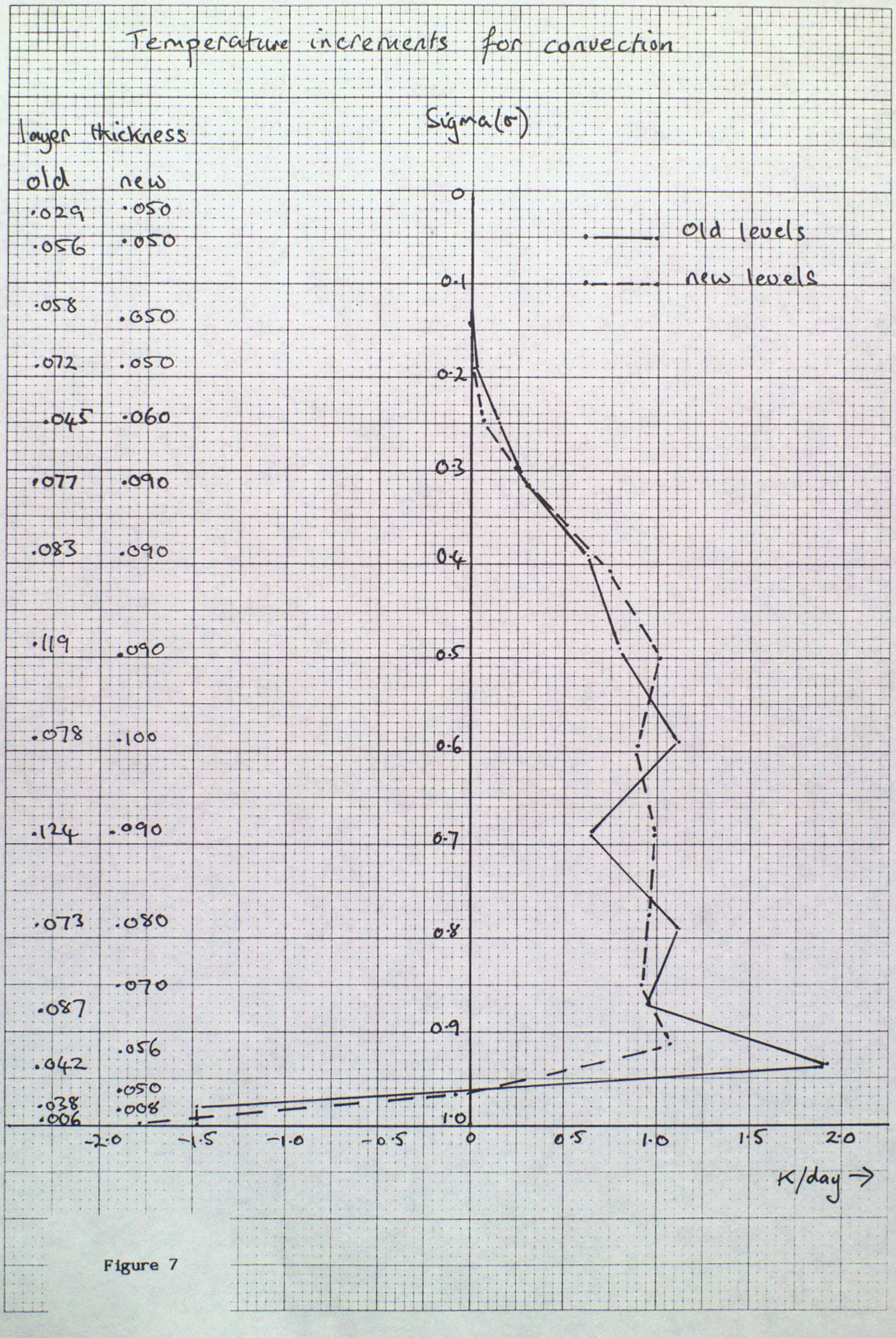
Temperature increments for convection
Sigma(σ)
layer thickness
old new
.029 .050
.056 .050
.058 .050
.072 .050
.045 .060
.077 .090
.083 .090
.119 .090
.078 .100
.124 .090
.073 .080
.087 .070
.042 .056
.038 .050
.006 .008
old levels
new levels
0
0.1
0.2
0.3
0.4
0.5
0.6
0.7
0.8
0.9
1.0
-2.0
-1.5
-1.0
-0.5
0
0.5
1.0
1.5
2.0
K/day →

Figure 7

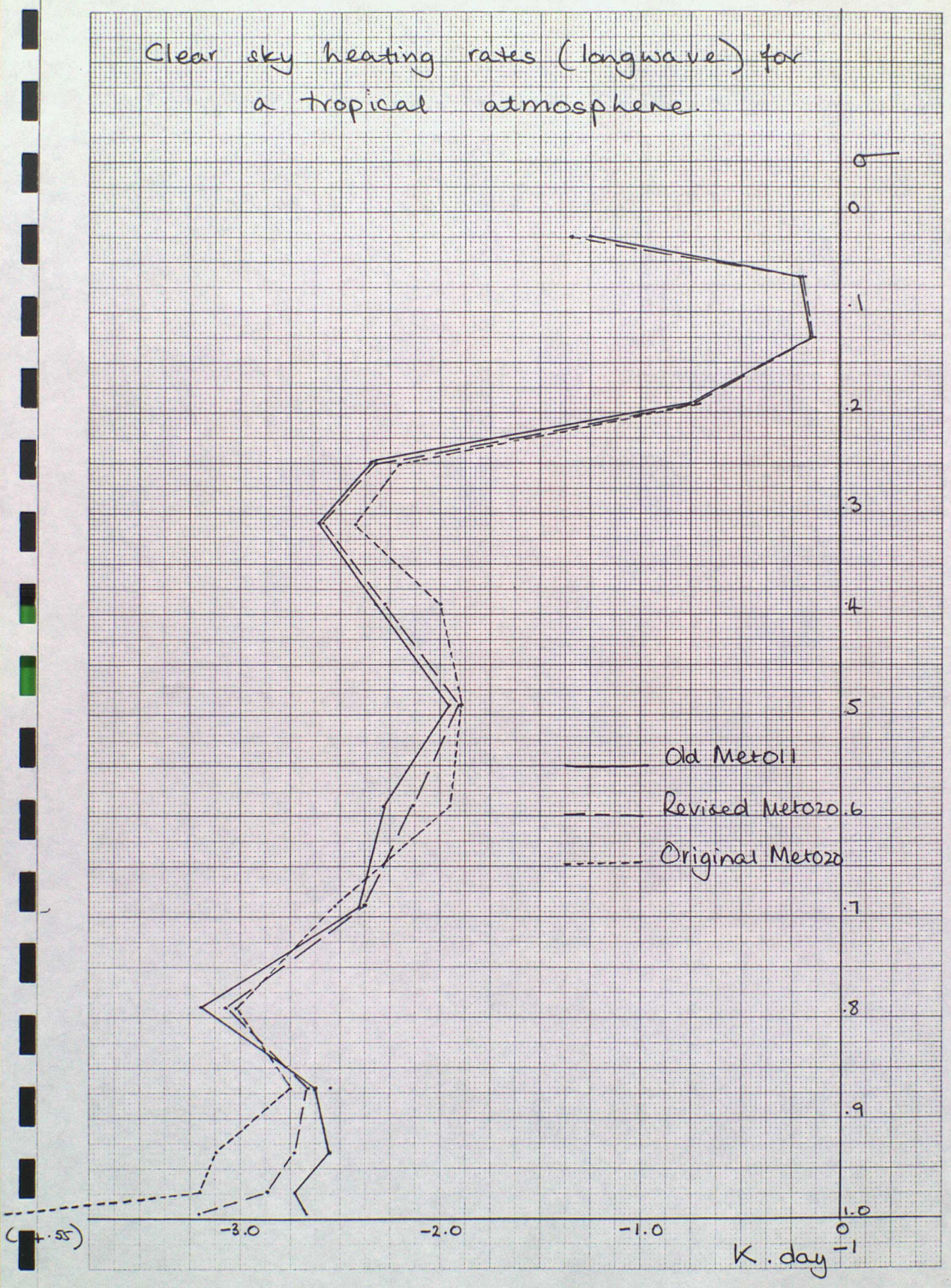

Figure 8

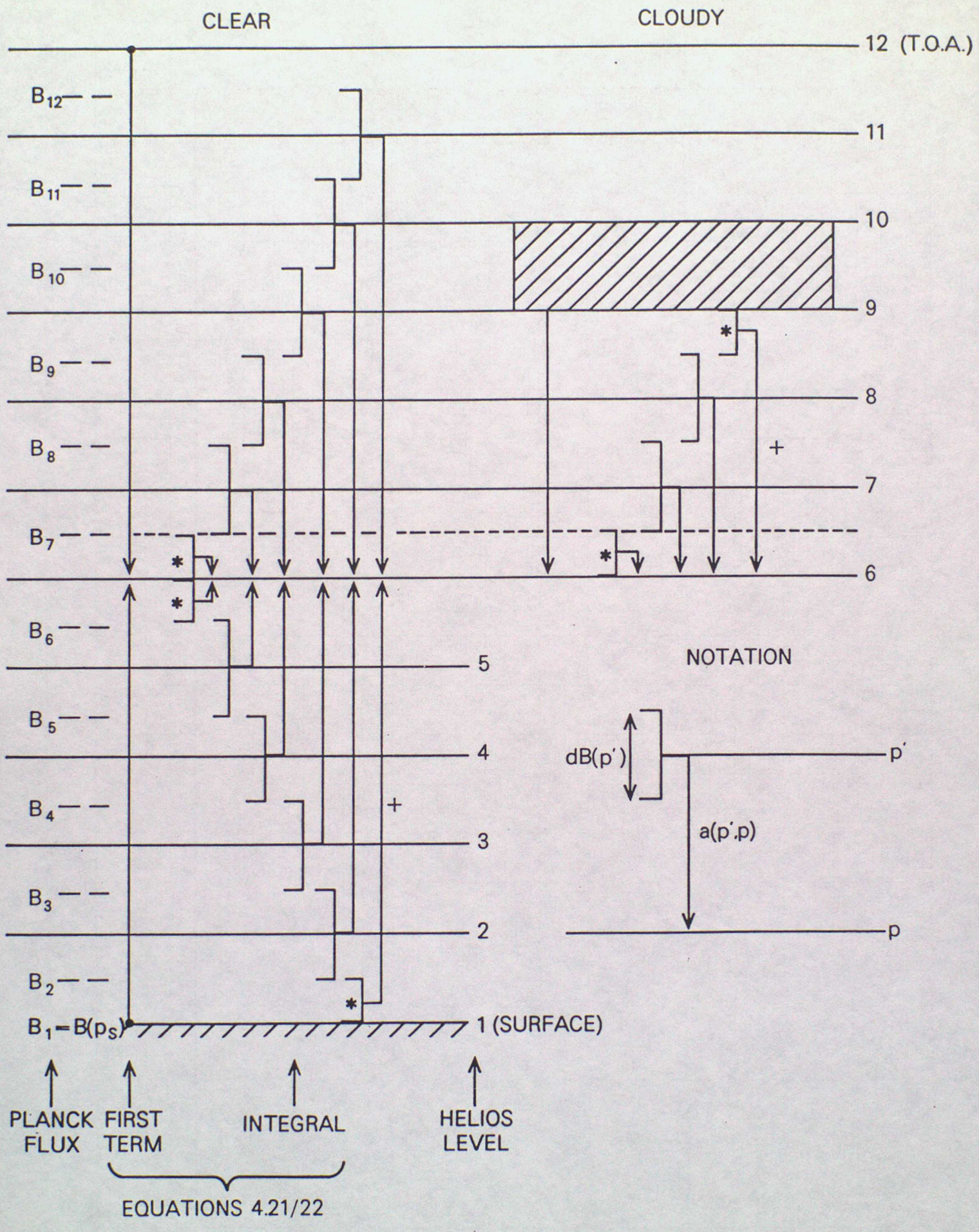
CLEAR
CLOUDY
12 (T.O.A.)
11
10
9
8
7
6
5
4
3
2
1 (SURFACE)
B_{12}
B_{11}
B_{10}
B_9
B_8
B_7
B_6
B_5
B_4
B_3
B_2
$B_1 = B(p_S)$
NOTATION
dB(p')
p'
a(p',p)
p
PLANCK FLUX
FIRST TERM
INTEGRAL
HELIOS LEVEL
EQUATIONS 4.21/22

Figure 9

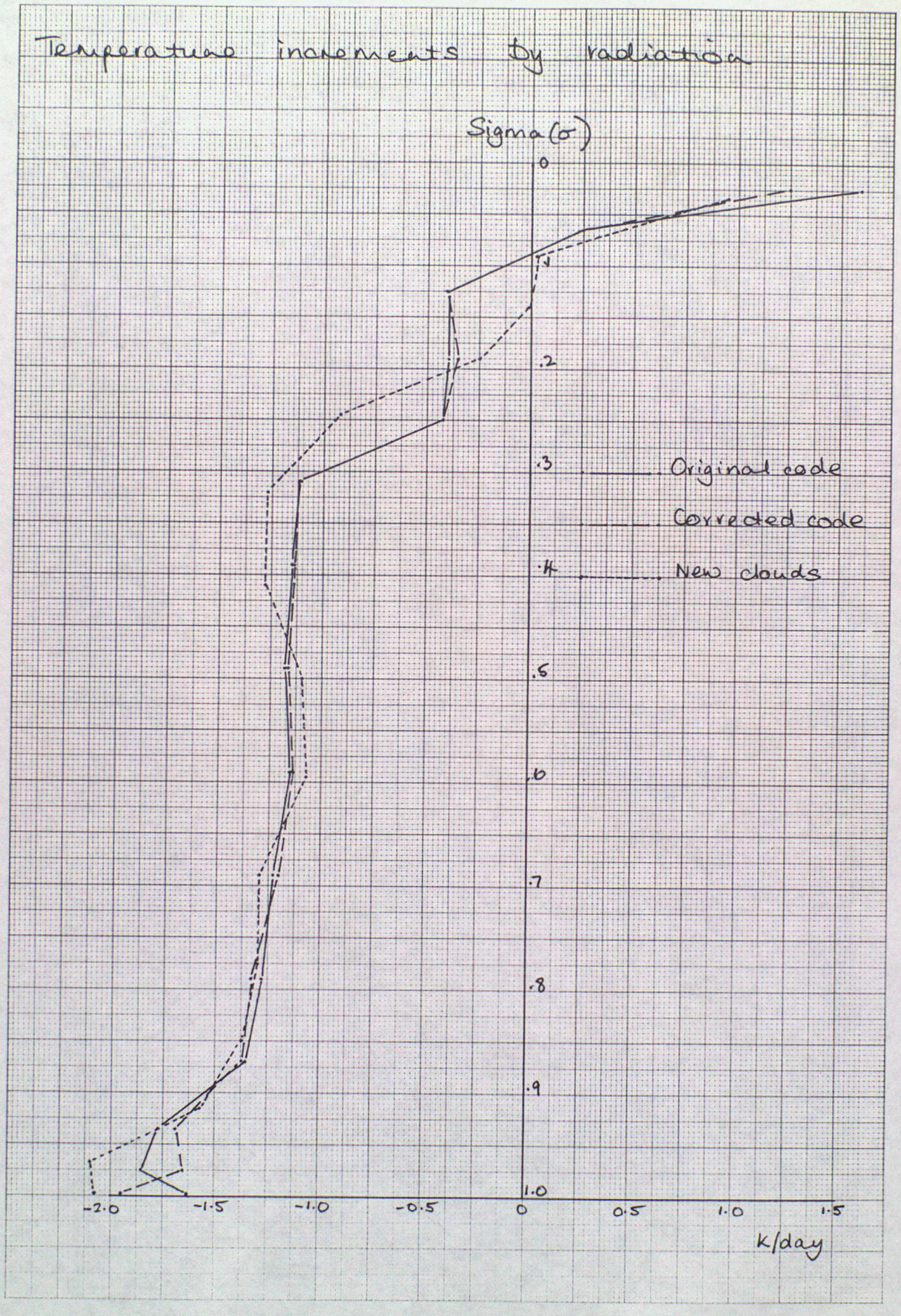
Temperature increments by radiation
Sigma (σ)
0
.2
.3
.4
.5
.6
.7
.8
.9
1.0
Original code
Corrected code
New clouds
-2.0
-1.5
-1.0
-0.5
0
0.5
1.0
1.5
K/day

Figure 10

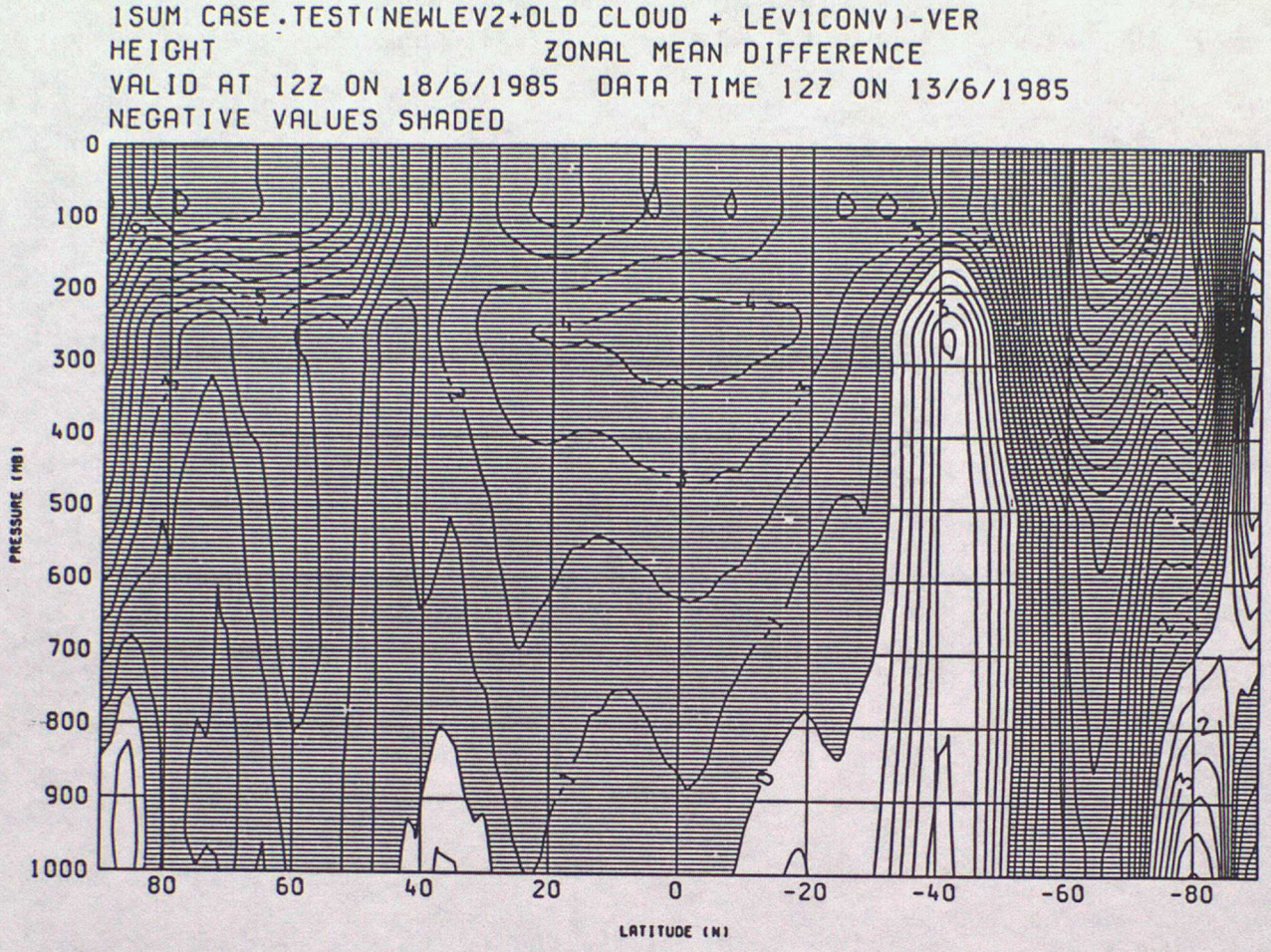
1SUM CASE.TEST(NEWLEV2+OLD CLOUD + LEV1CONV)-VER
HEIGHT ZONAL MEAN DIFFERENCE
VALID AT 12Z ON 18/6/1985 DATA TIME 12Z ON 13/6/1985
NEGATIVE VALUES SHADED
PRESSURE (MB)
0
100
200
300
400
500
600
700
800
900
1000
80
60
40
20
0
-20
-40
-60
-80
LATITUDE (N)

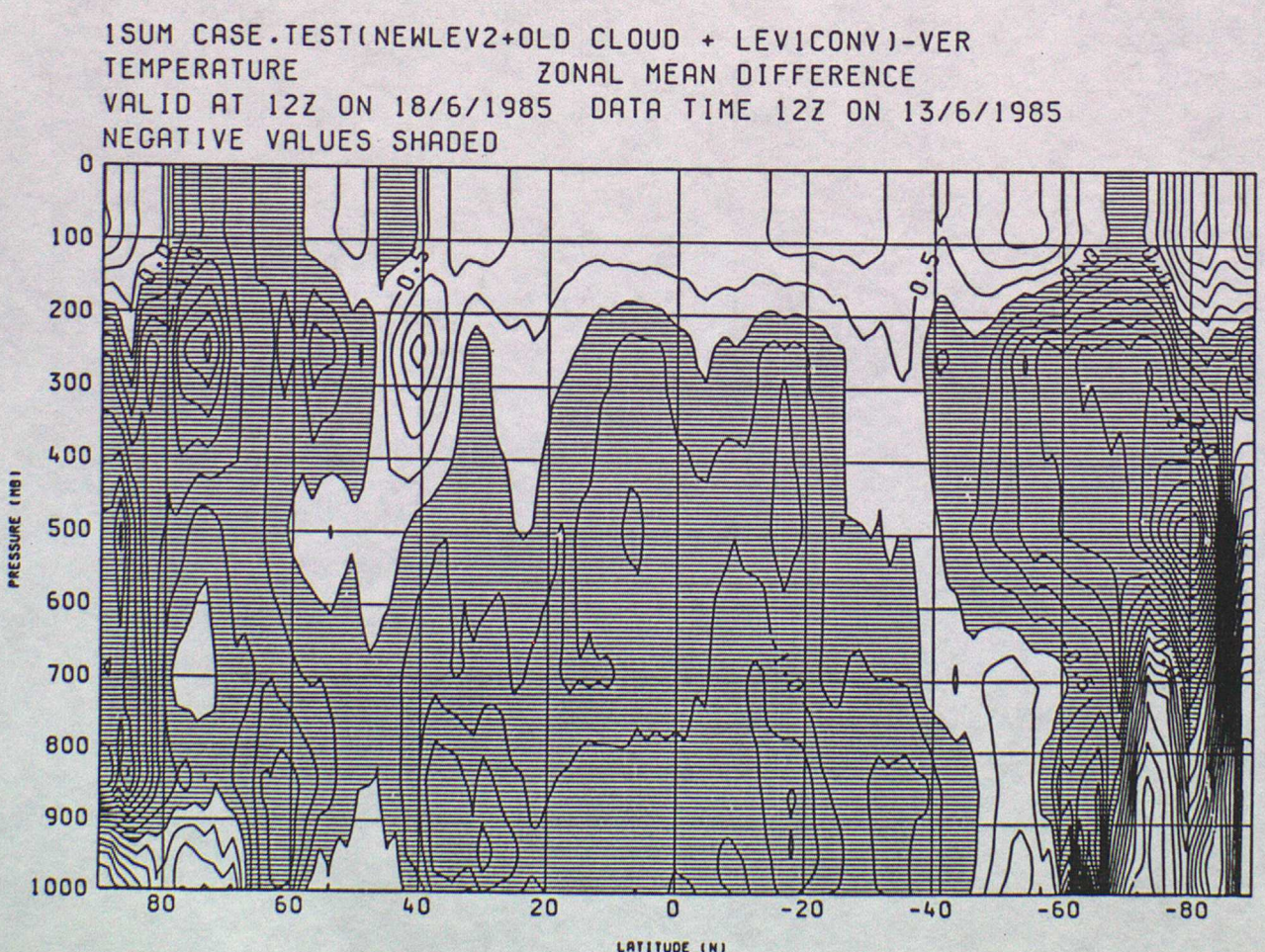
1SUM CASE.TEST(NEWLEV2+OLD CLOUD + LEV1CONV)-VER
TEMPERATURE ZONAL MEAN DIFFERENCE
VALID AT 12Z ON 18/6/1985 DATA TIME 12Z ON 13/6/1985
NEGATIVE VALUES SHADED
PRESSURE (MB)
0
100
200
300
400
500
600
700
800
900
1000
80
60
40
20
0
-20
-40
-60
-80
LATITUDE (N)

Figure 11

OLD SCHEME

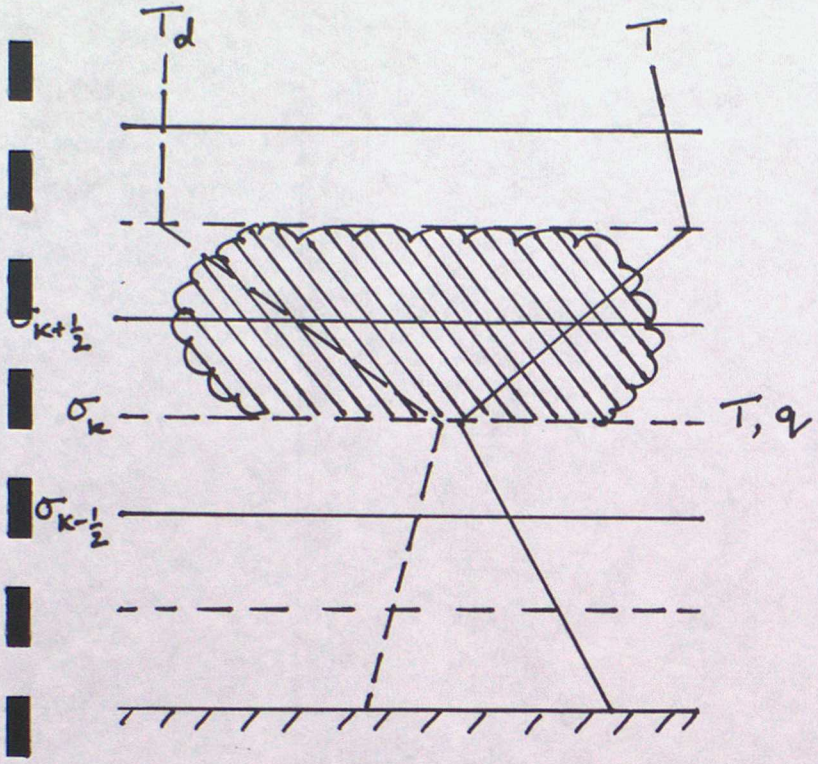

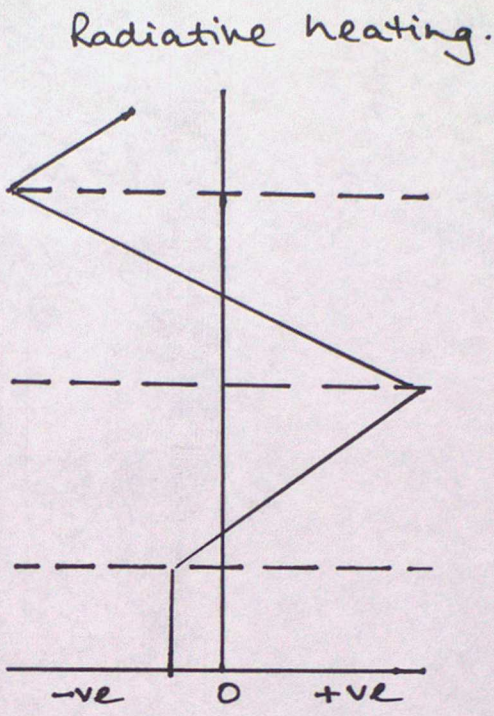

NEW SCHEME

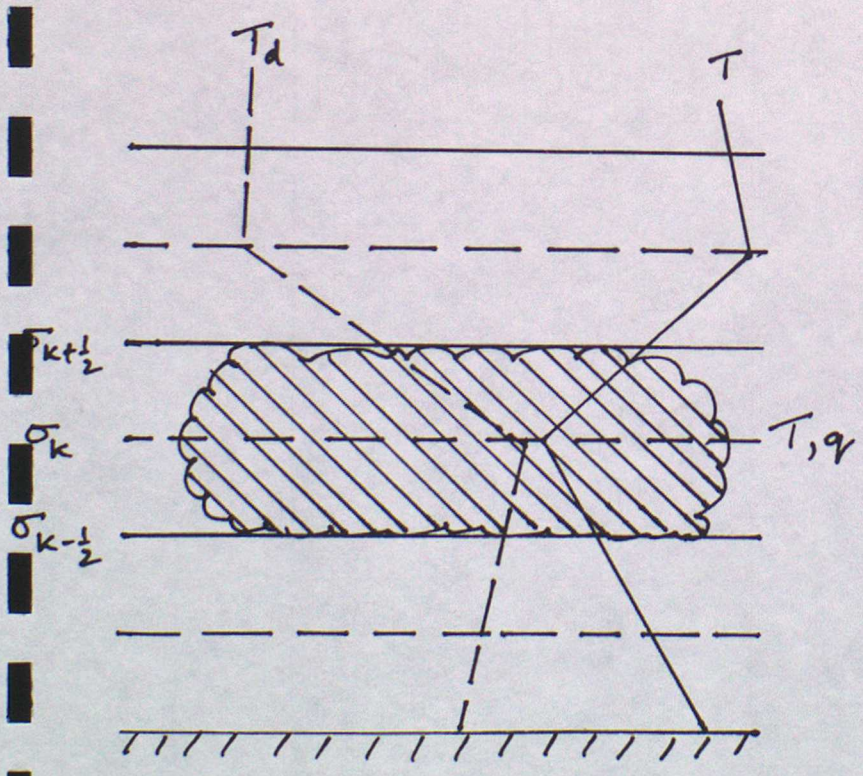

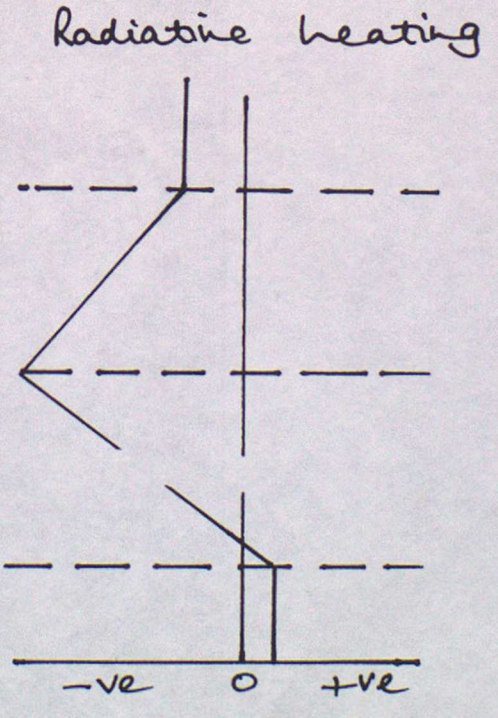

Figure 12

T+72 TEST(NEWLEV2+OLD CLOUD + LEV1CONV)
LOW CLOUD
VALID AT 12Z ON 16/6/1985 DATA TIME 12Z ON 13/6/1985
EXPERIMENT NO.: 1 T+72

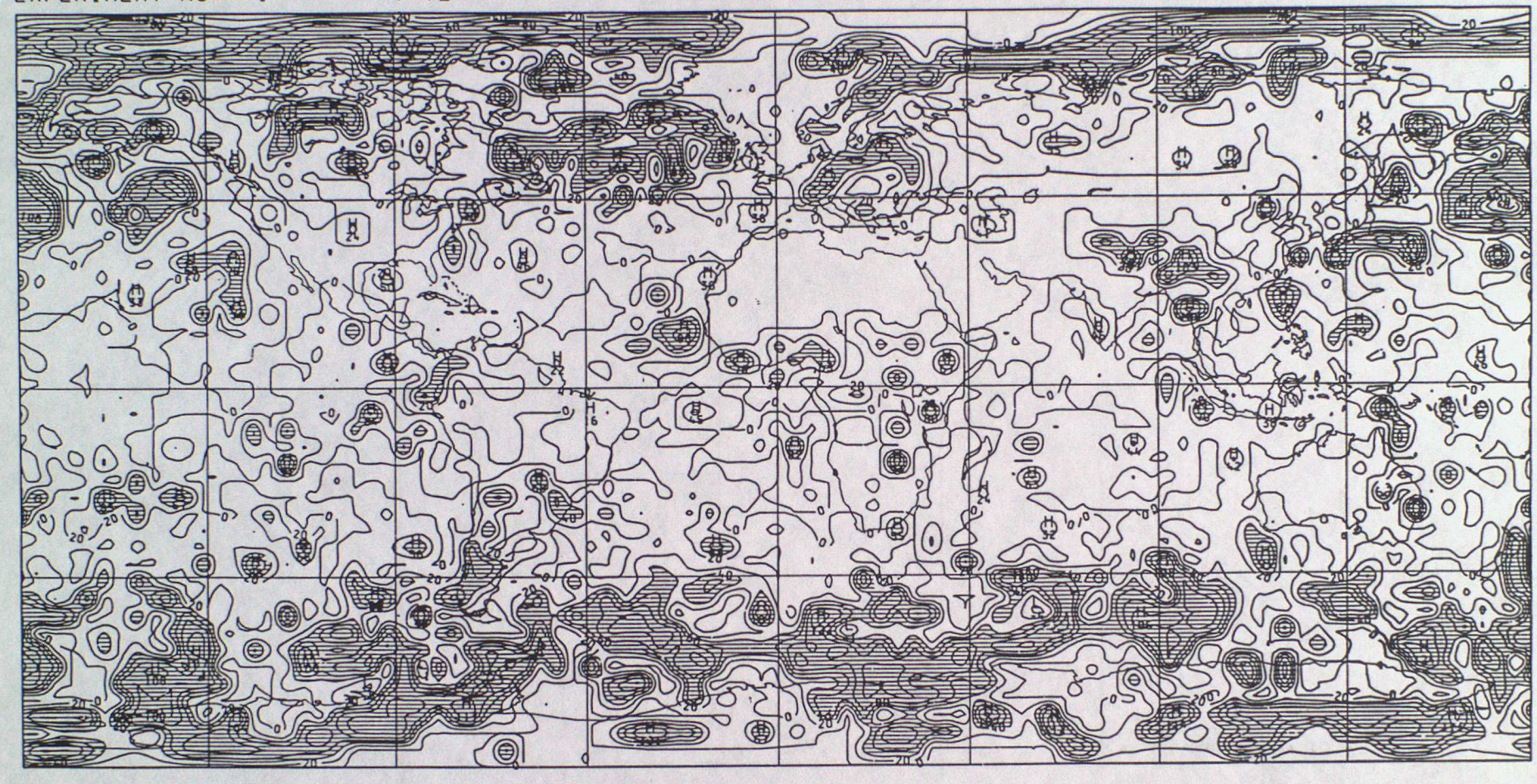

Figure 13a

T+72 TEST(NEWLEV2+CLOUDS IN LAYERS+RHDTHDP)
LOW CLOUD
VALID AT 12Z ON 16/6/1985 DATA TIME 12Z ON 13/6/1985
EXPERIMENT NO.: 1 T+72

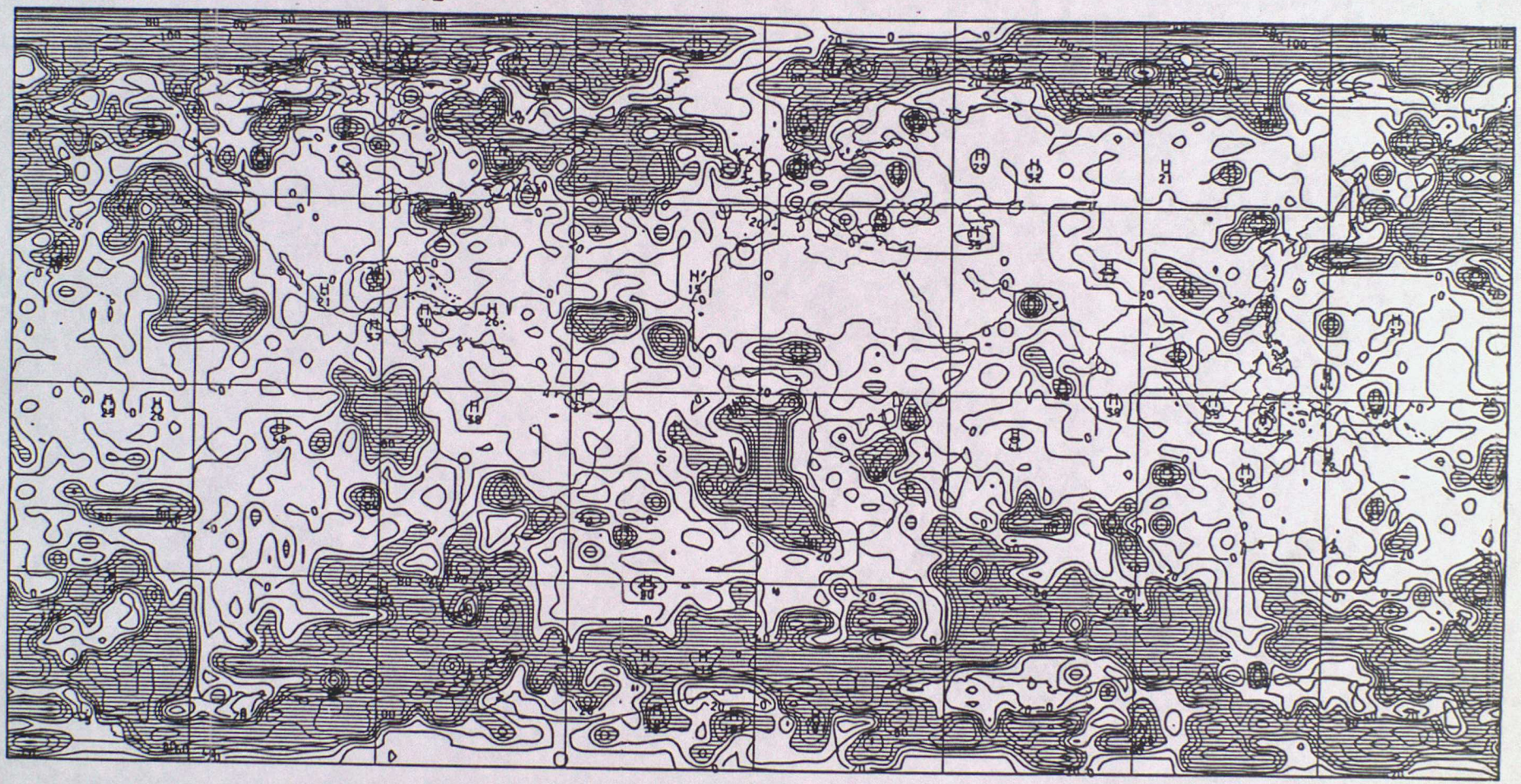

Figure 13b

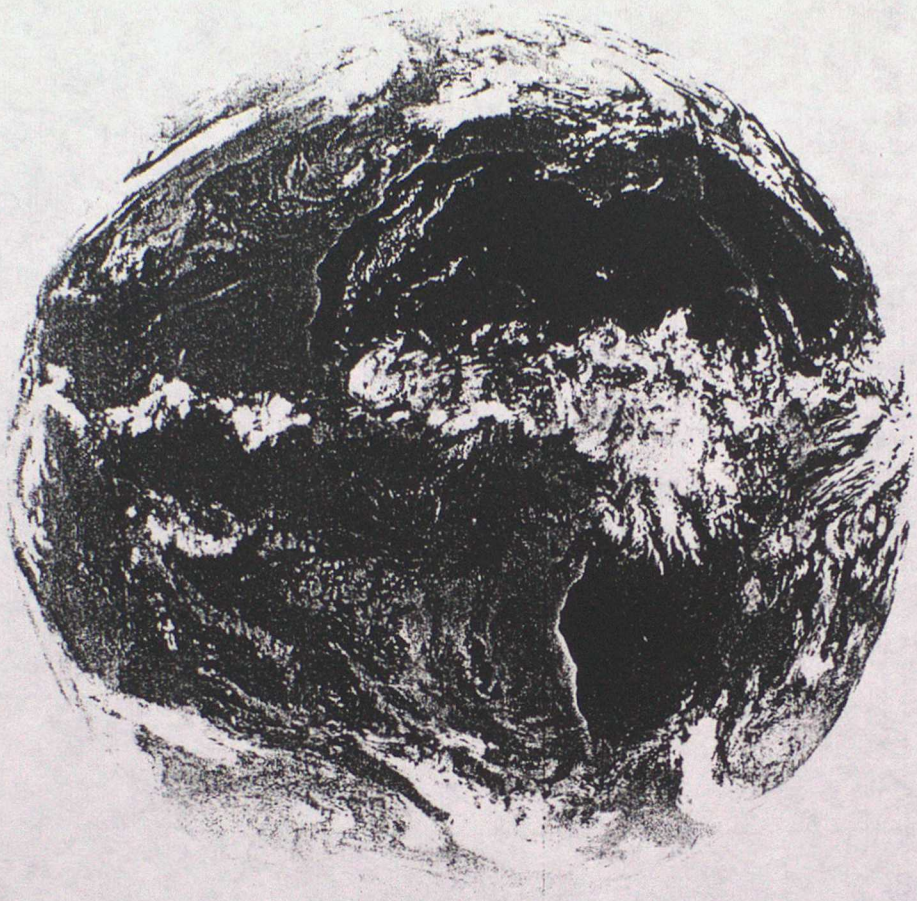

METEOSAT 1985 MONTH 6 DAY 16 TIME 1155 GMT (NORTH) CH. IR 1
NOMINAL SCAN/RAW DATA SLOT 24 COPYRIGHT - ESA -

Figure 13c

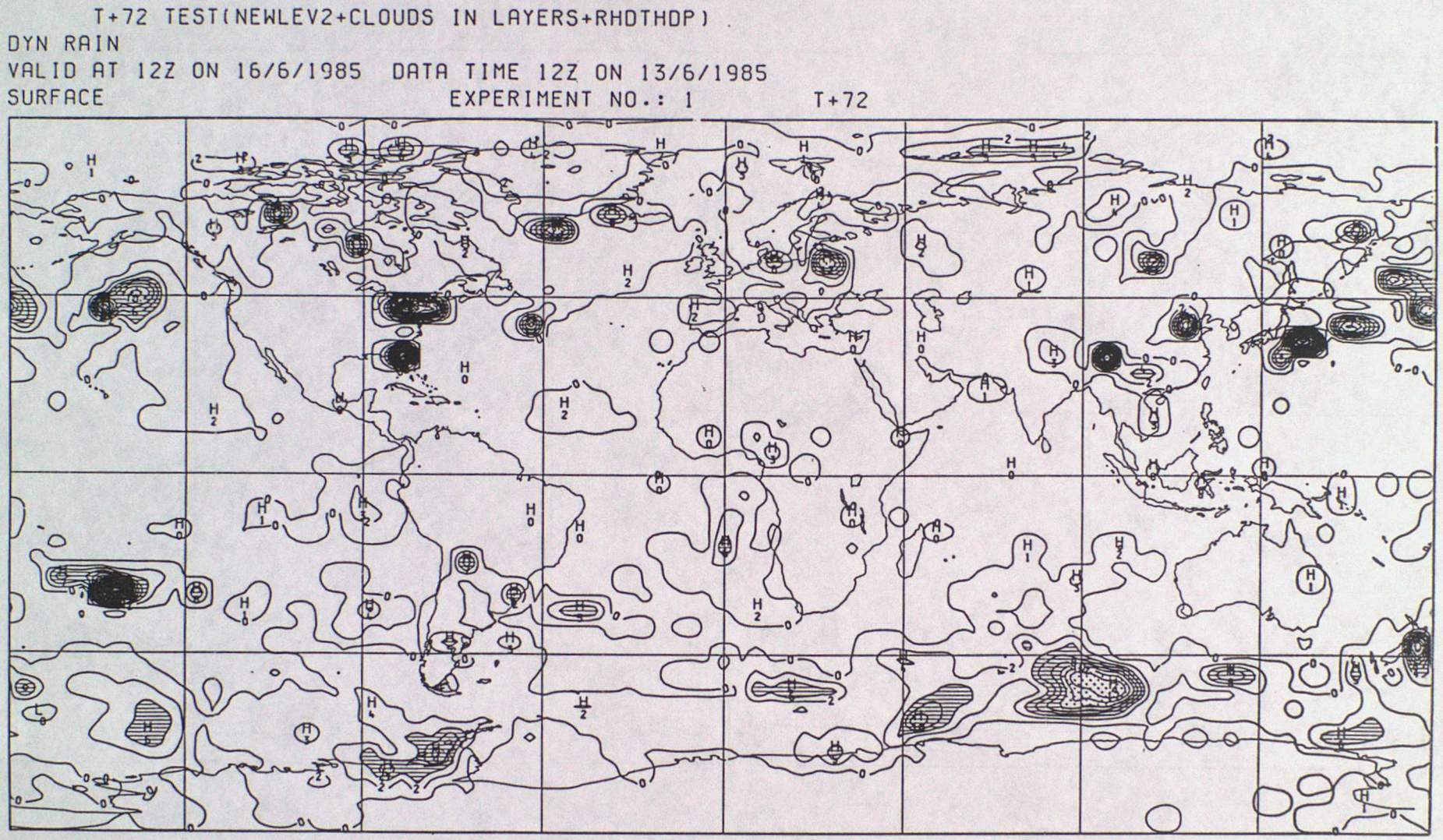
T+72 TEST(NEWLEV2+CLOUDS IN LAYERS+RHDTHDP)
DYN RAIN
VALID AT 12Z ON 16/6/1985 DATA TIME 12Z ON 13/6/1985
SURFACE
EXPERIMENT NO.: 1
T+72

Figure 14

T+72 TEST(NEWLEV2+ NEW CLOUD + LEVICONV)
DYN RAIN
VALID AT 12Z ON 16/6/1985 DATA TIME 12Z ON 13/6/1985
SURFACE EXPERIMENT NO.: 1 T+72

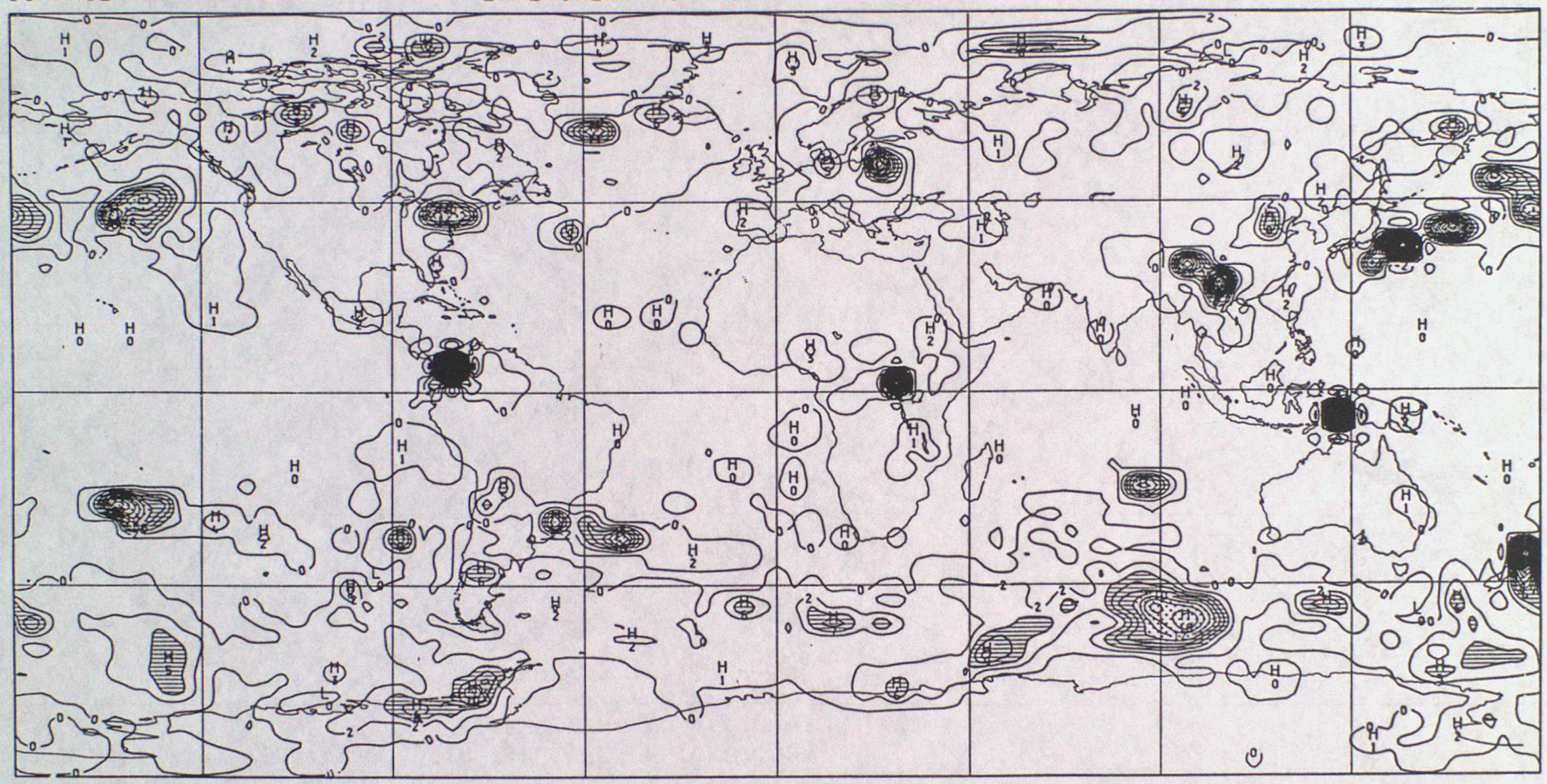

Figure 15

T+72 TEST(NEWLEV2+ NEW CLOUD + LEV1CONV)
LOW CLOUD
VALID AT 12Z ON 16/6/1985 DATA TIME 12Z ON 13/6/1985
EXPERIMENT NO.: 1 T+72

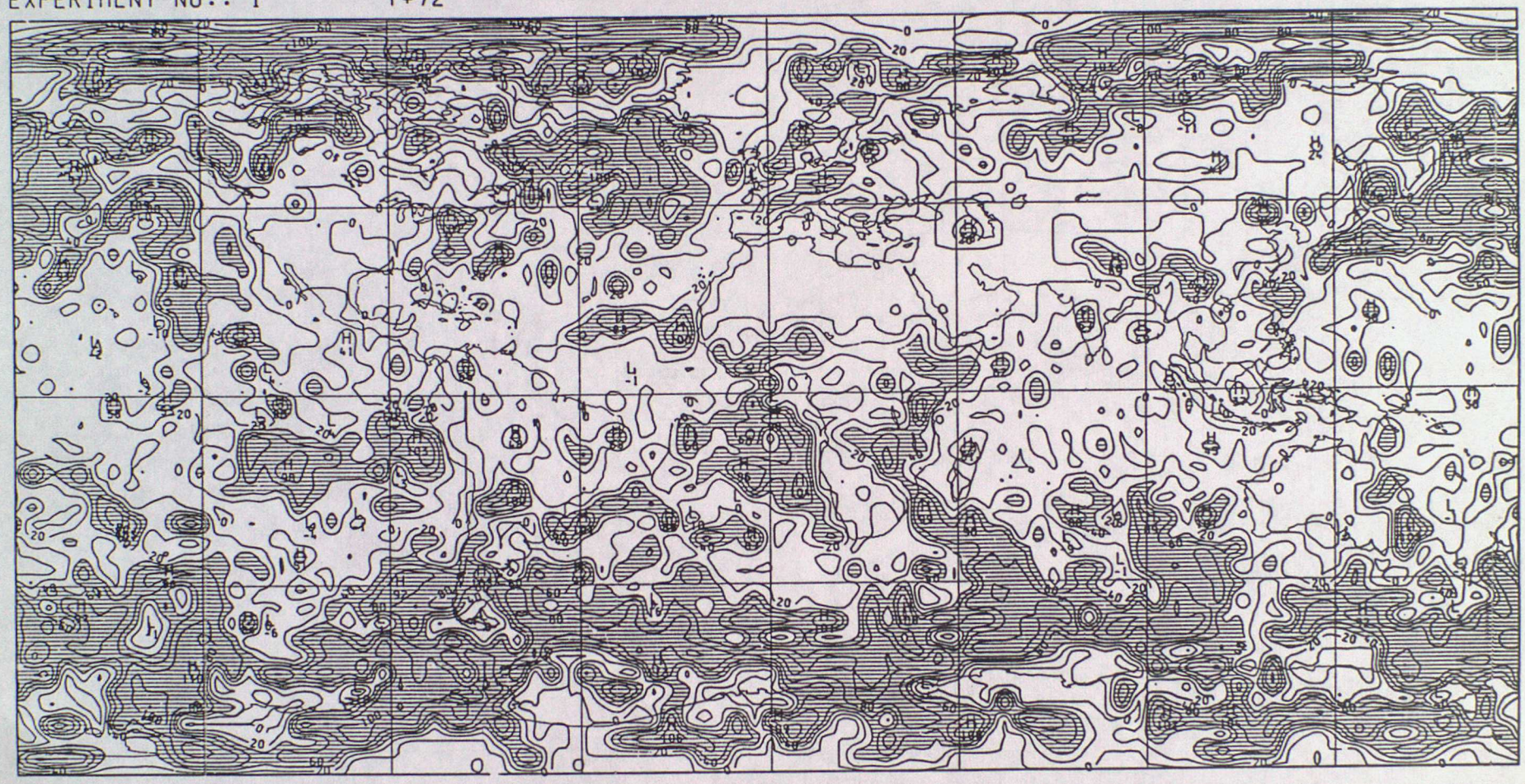

Figure 16

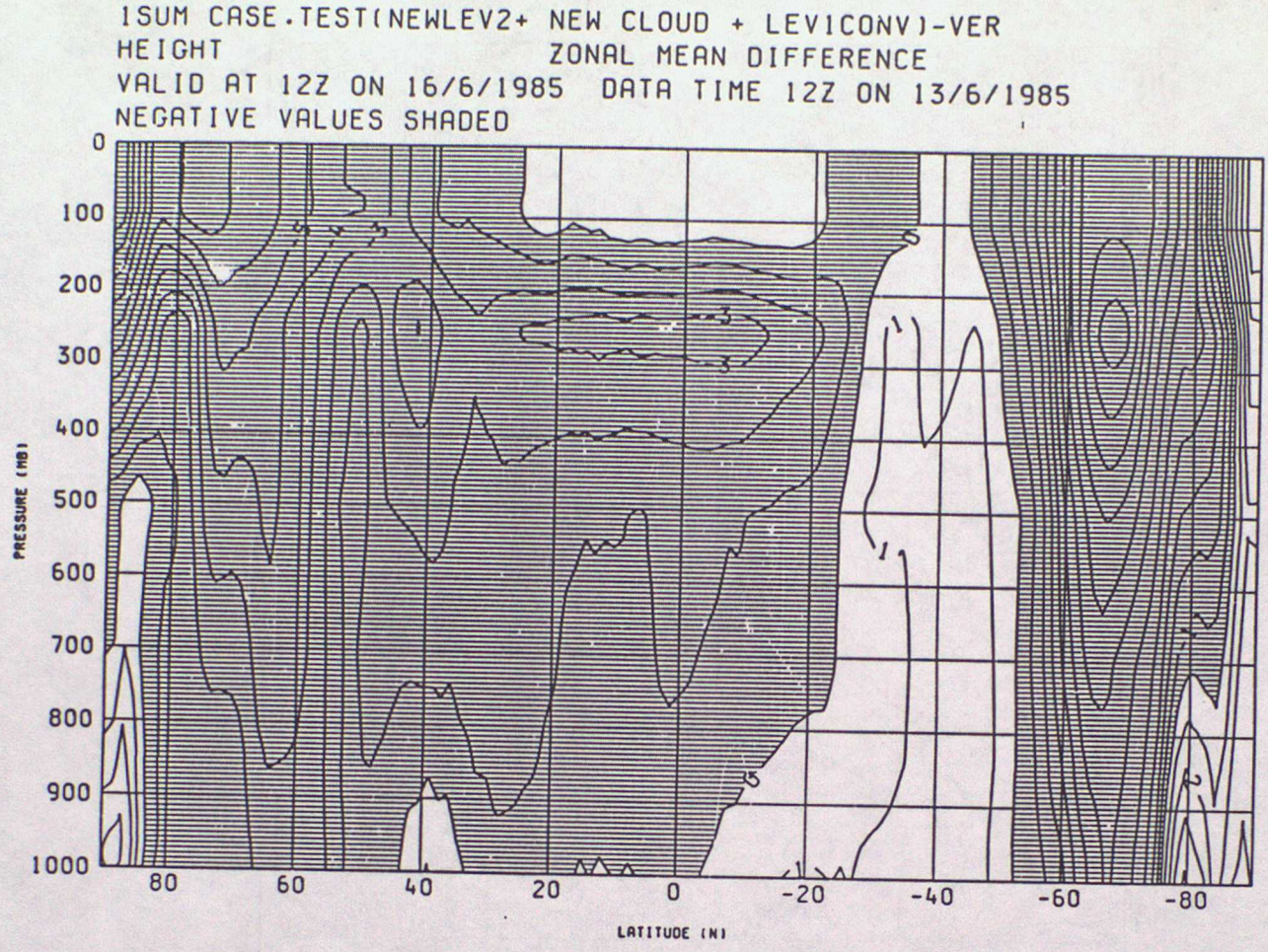
1SUM CASE.TEST(NEWLEV2+ NEW CLOUD + LEVICONV)-VER
HEIGHT ZONAL MEAN DIFFERENCE
VALID AT 12Z ON 16/6/1985 DATA TIME 12Z ON 13/6/1985
NEGATIVE VALUES SHADED
PRESSURE (MB)
0
100
200
300
400
500
600
700
800
900
1000
80
60
40
20
0
-20
-40
-60
-80
LATITUDE (N)

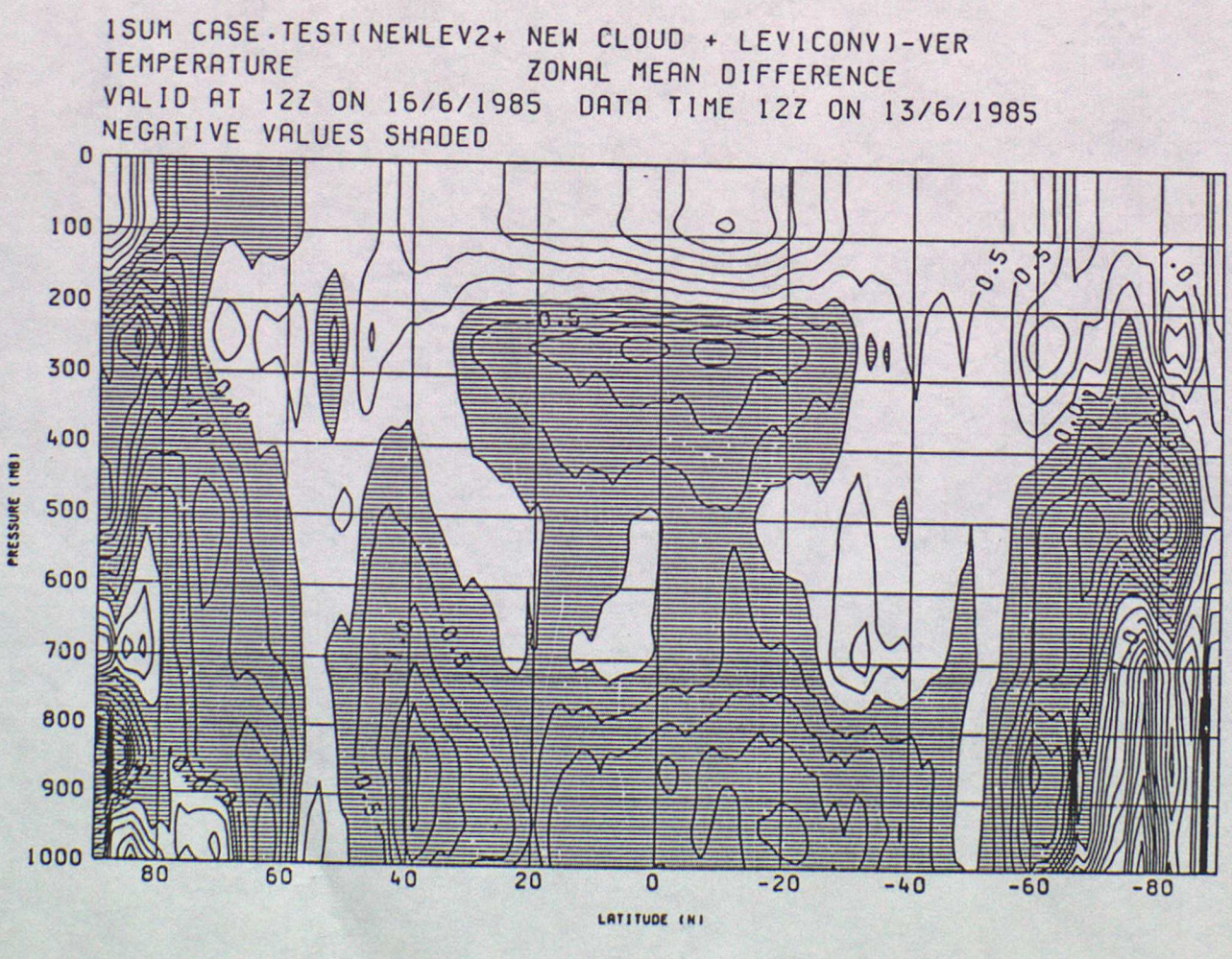
1SUM CASE.TEST(NEWLEV2+ NEW CLOUD + LEVICONV)-VER
TEMPERATURE ZONAL MEAN DIFFERENCE
VALID AT 12Z ON 16/6/1985 DATA TIME 12Z ON 13/6/1985
NEGATIVE VALUES SHADED
PRESSURE (MB)
0
100
200
300
400
500
600
700
800
900
1000
80
60
40
20
0
-20
-40
-60
-80
LATITUDE (N)

Figure 17

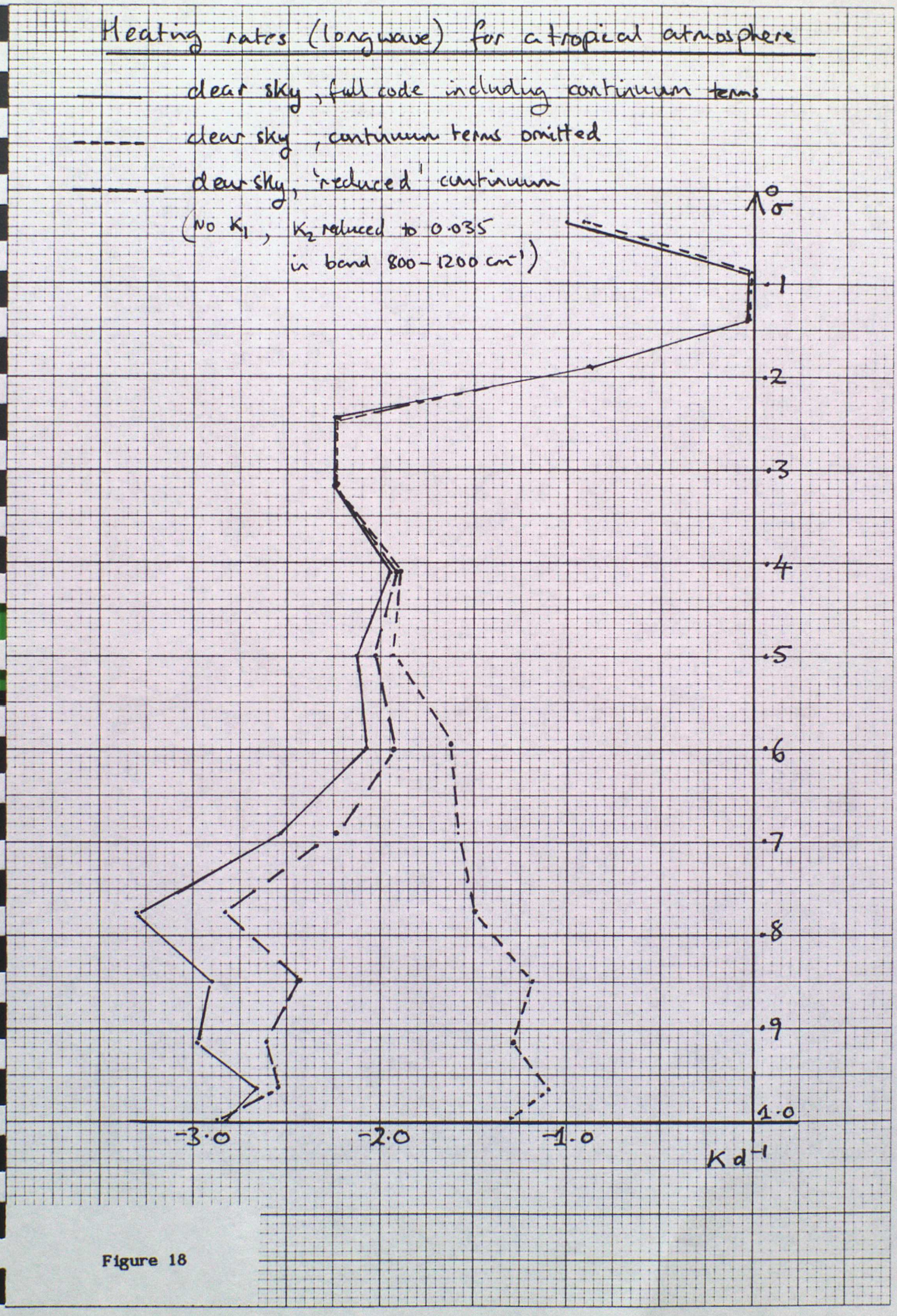
Heating rates (longwave) for a tropical atmosphere
clear sky, full code including continuum terms
clear sky, continuum terms omitted
clear sky, 'reduced' continuum
(No K_1, K_2 reduced to 0.035 in band 800–1200 cm^{-1})
0
.1
.2
.3
.4
.5
.6
.7
.8
.9
1.0
-3.0
-2.0
-1.0
K d^{-1}

Figure 18

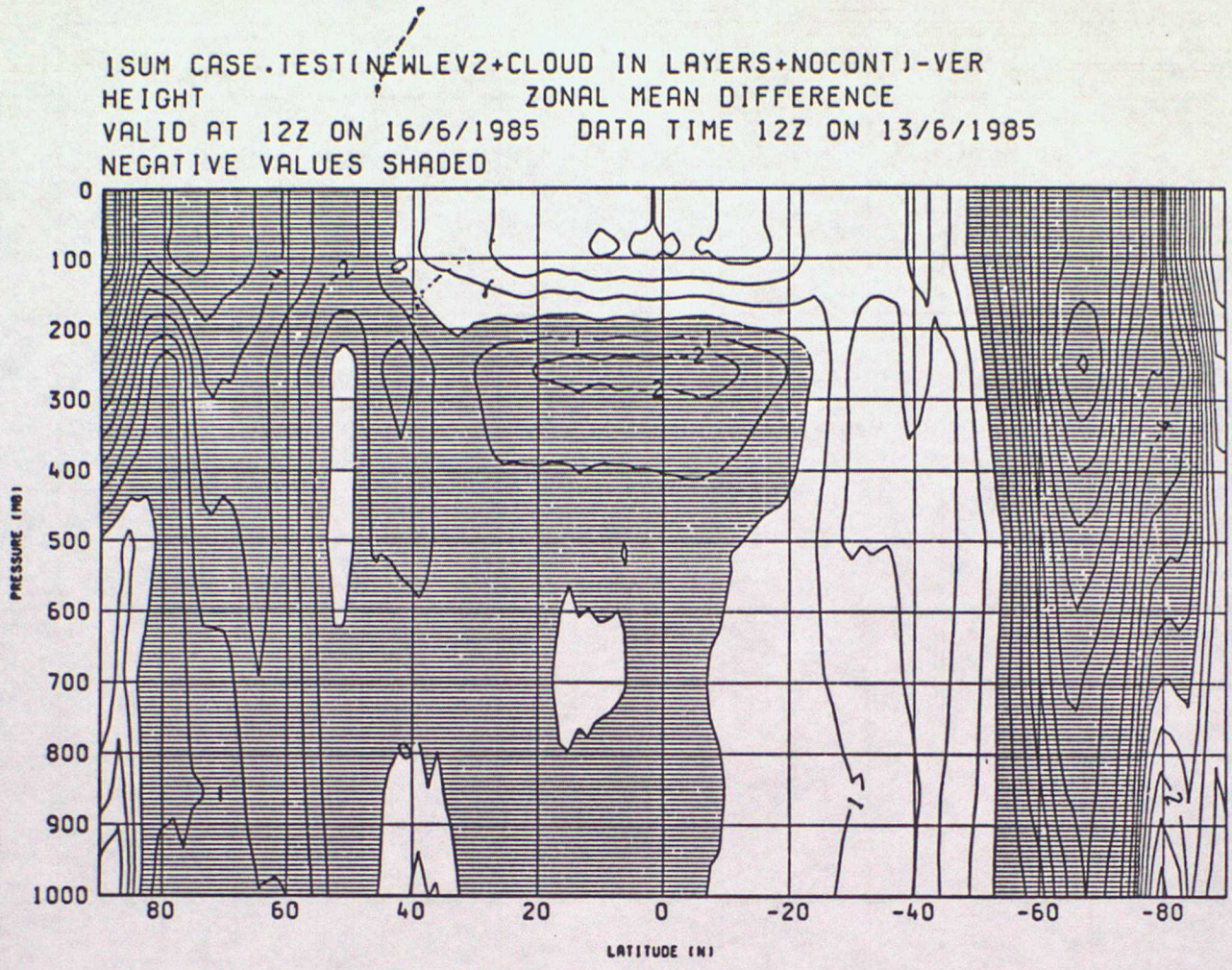
1SUM CASE.TEST(NEWLEV2+CLOUD IN LAYERS+NOCONT)-VER
HEIGHT ZONAL MEAN DIFFERENCE
VALID AT 12Z ON 16/6/1985 DATA TIME 12Z ON 13/6/1985
NEGATIVE VALUES SHADED
PRESSURE (MB)
0
100
200
300
400
500
600
700
800
900
1000
80
60
40
20
0
-20
-40
-60
-80
LATITUDE (N)

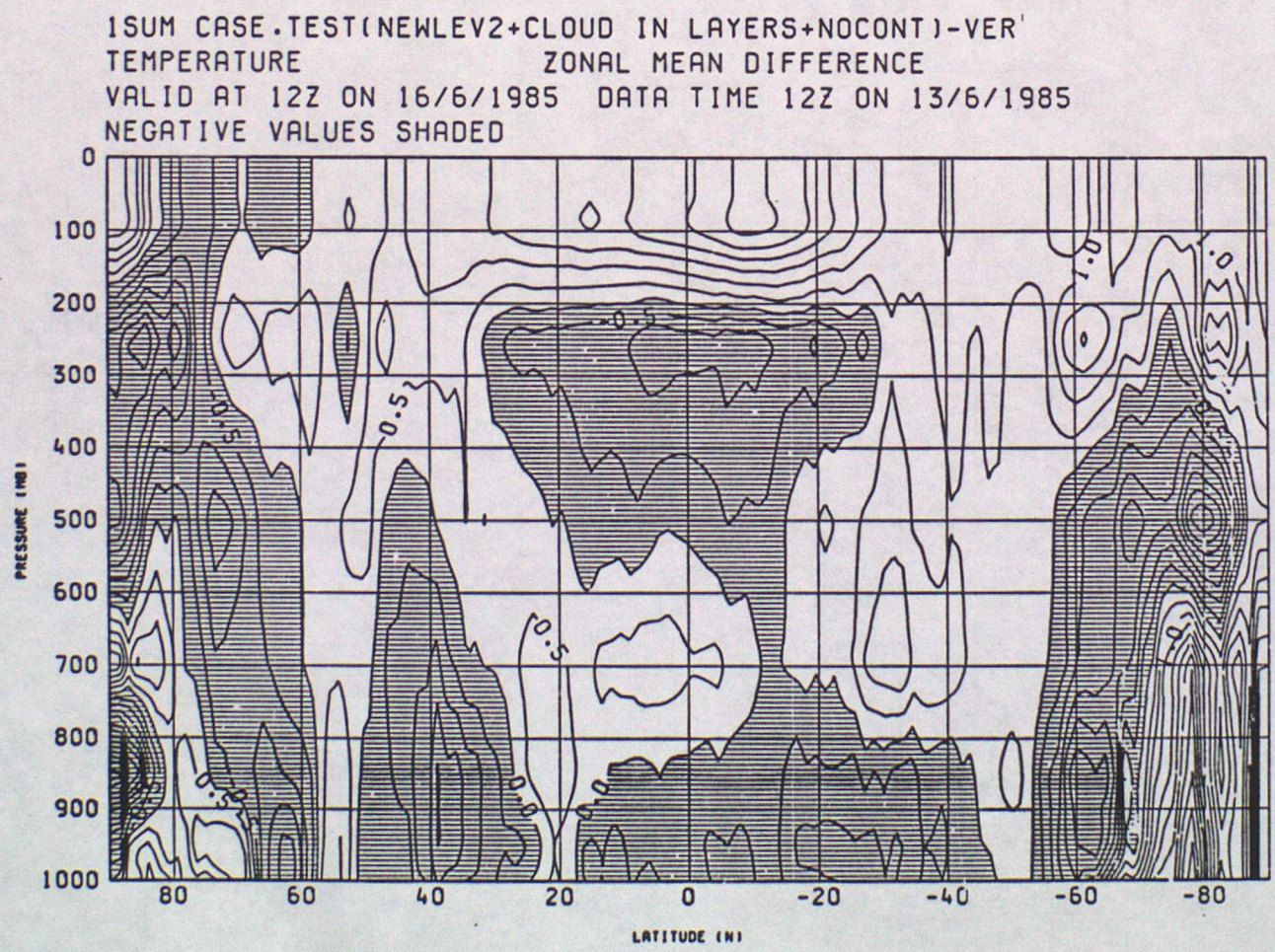
1SUM CASE.TEST(NEWLEV2+CLOUD IN LAYERS+NOCONT)-VER
TEMPERATURE ZONAL MEAN DIFFERENCE
VALID AT 12Z ON 16/6/1985 DATA TIME 12Z ON 13/6/1985
NEGATIVE VALUES SHADED
PRESSURE (MB)
0
100
200
300
400
500
600
700
800
900
1000
80
60
40
20
0
-20
-40
-60
-80
LATITUDE (N)

Figure 19

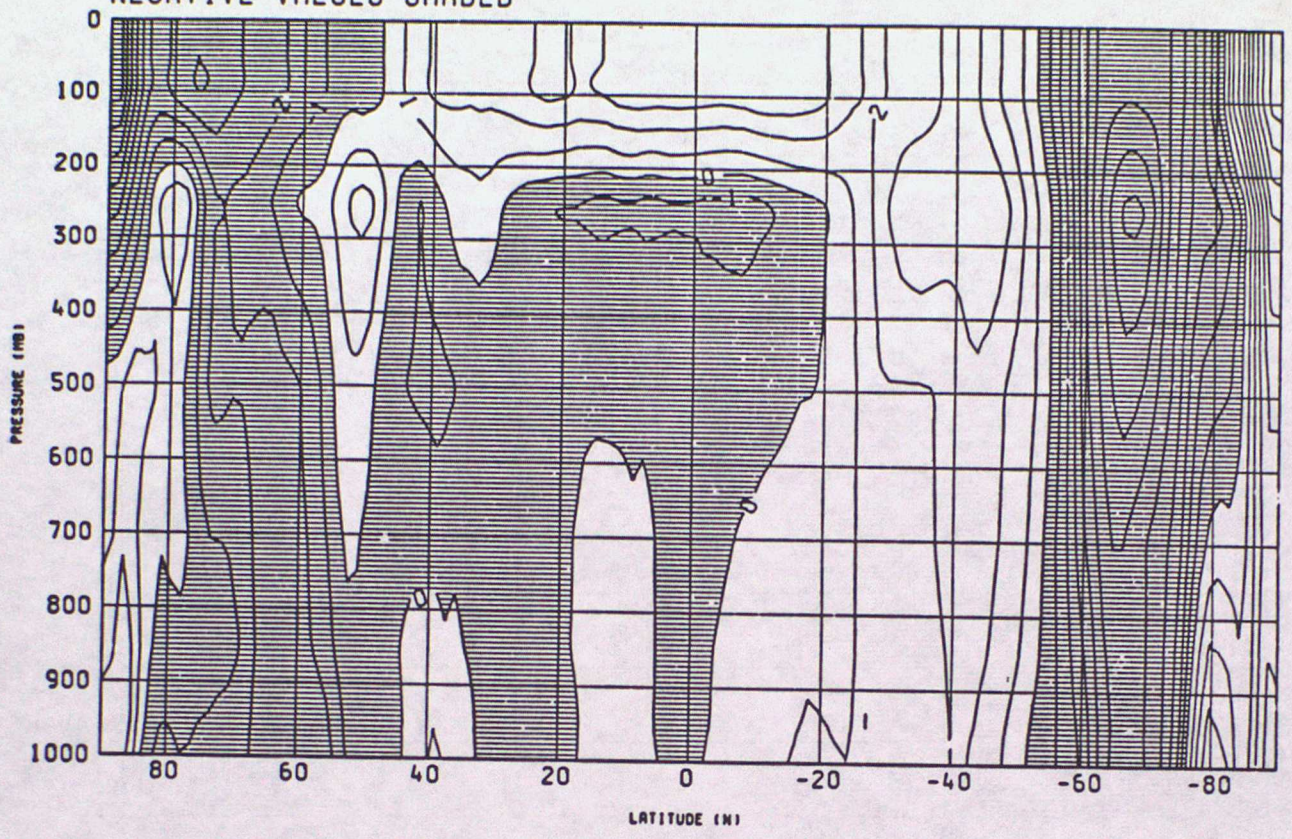
1SUM CASE.TEST(NEWLEV2+CLOUD IN LAYERS+PTHECON)-VER
HEIGHT ZONAL MEAN DIFFERENCE
VALID AT 12Z ON 16/6/1985 DATA TIME 12Z ON 13/6/1985
NEGATIVE VALUES SHADED
PRESSURE (MB)
0
100
200
300
400
500
600
700
800
900
1000
80
60
40
20
0
-20
-40
-60
-80
LATITUDE (N)

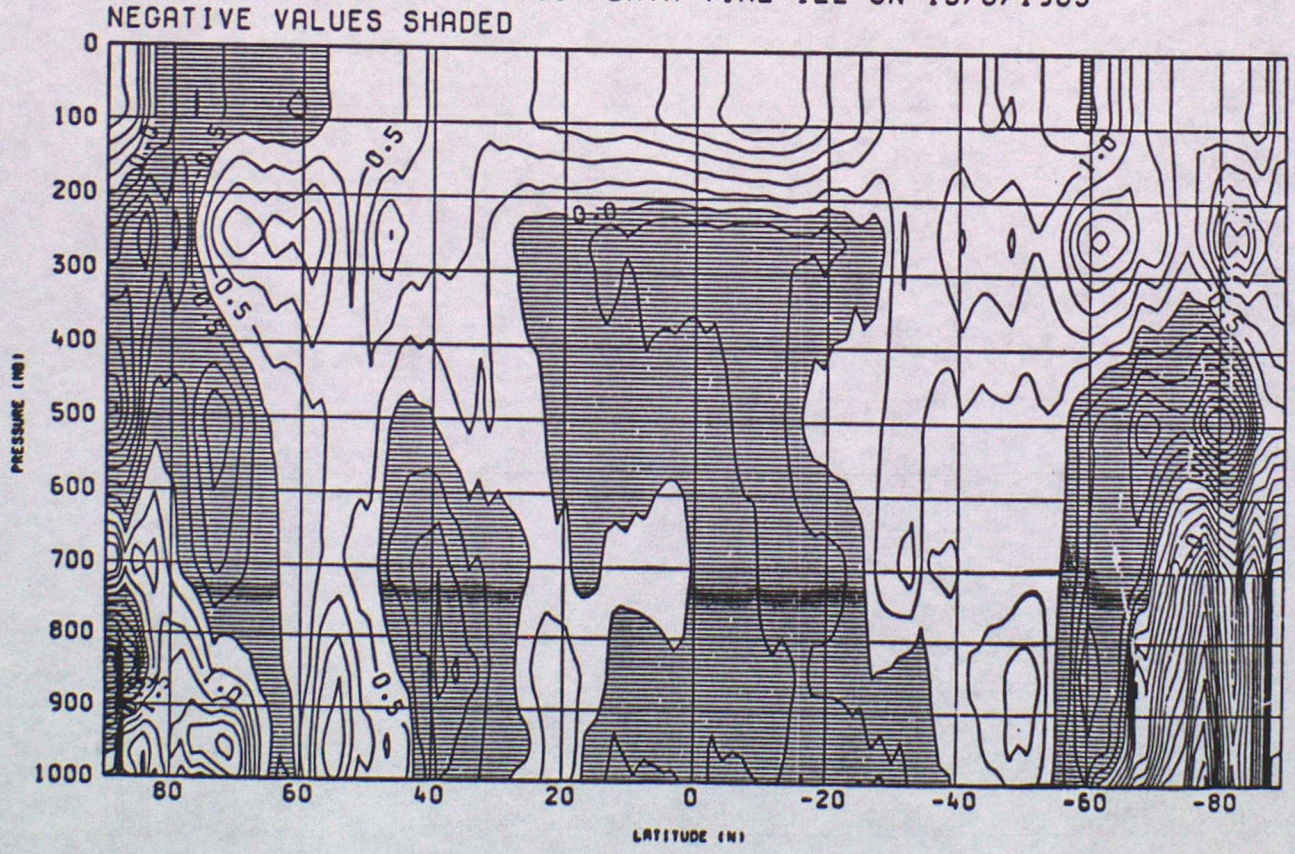
1SUM CASE.TEST(NEWLEV2+CLOUD IN LAYERS+PTHECON)-VER
TEMPERATURE ZONAL MEAN DIFFERENCE
VALID AT 12Z ON 16/6/1985 DATA TIME 12Z ON 13/6/1985
NEGATIVE VALUES SHADED
PRESSURE (MB)
0
100
200
300
400
500
600
700
800
900
1000
80
60
40
20
0
-20
-40
-60
-80
LATITUDE (N)

Figure 20

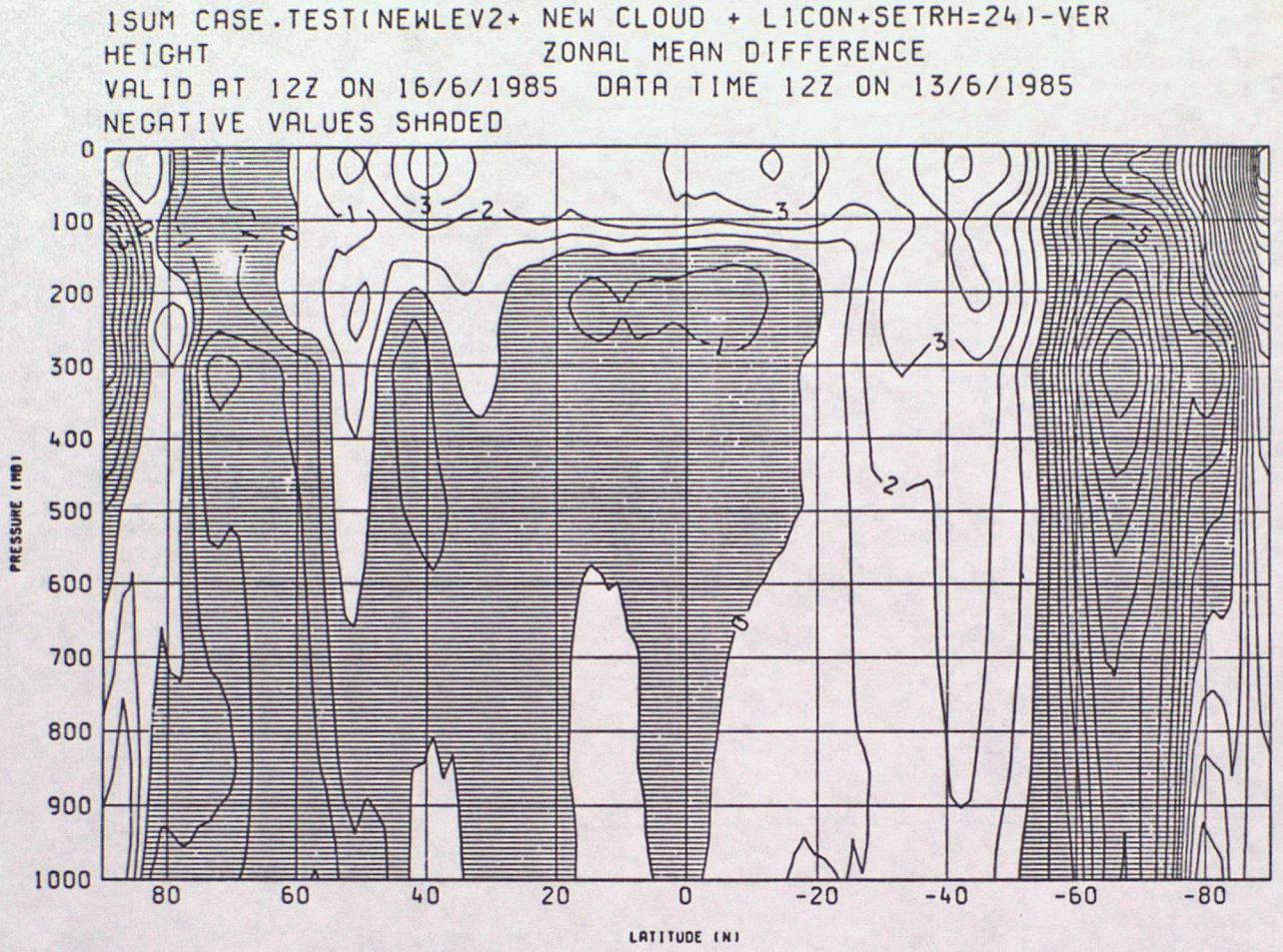
1SUM CASE.TEST(NEWLEV2+ NEW CLOUD + L1CON+SETRH=24)-VER
HEIGHT ZONAL MEAN DIFFERENCE
VALID AT 12Z ON 16/6/1985 DATA TIME 12Z ON 13/6/1985
NEGATIVE VALUES SHADED
PRESSURE (MB)
0
100
200
300
400
500
600
700
800
900
1000
80
60
40
20
0
-20
-40
-60
-80
LATITUDE (N)

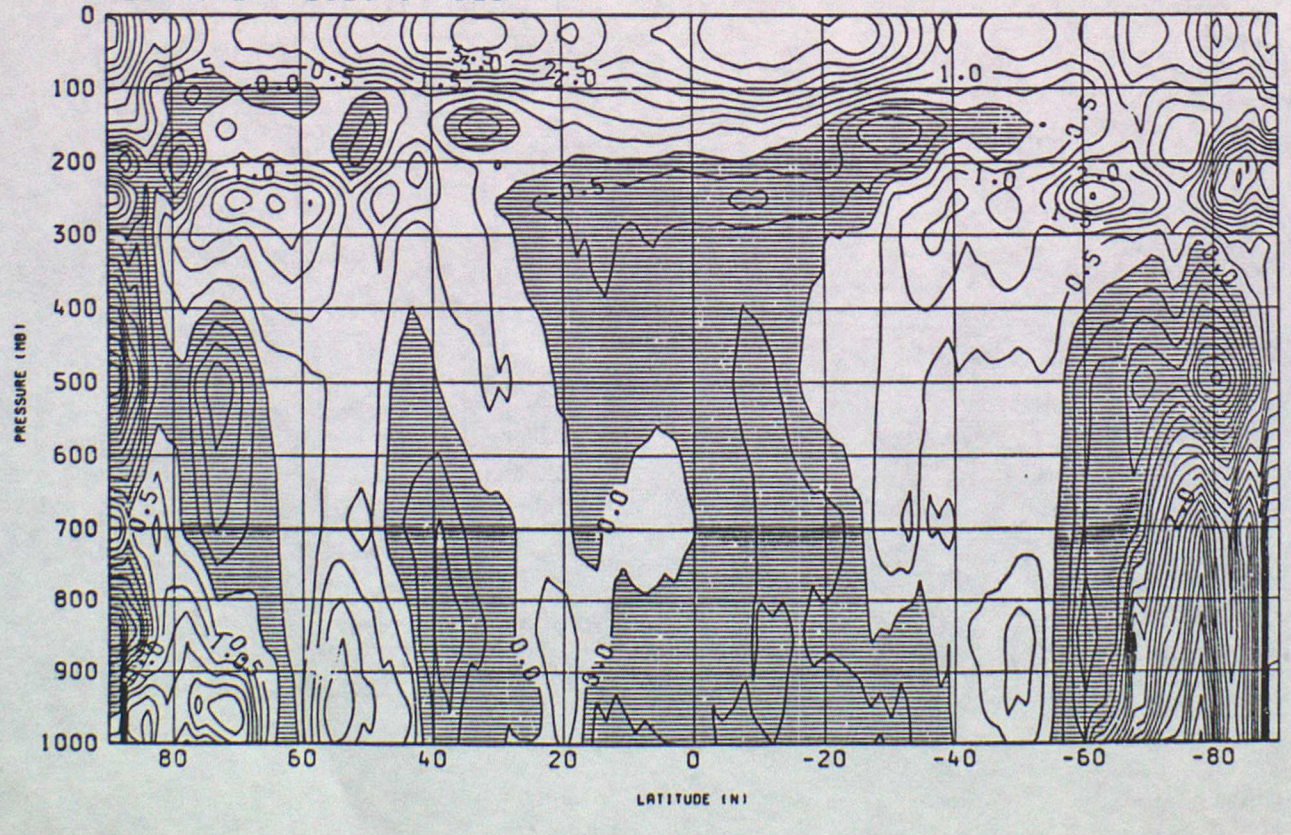
1SUM CASE.TEST(NEWLEV2+ NEW CLOUD + L1CON+SETRH=24)-VER
TEMPERATURE ZONAL MEAN DIFFERENCE
VALID AT 12Z ON 16/6/1985 DATA TIME 12Z ON 13/6/1985
NEGATIVE VALUES SHADED
PRESSURE (MB)
0
100
200
300
400
500
600
700
800
900
1000
80
60
40
20
0
-20
-40
-60
-80
LATITUDE (N)

Figure 21

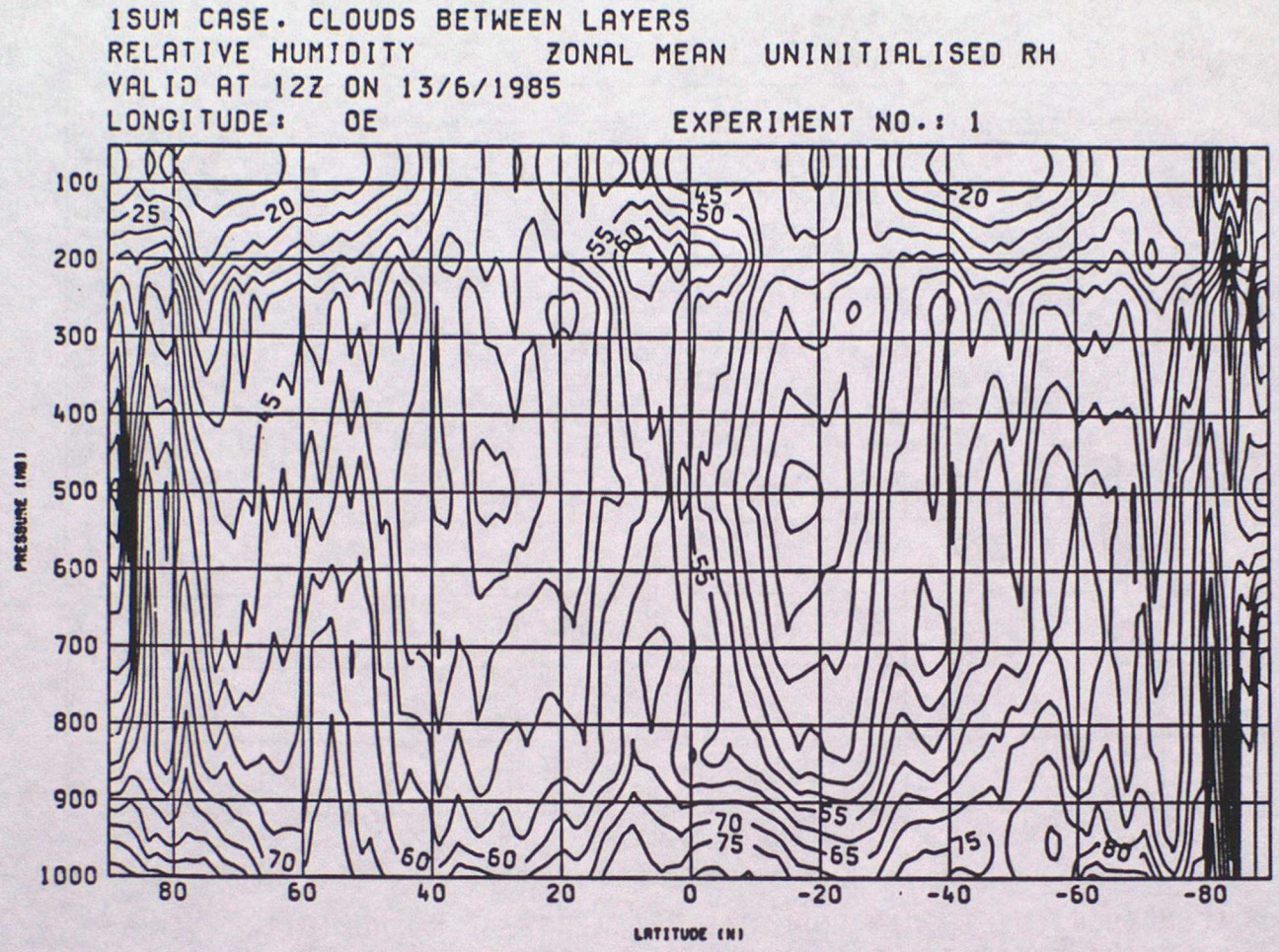
1SUM CASE. CLOUDS BETWEEN LAYERS
RELATIVE HUMIDITY ZONAL MEAN UNINITIALISED RH
VALID AT 12Z ON 13/6/1985
LONGITUDE: 0E
EXPERIMENT NO.: 1
PRESSURE (MB)
LATITUDE (N)

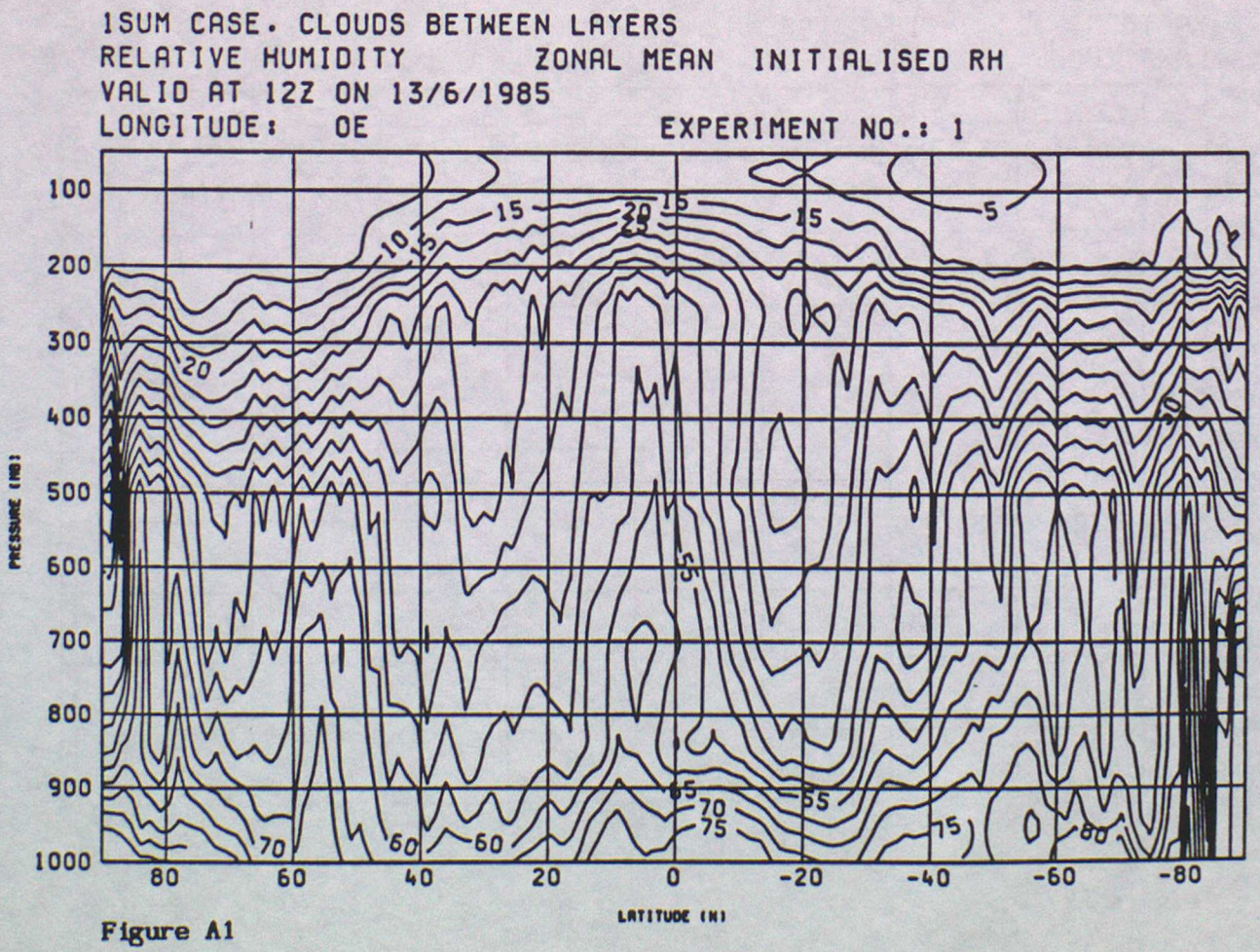
1SUM CASE. CLOUDS BETWEEN LAYERS
RELATIVE HUMIDITY ZONAL MEAN INITIALISED RH
VALID AT 12Z ON 13/6/1985
LONGITUDE: 0E
EXPERIMENT NO.: 1
PRESSURE (MB)
LATITUDE (N)

Figure A1

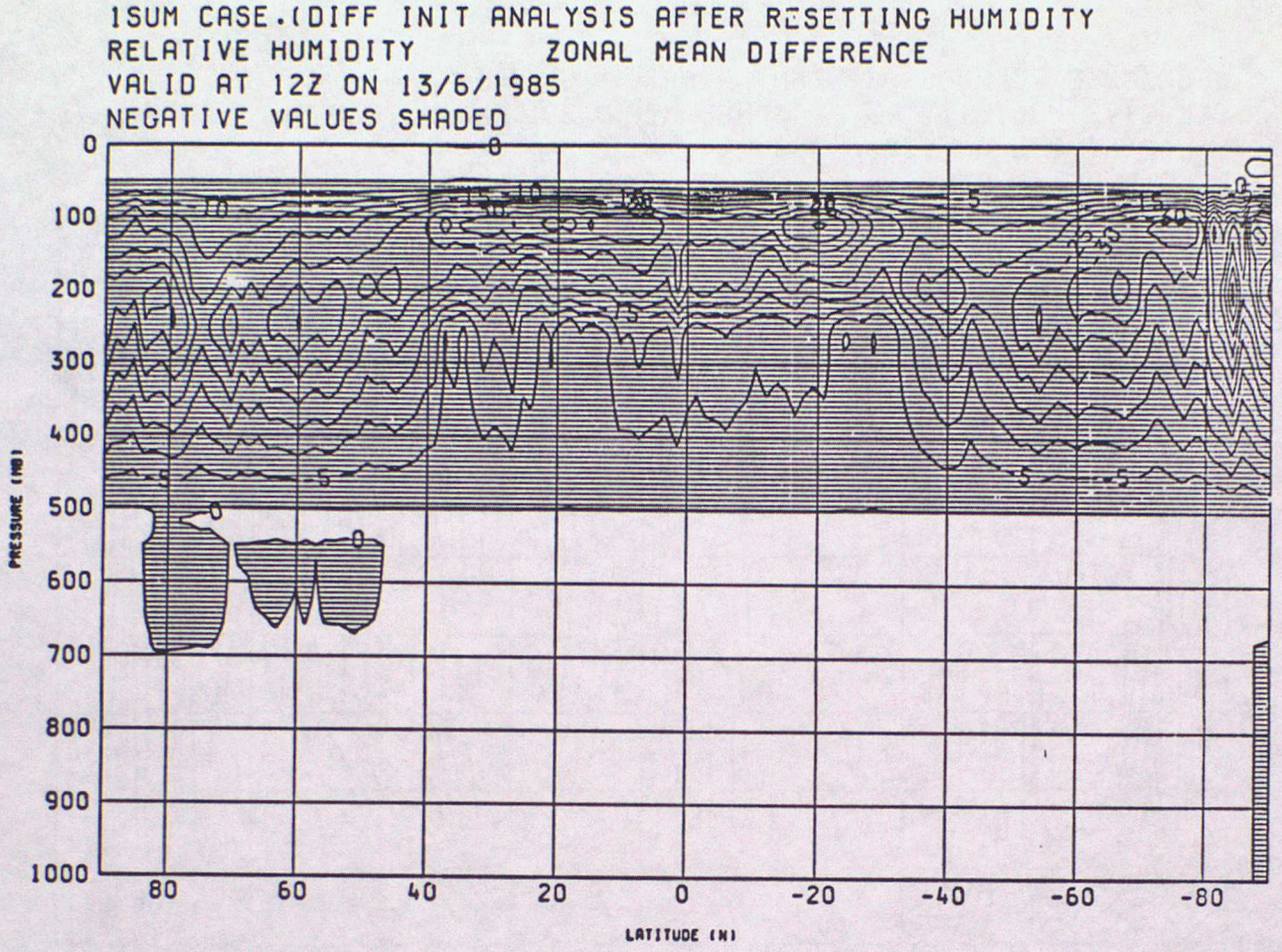
1SUM CASE.(DIFF INIT ANALYSIS AFTER RESETTING HUMIDITY
RELATIVE HUMIDITY ZONAL MEAN DIFFERENCE
VALID AT 12Z ON 13/6/1985
NEGATIVE VALUES SHADED
PRESSURE (MB)
LATITUDE (N)

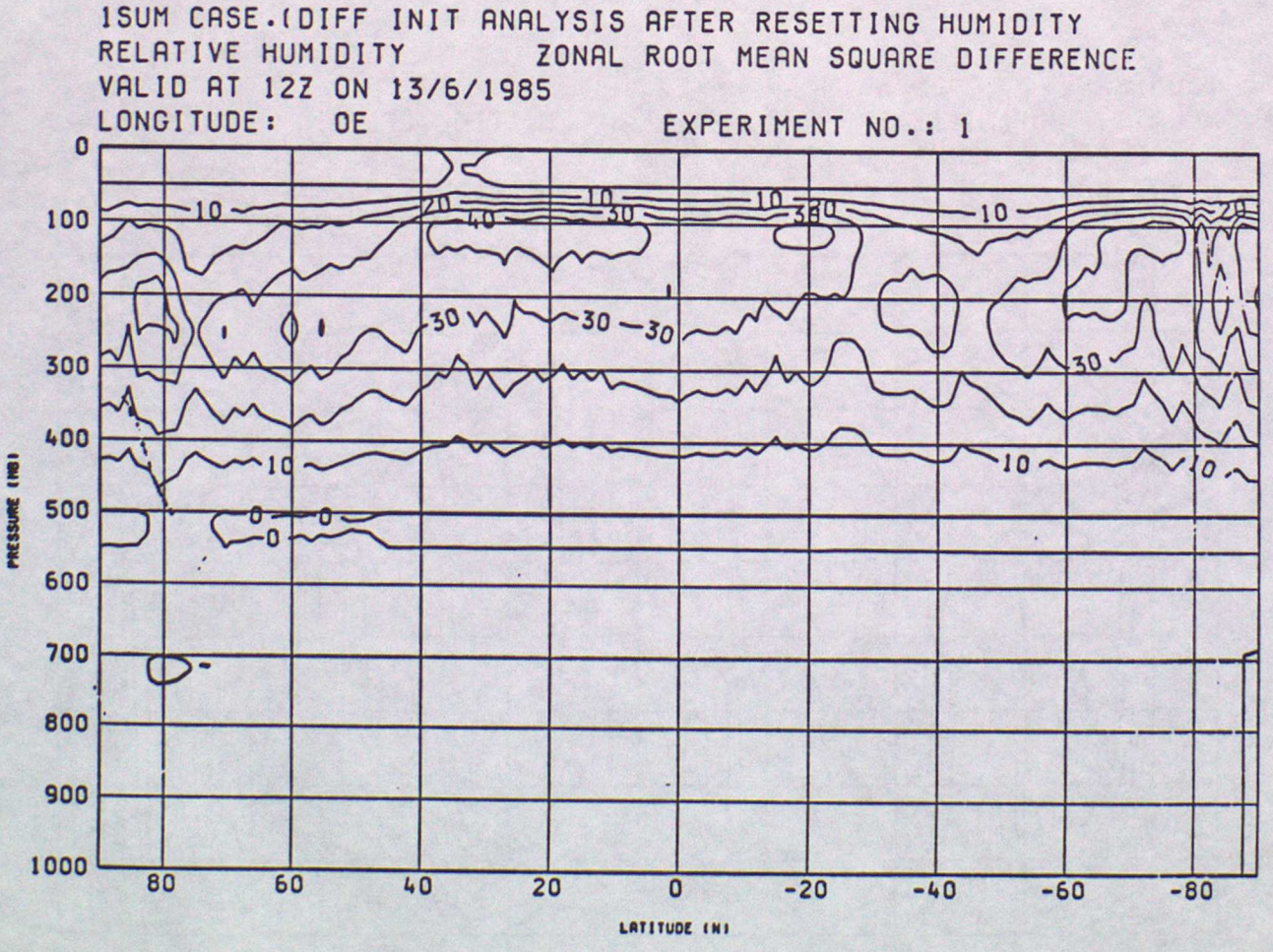
1SUM CASE.(DIFF INIT ANALYSIS AFTER RESETTING HUMIDITY
RELATIVE HUMIDITY ZONAL ROOT MEAN SQUARE DIFFERENCE
VALID AT 12Z ON 13/6/1985
LONGITUDE: 0E
EXPERIMENT NO.: 1
PRESSURE (MB)
LATITUDE (N)

Figure A2

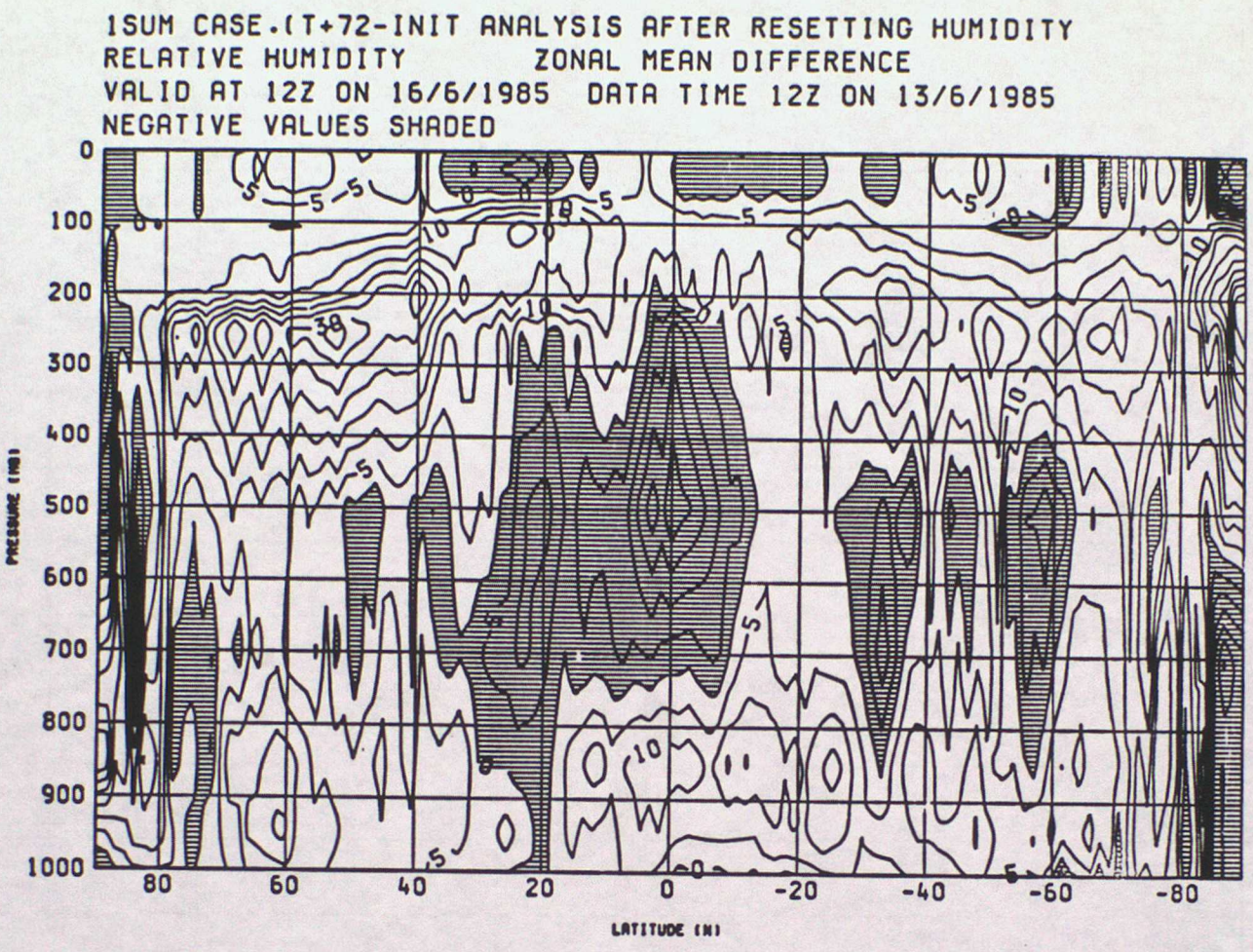
1SUM CASE.(T+72-INIT ANALYSIS AFTER RESETTING HUMIDITY
RELATIVE HUMIDITY ZONAL MEAN DIFFERENCE
VALID AT 12Z ON 16/6/1985 DATA TIME 12Z ON 13/6/1985
NEGATIVE VALUES SHADED
PRESSURE (MB)
0
100
200
300
400
500
600
700
800
900
1000
80
60
40
20
0
-20
-40
-60
-80
LATITUDE (N)

Figure A3

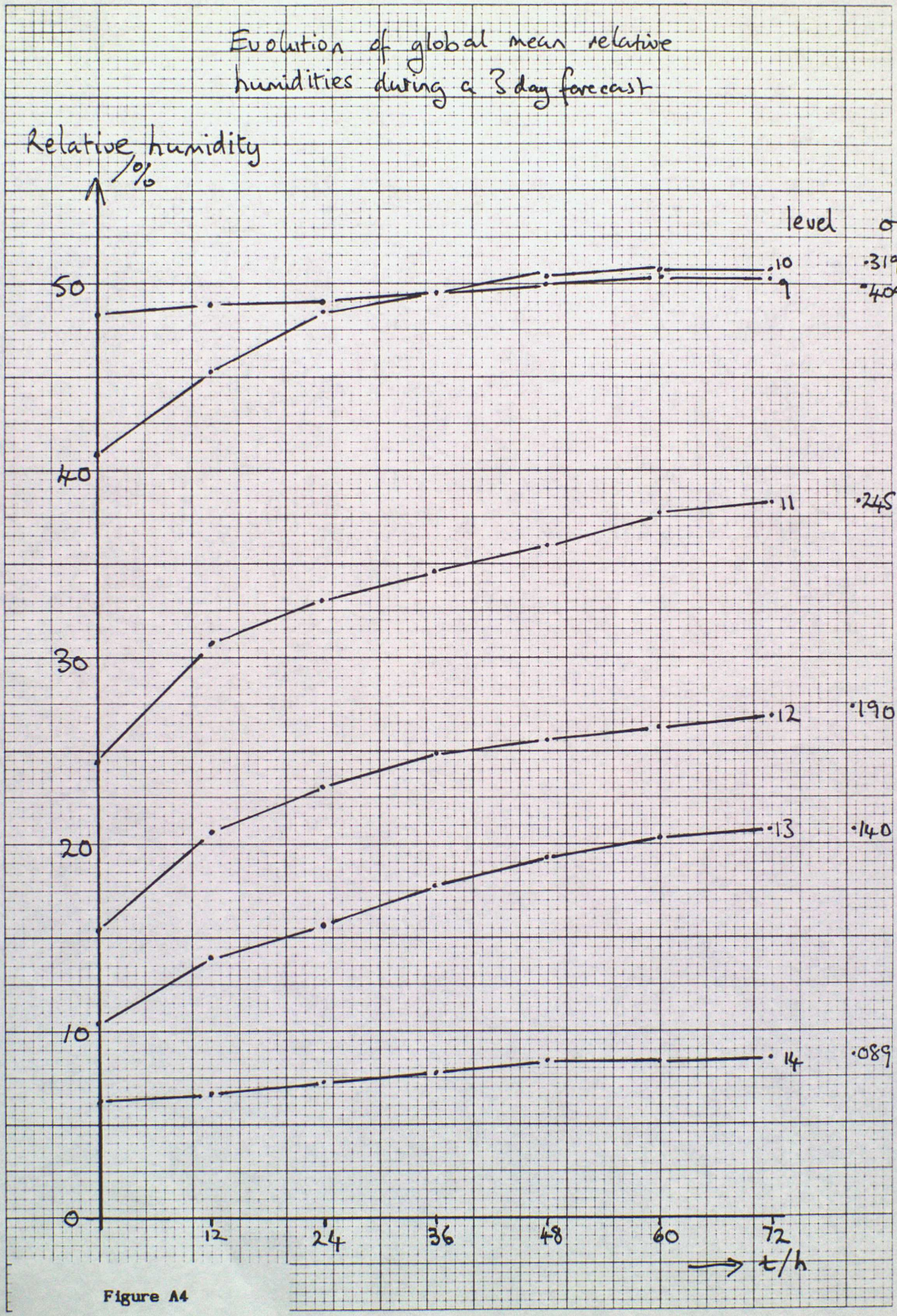
Evolution of global mean relative humidities during a 3 day forecast
Relative humidity
%
level
50
40
30
20
10
0
12
24
36
48
60
72
t/h
10
9
11
12
13
14
·319
·409
·245
·190
·140
·089

Figure A4

CURRENT MET O 11 TECHNICAL NOTES (JANUARY 1989)

The Met O 11 Technical Notes which contain information of current use and *which have not been published* elsewhere, are listed below. The complete set of Technical Notes is available from the National Meteorological Library on loan, if required.

186. **The representation of boundary layer turbulence in the mesoscale model. Part 1. The scheme without changes of state.**
R.N.B. Smith
April 1984

187. **The representation of boundary layer turbulence in the mesoscale model. Part 2. The scheme with changes of state.**
R.N.B. Smith
April 1984

195. **Assessment of HERMES data: a case study comparison with the operational analysis for 2nd March 1984.**
W. Adams
August 1984

196. **Solutions in flow over topography using a geometric Lagrangian flow.**
S. Chynoweth
November 1984

197. **An investigation into the likely causes of spurious rain in anticyclones in the fine mesh model.**
W. Hand
October 1984

199. **The impact of data from the HERMES system on the fine mesh data assimilation scheme - a case study.**
R.S. Bell and O.M. Hammon
February 1985

203. **Using an interactive radiation scheme in the fine mesh model.**
A.D. Darlington
March 1985

204. **Snow forecasts from NWP models during the winter of 1984/85.**
O.M. Hammon
March 1985

205. **Results of a trial of a parametrization of gravity wave drag in the operational forecast model.**
J.E. Kitchen, M.J. Carter and A.P. Day
April 1985

206. **Parametrization of viscosity in three dimensional vortex methods and finite difference models.**
S.P. Ballard
April 1985

207. **A mesoscale simulation of the cold front of 12.11.84.**
B.W. Golding
October 1985

208. **Subgrid-scale cloudiness in the UKMO mesoscale model.**
N. Machin
May 1985

209. **An examination of the structure of fronts in the Met. Office and ECMWF models.**
W. Hand
August 1985

211. **Solutions of a Lagrangian conservation law model of atmospheric motions**
M.J.P. Cullen, J. Norbury and R.J. Purser
August 1985

212. **The analysis of high resolution satellite data in the Met Office.**
A.C. Lorenc, W. Adams and J. Eyre
August 1985

215. **A shortcoming of the operational convection scheme at higher resolution**
M.W. Holt
September 1985

219. **Three dimensional vortex methods and their application to the direct simulation of turbulence.**
S.P. Ballard
October 1985

222. **An implicit version of the operational model boundary layer routine.**
J.E. Kitchen
1986

224. **Four-dimensional analysis by repeated insertion of observations into a NWP model.**
A.C. Lorenc and R. Dumelow
December 1985, revised July 1987

226. **A study of the structure of mid-latitude depressions in a numerical model using trajectory techniques, II. Case studies.**
B.W. Golding
1986

228. **Investigation of balance in the operational global model with normal mode initialization.**
B. Macpherson
April 1986

229. **A parametrization of deep convection for use in a non-hydrostatic mesoscale model.**
R.T.H. Barnes and B.W. Golding
March 1986

230. **Boundary layer structures and surface variables in operational forecasts.**
R.S. Bell
April 1986

231. **Meteorological Office mesoscale model: an overview, version 1.**
B.W. Golding
December 1986

235. **Snow forecasts from the fine mesh model and mesoscale model during the winter 1985/86.**
O.M. Hammon
June 1986

236. **Vertically-propagating quasi-inertia waves: simulated and observed.**
M.M. Booth and G.J. Shutts
November 1986

239. **Mesoscale case study - Project Haar.**
W.R.P. Taylor
February 1987

240. **A trial of modified diffusion in the coarse mesh model.**
R.S. Bell and R.A. Downton
September 1986

243. **The global impact of the recent developments of the physical parameterisation schemes.**
R.S. Bell
November 1986

247. **Some experiments with two-dimensional semi-geostrophic and primitive equation models, with sigma as the vertical coordinate.**
C.A. Parrett
February 1987

248. **Moist frontogenesis in the geometric model.**
M.W. Holt
March 1987

249. **Mesoscale model trial of a revised convection scheme and cloud modifications.**
O.M. Hammon
May 1987

250. **Results from the fine mesh trial of a modified physics package.**
O.M. Hammon
July 1987

251. **Verification of mesoscale model forecasts during the winter, November 1986 - February 1987.**
O.M. Hammon
March 1987

252. **Mountain wave generation by models of flow over synoptic-scale orography.**
M.J.P. Cullen and C.A. Parrett
March 1987

253. **Development of the analysis correction scheme, I. The observational weights.**
B. Macpherson
September 1987

256. **Experiments with divergence damping and reduced diffusion in the mesoscale model.**
S.P. Ballard
May 1987

258. **Trials of the interactive radiation scheme in the global model.**
M.D. Gange
May 1987

261. **Modifications to the automatic quality control of ship data and an assessment using case studies.**
B.R. Barwell and C.A. Parrett
1987

263. **Results from a fine mesh model trial using a modified evaporation scheme.**
O.M. Hammon and C.A. Wilson
August 1987

NEW SERIES (Commenced October 1987)

1. **An assessment of the results of trials of a new analysis scheme for the operational global model.**
R.S. Bell
October 1987

2. **A case study showing the impact of analysis differences on medium range forecasts.**
R.A. Downton and R.S. Bell
January 1988

3. **Development of the analysis correction scheme. II. Inclusion of an observation density analysis.**
B. Macpherson
September 1988

4. **An assessment of a trial to test small changes to the Convection scheme in the mesoscale model.**
O.M. Hammon
January 1988

5. **Trial of proposed changes to the Mesoscale model for November 1987.**
O.M. Hammon
December 1987

6. **Assessment of HERMES soundings processed using the new cloud-clearing scheme.**
R. Swinbank
March 1988

7. **An assessment of the impact of a correction to the Mesoscale model turbulence/vertical diffusion scheme implemented in March 1988.**
S.P. Ballard and O.M. Hammon
April 1988

8. **Comparison of algorithms for the solution of cyclic, block, tridiagonal systems.**
M.H. Mawson
May 1988

9. **A comparison of alternating direction implicit methods for solving the 3-D semi-geostrophic equations.**
M.H. Mawson
May 1988

10. **The automatic quality control of surface observations from ships: the final trial, latest statistics, operational implementation and future work.**
C.A. Parrett
May 1988

11. **"Panel-beater": a proposed fast algorithm for semi-geostrophic finite-element codes.**
R.J. Purser
June 1988

12. **The 5-day forecast trial of the AC scheme.**
R.A. Downton, R.A. Bromley and M.A. Ayles
September 1988

13. **A theoretical study of the information content of the ERS-1 scatterometer data.**
R.J. Purser
August 1988

14. **A further global trial of the analysis correction scheme - Christmas 1987.**
R.S. Bell
August 1988

15. **The sensitivity of a medium range forecast with the analysis correction scheme to data selection in the horizontal.**
B. Macpherson and R.A. Downton
Not yet issued.

16. **The sensitivity of fine-mesh rainfall forecasts to changes in the initial moisture fields.**
R.S. Bell and O.M. Hammon
August 1988

17. **Conservative finite difference schemes for a unified forecast/climate model.**
M.J.P. Cullen and T. Davies
July 1988

18. **Interpreting results from numerical models.**
T. Davies
August 1988

19. **A comparison of the OWSE assimilation scheme with the operational global assimilation scheme.**
D.N. Reed and M.A. Ayles
October 1988

20. **Improvements to low cloud forecasts from the mesoscale and fine mesh models.**
O.M. Hammon
October 1988

21. **The effect of route choice on aircraft wind observations over the North Atlantic.**
D. Lang and N.B. Ingleby
October 1988

22. **Maximum liklihood de-aliasing of simulated scatterometer wind fields using adaptive descent algorithms.**
R.J. Purser
January 1989

23. **A proposal for assimilating detailed aircraft wind data in a local area.**
R.J. Purser
January 1989

24. **Basic formulation and boundary conditions of the mesoscale model.**
S.P. Ballard
Not yet issued.

25. **Development of a new physics package for the global forecast model.**
C.A. Wilson and J. Slingo
January 1989